Review

Biomedical Applications of Graphene Nanomaterials and Beyond

Krishanu Ghosal, and Kishor Sarkar

ACS Biomater. Sci. Eng., **Just Accepted Manuscript** • DOI: 10.1021/acsbiomaterials.8b00376 • Publication Date (Web): 29 Jun 2018

Biomedical Applications of Graphene Nanomaterials and Beyond

Krishanu Ghosal and Kishor Sarkar*

Gene Therapy and Tissue Engineering Lab

Department of Polymer Science & Technology, University of Calcutta, 92, A.P.C. Road,

Kolkata-7 00 009

Abstract- Graphene nanomaterials have been considered as a novel class of nanomaterials that showed exceptional structural, optical, thermal, electrical and mechanical properties. As a consequence it has been extensively studied in various fields including electronics, energy, catalysis, sensing and biomedical fields. In the previous couple of years a significant number of studies have done on graphene based nanomaterials, where it is utilized in a wide range of bioapplications which includes; delivery of small molecule drugs/genes, biosensing, tissue engineering, bioimaging and photothermal and photodynamic therapies due to its excellent aqueous processability, surface functionalizability, outstanding electrical and mechanical properties, tunable fluorescence properties and surface enhanced Raman scattering (SERS).Therefore, it is necessary to get detailed knowledge about it. In this review we will highlight the various synthesis procedures of graphene family nanomaterials including graphene oxide (GO), reduced graphene oxide (rGO) and graphene quantum dots (GQDs) as well as their biomedical applications. We will also highlight the biocompatibity of graphene nanomaterials as well as its possible risk factors for bioapplications. In conclusion we will outline the future perspective and current challenges of graphene nanomaterials for clinical applications.

Keywords: Grpahene, Nanomaterials, Biomedical application, Biosensor, Drug Delivery

*Corresponding author

Email: kishorpst@gmail.com/ kspoly@caluniv.ac.in

Ph. no: +91-33-2350-1397 (Ext- 285, 484, 485), ORCID id: orcid.org/0000-0002-1451-426X

Table of Contents

1) Introduction:- In the last few decades' nanoscience and nanotechnology have been developed as a new prospect across many scientific disciplines due to their specific optoelectronic and physicochemical properties. Invention of nanoscience and nanotechnology is one of the largest revolutions since the beginning of modern science & technology[1]. In this context, carbonaceous nanomaterials like graphene, carbon dot, graphene quantum dots (GQDs), graphene oxide (GO) and reduced graphene oxide (rGO) have attracted much attention over the last decades owing to their unique properties such as large surface area, superior mechanical properties, exceptional thermal or electrical conductivity and optical property[2-6] .

Graphene is one-atom-thick 2D carbonaceous nanomaterial. It contains sp^2 hybridized carbon atoms with honeycomb structure. Since the revolutionary discovery by Prof. A.Geim and Prof. K.Novoselov in 2004, graphene has emerged as a new field of research due to its unique properties[7]. These one atom thick single layer graphene sheets have several unique properties like very high electron transport capability at room temperature[7], high elasticity[8] and thermal conductivity[4], high mechanical strength[9], tuneable optical properties[6, 10], quantum Hall effect at room temperature[11] and tunable band gap[12]. Unlike graphene, several fascinating properties also showed by double-, few-, and multilayer sheets of graphene. Subsequently, graphene is a conductive transparent nanomaterial, with low cost and substantial green environmental impact makes it suitable for catalysis[13], sensing[14], energy[15], drug delivery[16], electrical and bioelectronics applications[17]. Recent progress in the biomedical applications of graphene nanomaterials already provides us some of the sustainable biomedical devices such as deep brain stimulators[18], blood glucose sensors[19-20]. Beside these biomedical devices graphene

nanomaterials also have been used in tissue engineering[21-22], gene therapy[23], cell imaging[24], and bioelectronics[25]. Although there are many successful implementations of graphene nanomaterials already done in the field of physics, chemistry and biology. Still, it is an extremely hot topic of research for researchers and many applications yet to come in near future.

In this concern versatile range of nanomaterials including nanoparticles, quantum dots, nanowires and nanosheets have emerged from last few years, with extensive progress in synthesis, characterization and processing. One of the main reason to evaluate these efforts to how the size, composition and structure of these nanomaterials lead to novel optical, electronic, mechanical, thermal and magnetic properties. These enhanced and extraordinary physical and chemical properties of such nanomaterials open up exclusive opportunities in the field of biology.

In this review, we mainly discuss about biomedical applications of graphene family nanomaterials, as well as their synthesis procedure, biocompatibility and biomedical applications including biosensors, bio-imaging, tissue engineering, drug delivery, gene therapy, photodynamic and photothermal therapy and their future perspective.

2) Synthesis of graphene and graphene based nanomaterials:- Graphene has mainly four forms, which are graphene itself, oxidized form of graphene i.e. GO, reduced form of graphene oxide i.e. rGO and graphene quantum dots i.e. GQD which has a size less than 20 nm. GO is the oxidized form of chemically modified graphene and it can be synthesized by rapid oxidation of crystalline graphite followed by some dispersion methods or sonication of colloidal suspensions of graphite oxide in a wide variety of organic solvents[26]. Whereas high temperature under reducing conditions will convert GO to reduced graphene oxide. In this section, we mainly focus on relevant synthesis procedures of these nanomaterials.

2.1) Synthesis of graphene- There are several reported synthesis procedures for the synthesis of graphene; including mechanical exfoliation[7], chemical vapour deposition (CVD)[27], plasma enhanced chemical vapour deposition (PE-CVD)[28], cleavage of natural graphite[29], hydrogen arc discharge[5], epitaxial growth of electrically insulating material like boron nitride[30], solution processable methods[31-33] and microwave synthesis method[34-35].

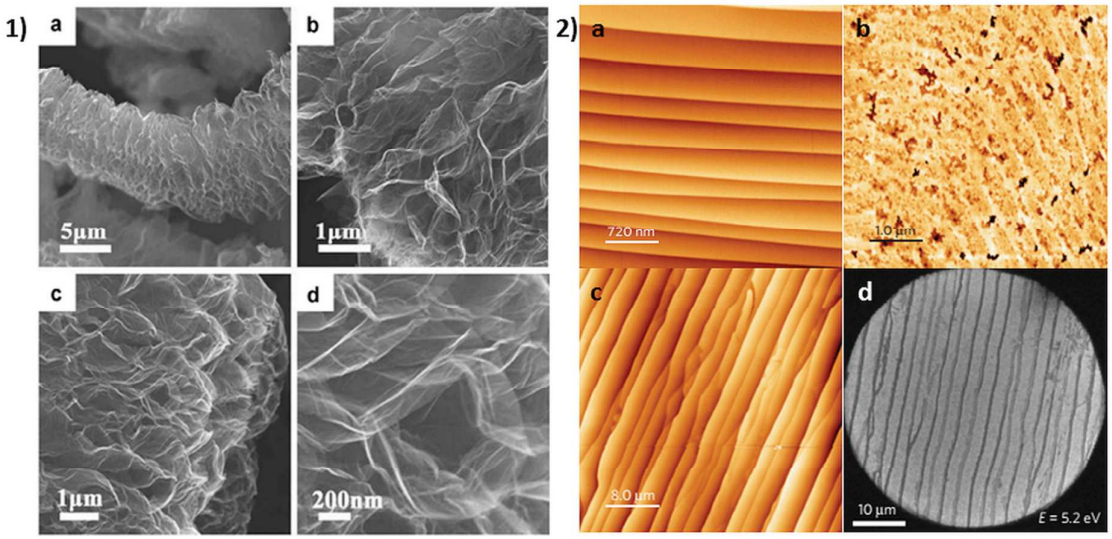

Figure 1. 1) SEM images of hydrogen arc discharge-exfoliated graphene sheets(GS); (a) GS with a transparent wormlike morphology, (b) top view and (c) side view of the GS, (d) magnification of a part of the GS in panel c. Reproduced with permission from ref[5]. Copyright 2009 American Chemical Society. 2) Morphological changes of 6H–SiC(0001) during graphene growth ; (a) Initial surface after H-etching imaged by AFM. The step height is 15 Å. (b), AFM image of graphene on 6H–SiC(0001) with a nominal thickness of 1 ML formed by annealing in UHV at a temperature of about 1,280 ^{O}C (c)AFM image of graphene on 6H–SiC(0001) with a nominal thickness of 1.2 ML formed by annealing in Ar (p= 900 mbar, T =1,650 ◦C). **(d)**, LEEM image of a sample equivalent to that of **c** revealing macro-terraces covered with graphene up to 50 µm long and at least 1 µm wide. Reproduced with permission from ref[36]. Copyright 2009 Nature Publishing Group.

Graphene was first synthesized by mechanical exfoliation in 2004[7]. This simple cost effective synthesis procedure created an explosive growth in the research field of graphene and consequently demands graphene flakes which are valuable for research to clarify graphene properties. But unfortunately, graphene flakes are usually available in few microns in this method with irregular shapes due to their deterministically uncontrolled azimuthal alignment. To overcome this problem, CVD technique was developed to synthesize graphene flakes in large scale production. CVD is generally carried out from carbon containing gases in a catalytic converter where metal surfaces act as a catalyst or by surface segregation of carbon at high temperature and then dissolved in bulk of metals like Ni, Cu etc[2, 37].

The first interpretation of single layer graphite was reported by J.W. May in 1969[38]. Since then, a lot of research experiments were performed to synthesise single or few layers of graphite by surface segregation of carbon throughout the annealing period of various carbon doped metals e.g. Fe, Pt, Co, Ni, Pd. In a study done by Yu and his co-workers showed that an atomically cleaned single crystal Ni (111) surface in absence of grain boundaries can produce more uniform and thinner few layered graphene, while polycrystalline Ni with grain boundaries formed multilayer graphene. Here grain boundaries act as a nucleation site. They also noticed that different cooling rate substantially affects the quality, amount of defects and thickness of graphene. Another very important observation they reported that annealing of Ni surface in H_2 atmosphere before graphene synthesis produce more uniform graphene films. They explained the reason behind this phenomenon that hydrogen removes impurities like S, P that cause local alteration of carbon solubility in metals and affecting graphene thickness[39]. Land and his co-workers used hydrocarbon decomposition on Pt (111) surface to synthesise single-layer graphite[40], while ambient pressure CVD on polycrystalline nickel produced 1-12 layer graphene films[41]. By using CVD technique, Colombo and his co-worker synthesized large-area graphene films in the order of centimetres on the copper surface using methane as

s source of carbon[2]. The reason behind this phenomenon is explained based on differential solubility of carbon in metal. The solubility of carbon in nickel much greater than copper (solubility of C in Ni is 1.3 atom% at 1000^{o} C[42] ,while in case of copper it is less than 0.001 atom% at 1000^{o}C[43]). Similarly large area monolayer and multilayer graphene films were synthesized by Chen et al., specifically bilayer graphene films on commercial Cu-Ni alloy foils by CVD using hydrogen and methane as precursors. They also noticed that, the quality and thickness of graphene obtained on Cu-Ni foils substantially dependent on decomposition temperature and cooling rate[43]. Graphene can be also prepared by surface segregation of C atoms under ultra-high vacuum at 1400 K on Ru(0001) surface[44] and by low pressure CVD on Ir(111) surface[45]. In another work, Ruoff and his co-workers discovered that, the single crystals graphene can be synthesized by low-pressure CVD technique on a copper foil[46].

Although exfoliated graphene flakes exhibit electrical transport properties like CVD based graphene but when it comes to single graphene domain, grain boundary plays an important role. This is the main reason behind variability of electron mobility which is frequently observed in CVD based graphene. In addition to the CVD technique, another technique i.e. epitaxial growth technique is also used to produce large scale monolayer graphene where graphene is grown on a single-crystal silicon carbide (SiC) wafer by vacuum graphitization.

Compared to the above techniques, epitaxial growth method simply provides the fabrication of low-defect-density, large-scale graphene films on a semi-insulating SiC surface and it can be used without transfer to any insulating substrate[47]. In the year of 1978, Tairov and Tzvetkov developed a modified sublimation growth process for 6H-SiC[48]. A few years earlier in 1975 Tooren and his group showed that segregation of silicon from SiC (0001) single crystal leads to the formation of a graphite layer on the SiC surface. They also noticed that under ultrahigh vacuum ($<10^{-10}$ Torr) and at elevated temperature, Si-face consist with monocrystalline graphite layer whereas C-face consists with polycrystalline graphite layer[49].

Graphene formation starts on the top of the SiC surface and proceeds inner wards. One graphene layer is formed from decomposition of approximately three SiC bilayer. Initially, a carbon-rich surface layer also called buffer layer reconstruction starts where carbon atoms situated isostructurally to the graphene, however there are neither sp^2 structure nor covalent bonds are attached to underlying Si atoms. This silicon layer acts as an insulator and does not show graphene-like electronic properties. It is also observed that the sublimation rate of SiC is reduced drastically, when an inert gas atmosphere (up to 1 bar) is introduced, and graphene starts to grow at temperature more than 1400-1500 ℃, at this temperature carbon atom form high-quality graphene (only 1-2 layers) due to greater mobility of C atoms[36]. Synthesis of graphene by reduction of graphite oxide is another easy route of graphene synthesis. Wei and his co-workers demonstrated a green and sustainable approach for the synthesis of graphene[50]. They synthesized graphene nanosheets from exfoliated graphite oxide by Fe reduction. Fe eliminates, oxygen functionalities from graphite oxide and produce graphene. This technique offers a large scale, eco-friendly and cost-effective production of graphene. In 2008 Mullen and his group discovered another novel approach for synthesis of 2D graphene nanoribbons[51]. They produced graphene nanoribbons with the help of Suzuki-Miyaura coupling reaction using 1,4-diiodo-2,3,5,6-tetraphenylbenzene and 4-bromophenylboronic acid as a starting material. They developed graphene nanoribbons up to 12 nm in length, further microscopic studies also confirmed that these nanoribbons have a high tendency to self-assemble[51]. Graphene nanoribbons were also synthesized by electron beam irradiation on poly(methyl- methacrylate) nanofibers. This low temperature one step synthesis process provide a designed and controlled way to obtain graphene[52]. P*é*nicaud and their group manufactured graphene from graphite by liquid-phase exfoliation technique. In this process they first dispersed graphite in organic solvents followed by exfoliation[53]. Recently another

large scale graphene synthesis process was developed by Stride research group[54]. They synthesized graphene from ethanol reduction by sodium followed by pyrolysis.

Recently solution processable synthesis of graphene has gained tremendous attraction due to its several advantages like eco-friendly, scalability and easy synthesis method than CVD or epitaxial growth or hydrogen arc discharge. In this concern, Wallace and co-workers reported for the first time solution processable synthesis of graphene sheets in large scale. They synthesised graphite oxide from graphite by modified Hummers method. Then they purified the graphite oxide by dialysis followed by dispersion using ultrasonication to get GO. After that they removed the unexfoliated graphite oxide by centrifugation and finally the GO dispersion treated with hydrazine and ammonia solution to get processable graphene sheets. During the reaction they maintained the hydrazine to GO ratio at about 7:10 which is optimal for synthesis[55]. Shams et al. synthesized solution processable few layer graphene nanosheets from dead camphor leaves. They used a greener approach for the synthesis of graphene sheets. For the synthesis they used dirt free vacuum dried camphor leaves as a starting material and heated in a vacuum oven under nitrogen atmosphere up to 1200°C at 10°C/min and maintained for 4 min. After that they cooled the product and mixed with D-Tyrosine and trichloromethane with sonication for 15 min followed by centrifugation to precipitate large carbon particles to acquire the few layer graphene sheets[33]. In a recent work, Verramani et al. also reported the synthesis of solution processable graphene sheet like porous activated carbon (GPAC). For the preparation of GPAC they cut the Bougainvllea glabra flowers into small pieces, washed with water and dried in an oven at 100°C. Then they preheated the dried material at 200°C for 6 h. After that they carried out activation process where they mixed the preheated carbon powder with 10% $ZnCl_2$ and stirred at 60°C under N_2 atmosphere for 24 h followed by carbonization in a tubular furnace for 3 h in N_2 atmosphere. Finally they washed the carbonized product with HCl and distilled water for neutralization and drying[56].

Microwave synthesis method another newer synthesis process for graphene. Hazmi and co-workers reported, synthesis of monolayer, bilayer and multilayered graphene using precise microwave power and temperature. In details, they treated graphite flakes with ice cold glutaric acid to separate out graphite flakes at a distance equal to the glutaric acid molecule (0.88nm). After that, they dispersed the pre-treated graphite flakes in methanol and introduced in Teflon autoclave and finally placed into a microwave oven. The microwave power, time and reaction temperature determine the faith of the graphene layers[34].

In addition to these, there are some other graphene synthesis methods having various advantages and disadvantages which are enlisted in Table 1.

Table 1. Comparison between various graphene synthesis methods

Synthesis Methods	Starting Materials	Advantages	Disadvantages	Applications	References
Mechanical exfoliation	Highly oriented pyrolytic graphite	Very simple process, large scale production, good structural and electronic quality	Low yields, time consuming	Fundamental research applications	7
Epitaxial growth on Silicon Carbide	6H-6SiC	Wafer scale production, high qualities	Low yields, very high temperature requirement, high synthesis	Electronics applications	57

			cost		
Reduction of graphite oxide	Graphite	Low cost, high yields, very good processability	Structural defects	Optoelectronics, composite materials	[58]
Chemical vapour deposition on transition metals	Hydrocarbon gas	Uniform, high quality, large scale production	High cost, complicated technique, high temperature requirement	Fundamental research and electronic applications	[59]
Reduction of ethanol by Na	Ethanol and sodium	Low cost, gram scale production, starting material other than graphite	Impure low quality graphene, violent reaction	Composite materials applications	[54]
Conversion of nanodiamond	Nanodiamond	Simple process	High manufacture cost, high temperature requirement	Composite materials applications	[60]
Organic	Polyacyclic	Good	Difficult	Electronics and	

synthesis	hydrocarbons	structural quality, very good processability	synthesis process, limited size range	optoelectronic applications	[51]
Arc discharge of graphite	Graphite	Low cost, one step synthesis procedure	Impure graphene, nonuniform	Composite materials applications	[61]
Electron beam irradiation on PMMA nanofibers	PMMA	Low temperature process, controlled way to produce graphene	Nonuniform, yield is low	Electronics and optoelectronic applications	[52]
Unzipping of carbon nanotubes	Carbon nanotubes	Low cost, very simple process, large scale production, graphene nanoribbons with controlled edges and widths	Time consuming process	Electronics applications	[62]
Thermal reaction of polyaromati	Polyaromatic hydrocarbons	Wafer scale, low-cost production	High-temperature requirement,	Electronics and optoelectronics applications	[63]

c hydrocarbon			Non-uniform		
Liquid-phase exfoliation	Graphite	Low cost, large scale production, direct synthesis procedure	Impurity present in final product, time-consuming process	Transparent electrodes, electronic applications	[64]
Transfer batch fabrication	Acetic acid, CH_4, H_2	Uniform single layer graphene, good carrier mobility, electrical and mechanical continuation over a large distance	Complicated, high temperature required	Electronics applications	[65]
Molecular beam deposition	Acetylene	Large area, high quality graphene, good control over process	High temperature required	Electronics applications	[66]

2.2. Synthesis of graphene oxide (GO) and reduced graphene oxide (rGO):- One of the most significant branches of graphene research concerns with GO and rGO. GO contains many oxygen functionalities, as it is prepared by oxidation of graphite and reduction of graphene oxide produce reduced graphene oxide. Till now there are three well-known methods for synthesis of GO, these methods are Boride[67], Staudenmaier[68] and Hummers method[69] or by slight modifications of these procedures. In all these procedures oxidation of graphite involves at different level. Boride performed a reaction involving a mixture of nitric acid (HNO_3) and potassium chlorate ($KClO_3$) to oxidize graphite and produced graphite oxide[67]. Nearly four decades later Staudenmaier modified and improved Boride's method by adding several aliquots of chlorate during the course of the reaction. Staudenmaier also added some concentrated sulfuric acid to increase the acidity of the reaction medium. This slight modification in the procedure resulted in overall oxidation of graphite similar to Boride's method but performed more efficiently in a single reaction vessel[68]. After 60 years later Hummers developed another alternative method to synthesize GO by reacting graphite with sodium nitrate ($NaNO_3$), concentrated sulphuric acid (Con H_2SO_4), and potassium permanganate ($KMnO_4$)[69]. Apart from these well-known methods, researchers have also developed few modified methods (Such as addition of one or two additional oxidising agents during synthesis steps) to synthesize GO based on previous methods as discussed earlier, however these three methods remains the main methods for synthesis of GO[70]. Although it has been observed that the final products of these reactions show a wide range of variance depending not only the specific oxidants used but also depends on reaction conditions of the medium and graphite source. Both Boride and Staudenmaier treated together potassium chlorate ($KClO_3$) and concentrated nitric acid (con HNO_3) for their method. Nitric acid is one of the most common oxidizing agent used for chemical reactions, it also reacts significantly

with aromatic carbon surfaces and forms various oxide containing species like ketones, lactones, carboxyl's etc.

In the case of Hummers method, a mixture of potassium permanganate and sulfuric acid is used. Potassium permanganate reacts with sulfuric acid and form dimanganeseheptaoxide (Mn_2O_7), this bimetallic heptaoxide is much more reactive than its monometallic tetraoxide analogue and it is well-known that this bimetallic heptaoxide detonates when placed in contact with organic compounds or when heated temperature higher than 55 ^oC[71-72] . Tour and his group developed an improved GO production method based on Hummers method[73]. They found that excluding $NaNO_3$, if the amount of $KMnO_4$ is increased and a mixture of 9:1 $H_2SO_4/H_3PO_4$are used then it improves the effectiveness of the oxidation process as shown in Fig 2. Polar oxygen group, that present in GO provide it good hydrophilicity, so it can be exfoliated in many polar solvents, particularly in water. GO offers a wide range of possibilities for the manufacture of the chemically modified graphene in industrial scale[74].

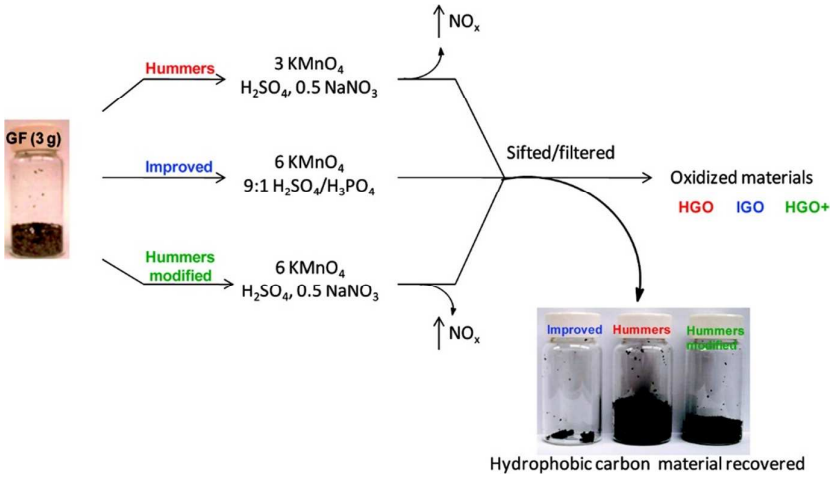

Figure 2. Representation of the synthesis procedures of GO followed starting with graphite flakes (GF). Under-oxidized hydrophobic carbon material recovered during the purification of IGO, HGO, and HGO+. The increased efficiency of the IGO method is indicated by the

very small amount of under-oxidized material produced. Reproduced with permission from ref[73]. Copyright 2010 American Chemical Society.

Other than Hummers and modified Hummers method recently researchers came with some alternative rapid an improved synthesis method like microwave synthesis method for the preparation of GO. As for example, Wang et al. synthesized GO nanosheets by microwave irradiation. Their synthesis method involved conc. H_2SO_4, graphite flakes and $KMnO_4$. They mixed in a three necked flask and placed in a microwave oven for 150 sec in a cycle of 30 sec. After that they stopped the reaction by adding 15 ml of 30% H_2O_2 followed by centrifugation and discarded the supernatant to get GO. Finally they ultrasonicated the mixture to get a homogeneous suspension of GO[75]. He and co-workers also reported one pot, one step microwave assisted synthesis of GO with a yield of 120%. Unlike previous work, they used conc. HNO_3 along with conc. H_2SO_4, graphite flakes and $KMnO_4$ for the preparation of GO. Under the microwave irradiation of 300 watt for 40 sec graphite flakes turned into GO[76]. In addition to microwave synthesis method Grossman and co-workers reported another improved synthesis method for preparation of GO[77]. Briefly, they demonstrated that a mild thermal annealing procedure (50-80°C) can enhance the sheet properties in GO produced by Hummers method in a large scale without affecting the oxygen content preserved and without involving any other chemical treatment. The thermal annealing facilitate to transform the mixed up sp^2-sp^3 hybrid phases into a distinct oxidized and well-ordered graphitic phases which resulted in improved optical and electronic properties than as synthesized GO produced by Hummers method. Yamaguchi et al. also revealed that, oxygen functionalization of GO can be controlled by thermal annealing which produce GO with enhanced electronic properties[78].

Till now only few preparation methods are reported for reduced graphene oxide (rGO). Most researchers used hydrazine hydrate for synthesis of rGO from GO[79-81]. However, some other

reducing agents also used for the preparation of rGO. Paredes and his group compared effect of different reducing agents on graphene oxide. They used ammonia, potassium hydroxide, sodium borohydride, pyrogallol, ascorbic acid(vitamin-C) and hydrazine monohydrate as reducing agents and reached in a conclusion that ascorbic acid is the ideal substitute for hydrazine for reduction of the GO[82].

Lee and his co-workers are used $NaBH_4$ for reduction of GO and found that, the electrical resistance of rGO reduced by $NaBH_4$ is much lower than reduced by hydrazine. They proposed that it might be formation of C-N groups in case of hydrazine, which can act as donors, recompensing the hole carriers in rGO but on the other hand in case of $NaBH_4$ reduction the interlayer spacing between two graphite oxide layer expanded to some extent by the formation of transitional boron oxide complexes and then contracted by subsequent removal of hydroxyl and carbonyl groups with boron oxide complexes[83].

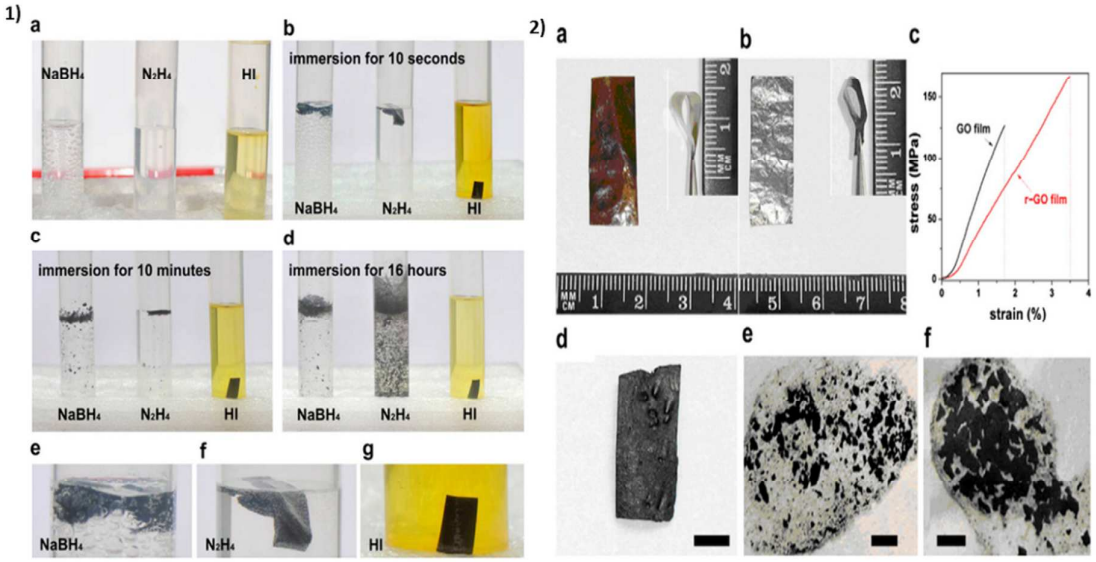

Figure 3. 1) Optical photographs of the reducing process by immersing a GO film into different reducing agents for different times at room temperature; (a) Three liquid reducing agents: 50 mM $NaBH_4$ aqueous solution ($NaBH_4$), 85% $N_2H_4.H_2O$ solution (N_2H_4), and 55% HI acid solution (HI). (b–d) The GO films reduced by the three agents for 10 s, 10 min and

16 h. (e–g) Enlarged views from (b) which show that the phenomenon occurred after 10 s immersion of GO films to the three liquid reducing agents; 2) Optical photographs and mechanical properties of the GO films reduced by different chemical agents. (a) As assembled GO film. (b) 1 h HI acid-reduced GO film at 100 C. (c) Stress–strain curve of the GO film and HI acid-reduced GO film. (d–f) Hydrazine vapor-, $N_2H_4.H_2O$ and $NaBH_4$-reduced GO films. The scale bar in (d–f) is 5 mm. Reproduced with permission from ref [84]. Copyright 2010 Elsevier.

Cheng research group reported a unique method for reduction of GO[84]. They used hydrohalic acid for reduction of GO. They demonstrated that hydrohalic acid can reduce GO very effectively at 100^{o}C for 1 hour without destroying their flexibility and integrity images are shown in Figure 3. They also checked electrical conductance of the produced rGO and figure out that its electrical conductance is much better than other rGO produced by other methods. Other than these studies, some research groups tried to understand the theoretical framework of the oxygen bonds during the reduction process of GO to rGO. Such as, Kumar et al. investigated the impact of oxygen clustering on the thermal reduction of graphene oxide[85]. They found that the number of oxygen and carbon atoms can be altered during the synthesis of rGO, depending on the degree of oxygen clustering without hampering the reduction temperature. Shen et al.[86] and Niu et al.[87] also tried to reveal the effect of low temperature thermal treatments during the synthesis of rGO from GO. Shen et al. demonstrated that during the low temperature thermal reduction process, the decomposition of functional groups present in GO occurs in 4 distinct steps ranging from below 160°C to above 300°C[86] whereas Niu et al. demonstrated that rGO can be prepared effectively by thermal treatment of GO at 200°C[87]. Till now these methods are most significant and well-known method for the synthesis of graphene oxide (GO) and reduced graphene oxide (rGO).

2.3. Synthesis of graphene quantum dots (GQDs):- The latest member of graphene family is graphene quantum dots (GQDs) which are smaller in size ranges from 3 to 20 nm[88-89] with sp^2- sp^2 carbon bonds similar to graphene and also possess large surface area, better surface grafting using π-π conjugation and surface functionalization[88]. In addition to above properties, GQDs exhibit new phenomena due to quantum confinement and edge effects which are similar to C-Dots. Typically, GQDs contain hydrophilic functional groups such as hydroxyl and carboxylic acid at the edge, which are similar to graphene or graphene oxide, thus imprinting them with excellent water solubility and subsequently allowing to modify with various organic, inorganic and biological species according to requirement. Owing to these superior properties, GQDs have been considered as one of the most promising nanomaterial and significant research efforts are giving to synthesize low toxic GQDs using eco-friendly alternative methods which is a major concern with other quantum dots (CdSe, PbS, CdS etc). In this regard, there are mainly two approaches to synthesize GQDs namely top-down method and bottom up method. Top down method includes chemical ablation from graphene and electrochemical exfoliation. Bottom up approaches consists of cage opening of fullerene and solution chemistry synthesis, microwave synthesis etc. Below we shall do a small discussion about various synthesis methods of GQDs.

2.3.1. Top-down methods:- Chemical ablation from graphene is one of the most common GQDs synthesis technique. It includes hydrothermal, solvothermal, hydrazine hydrate reduction method etc.

In 2010, Wu and his co-workers synthesized GQDs from graphene oxide sheets by hydrothermal method where large graphene oxide sheets were cut into small one by controlled oxidation in a mixture of sulfuric acid and nitric acid under mild ultra-sonication. The oxidized small graphene sheets were then reduced to GQDs under hydrothermal condition at a temperature of 200^{O}C for 10h[90]. Shen et al. reported GQDs surface passivation

with polyethylene glycol by hydrothermal reaction, using small GO sheets and polyethylene glycol as a starting material[91]. Yang group made green fluorescent GQDs by solvothermal method with PL quantum yield as high as 11.4% and average diameter of 5.3 nm and height of 1.2 nm. From which they concluded that most of the GQDs are single or bilayerd[92]. In addition to this GQDs were also synthesized by hydrazine hydrate reduction method from small graphene oxide sheets. Zhu and his group synthesized GQDs by hydrazine hydrate reduction of GO with their surface passivation by PEG diamine[93]. For this method, at first they oxidized GO with HNO_3 to cut into small pieces, then this small GO sheets passivated with PEG diamine and finally they reduced it by hydrazine hydrate to get the GQDs. The diameter of the synthesized GQDs lies between 5-19 nm suggesting that the formation of monodisperse GQDs. Prior to this work, Chhowalla and co-workers discovered that fluorescence intensity of the GO thin film was changed after each incremental when it is exposed to hydrazine-vapour (from 20seconds up to 60 min)[94].

Pang group synthesized GQDs by electrooxidation of graphite in aqueous solution. They electrochemically oxidized a graphitic at 3V against a saturated calomel electrode with a Pt wire counter electrode in a NaH_2PO_4 aqueous solution[95]. Chi group also prepared GQDs electrochemically[96]. They performed the experiment in an electrochemical cell consisting a graphite rod working electrode a Pt mesh as a counter electrode Ag/AgCl electrode reference electrode and pH 7.0 phosphate buffer solution. Li et al. reported an electrochemical synthesis procedure for green-luminescent functional GQDs with a uniform size of 3-5 nm. GQDs were formed by electrochemical oxidation of graphene film electrode in phosphate buffer solution. Due to oxygen containing functional groups on its surface it gained high stability in the aqueous medium. The aqueous dispersion of GQDs are stable upto 3 months[97].

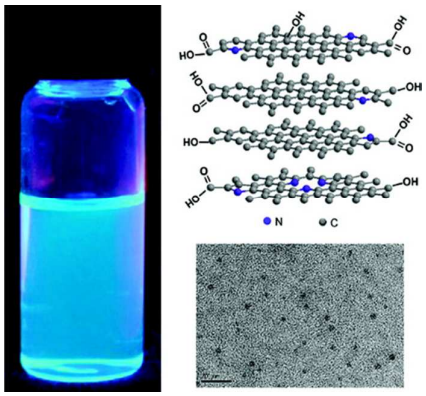

Figure 4. (a) Blue fluorescence of N-GQDs upon UV light exposure (b) Schematic structure of the GQDs(c) TEM images of N-GQDs. Reproduced with permission from ref [98]. Copyright 2012 American Chemical Society.

Qu and co-workers reported a simple electrochemical approach for N-doped GQDs with oxygen group functional groups[98]. They used graphene film as a working electrode, Pt wire and Ag/AgCl act as a counter and reference electrode. The electrolyte was 0.1M TBAP in acetonitrile. The synthesized N-GQDs have uniform diameter of 2-5 nm with a topographic height of 1-2.5 nm suggesting that each N-GQD consist of 1-5 graphene layers.

2.3.2. Bottom-up methods:- Loh group reported a mechanistic approach for synthesis of a series of atomically defined GQDs by metal catalysed of fullerene. They synthesized different geometrically shaped GQDs such as triangular, parallelogram, hexagonal and trapezoid-shaped on a Ru surface using C_{60} molecules as a starting compound. Although the formation of different shaped GQDs was temperature dependent. They suggested that GQDs are formed through the opening of C_{60} cage on ruthenium surface through the strong interaction between Ru surface-carbon atoms of C_{60}.

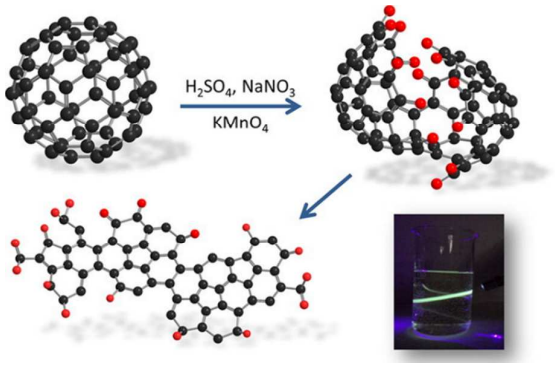

Figure 5. Illustration of the oxidation and cage-opening of fullerene C60 with treatment of strong acid and chemical oxidant. On the right side below luminescence of graphene QDs excited with a blue laser pointer (405 nm). Reproduced with permission from ref [99]. Copyright 2015 American Chemical Society.

The fragmentation of embedded fullerene molecules at elevated temperature then produces carbon cluster and subsequently under GO diffusion and aggregation to form GQDs[100]. Chua et al. also synthesized ultra-small graphene quantum dots by cage opening of Buckminster fullerene. For synthesis fullerene and sodium nitrate were stirred with sulfuric acid. Then the mixture was cooled to $0^{O}C$ temperature after that potassium permanganate (7.5 g) was added for a period of 2 h. Then the mixture was cooled and treated with H_2O_2 to remove the unreacted potassium permanganate and manganese dioxide followed by neutralization with NaOH. The size of the GQDs are 3-5 nm as depicted in Fig 5[99]. Among other bottom up methods it is the most common approach for synthesis of GQDs. Li and co-worker's synthesized large stable graphene quantum dot by solvothermal method using dendritic arene precursors. Their as prepared GQDs made with graphene moieties containing 168, 132, 170 conjugated carbon atoms[101]. Mullen and his co-workers reported multicolour photoluminescent GQDs with a uniform size of ~60 nm dia and thickness of 2-3 nm using unsubstituted hexa-peri-hexabenzocoronene as the precursor[102]. Zhao and his co-workers a synthesized GQDs with an average diameter of 4.66 ± 1.24 nm by solution chemistry

pyrolysis using L-glutamic acid as a precursor[103]. The quantum yield of the synthesized GQDs as high as 54.5%.

Recently Hu and co-workers prepared strong blue fluorescence emitting GQDs having 14% quantum yield using aspartic acid and NH_4HCO_3 as precursor with the help of microwave mediated pyrolysis technique[104]. One the other hand, Zhu and his team also reported the synthesis of GQDs having 11.7% quantum yield and greenish-yellow luminescence from GO nanosheets but they obtained GQDs by simultaneous cleaving and reduction of GO nanosheets under acidic condition without using any external reducing agent. The diameter of the synthesized GQDs lies between 2-7 nm with an average diameter of 4.5 nm. The topographic height of the GQDs were mostly between 0.5-2 nm with an average height of 1.2 nm suggesting that most of the GQDs are single or bilayered[105].

3. Cytocompatibility assessments of graphene nanomaterials:- Since the revolutionary discovery of graphene, graphene nanomaterials have gained tremendous attention in all the fields of science and technology. Till now different types of graphene nanomaterials have been devolved in terms of their sizes, shapes and surface functionalization which endow them with different physical chemical and biomedical characteristics. So *in vitro* cytocompatibility investigations are very essential in order to develop graphene related biomedical devices/ materials as well as it is very crucial for further in-vivo studies of graphene nanomaterials.

Cytocompatibility of graphene and graphene based nanomaterials with living cells and microorganisms play a crucial role for bio-applications. More specifically the cytocompatibility of graphene nanomaterials significantly depends on their physical and chemical properties (such as hydrophobicity, number of graphene sheets, size) and concentration[106-107]. The hydrophilic and nanosize graphene forms (e.g-GO, GQDs) are found to be less toxic compared to that of hydrophobic and large size graphene. As an example, Cui

and co-workers reported that in presence of GO, human fibroblast cells decreases the viability slightly (less than 20% when exposed for 4 days) at a concentration of less than 10μg/ml, however higher concentration and longer exposure time leads to significant amount of cell death. They found that, GO concentrations more than 50 μg/mL obviously cytotoxic even after only 1 day of exposure (>20%)[108]. The possible explanation of this phenomenon is due to the formation of agglomeration in physiological medium through π-π interactions between the GO layers. As a result, aggregated macroparticles are failed to enter into the cells and entrapped on the cell membrane and leads to disruption of the cytoskeleton, membrane deformation and increase in intercellular stress which consequently leads to cell death. These factors also applicable for other graphene family nanomaterials. So in order to get good and long term stability as well as low cytotoxicity for bioapplications purpose, the graphene nanomaterials should be stable in biological media without formation any aggregation and it is already well established that proper functionalization of graphene nanomaterials can increase its stability in biological media and consequently increased the cytocompatibility. In this concern, Koyakutty and co-workers reported that, cytocompatibility of pristine graphene can be increased significantly when it is subjected to carboxyl functionalization[109]. They discovered that, 24 h exposure by the carboxyl functionalized graphene at a concentration of 300 μg/ml did not significantly affect the viability of vero cells. In another work they studied the cytocompatibility and immune response of both pristine graphene and functionalized graphene[110]. They observed that the macrophage cells (RAW 264.7) uptake much higher amount of functionalized hydrophilic graphene to compared with hydrophobic pristine graphene, which was mainly retain at cell surface and induce ROS mediated apoptosis above the 50 μg/ml concentration. Whereas functionalized graphene showed better cytocompatibility with no stress effect up to 75 μg/ml concentration. However despite the cytocompatibility improvement of graphene through hydrophilic functionalization, the

reactive oxygen species (ROS) production in mammalian cells by all forms of graphene nanomaterials is a major drawback in biological application. Therefore care should be taken seriously when using graphene materials for biomedical applications[111-112]. It is also found that the synthesis methods of graphene effect on the hydrophilicity of graphene and consequently its cytotoxic effects. For example, graphene synthesized by CVD increased apoptosis, level of lactate dehydrogenase and generate ROS in neural cells[113].

Graphene nanomaterials, especially hydrophilic forms of graphene (e.g-GO) can strongly promote cell adhesion. More specifically, a number of studies have been done where graphene and its derivatives act as a substrate for various types of cells including stem cells[114]. Hong and co-workers showed the formation of neuron cells instead of glial cells through differentiation of human neural stem cell by laminin coated graphene without using any biological cues [114] as shown in Fig 6 where enhanced neural differentiation observed in presence of graphene films.

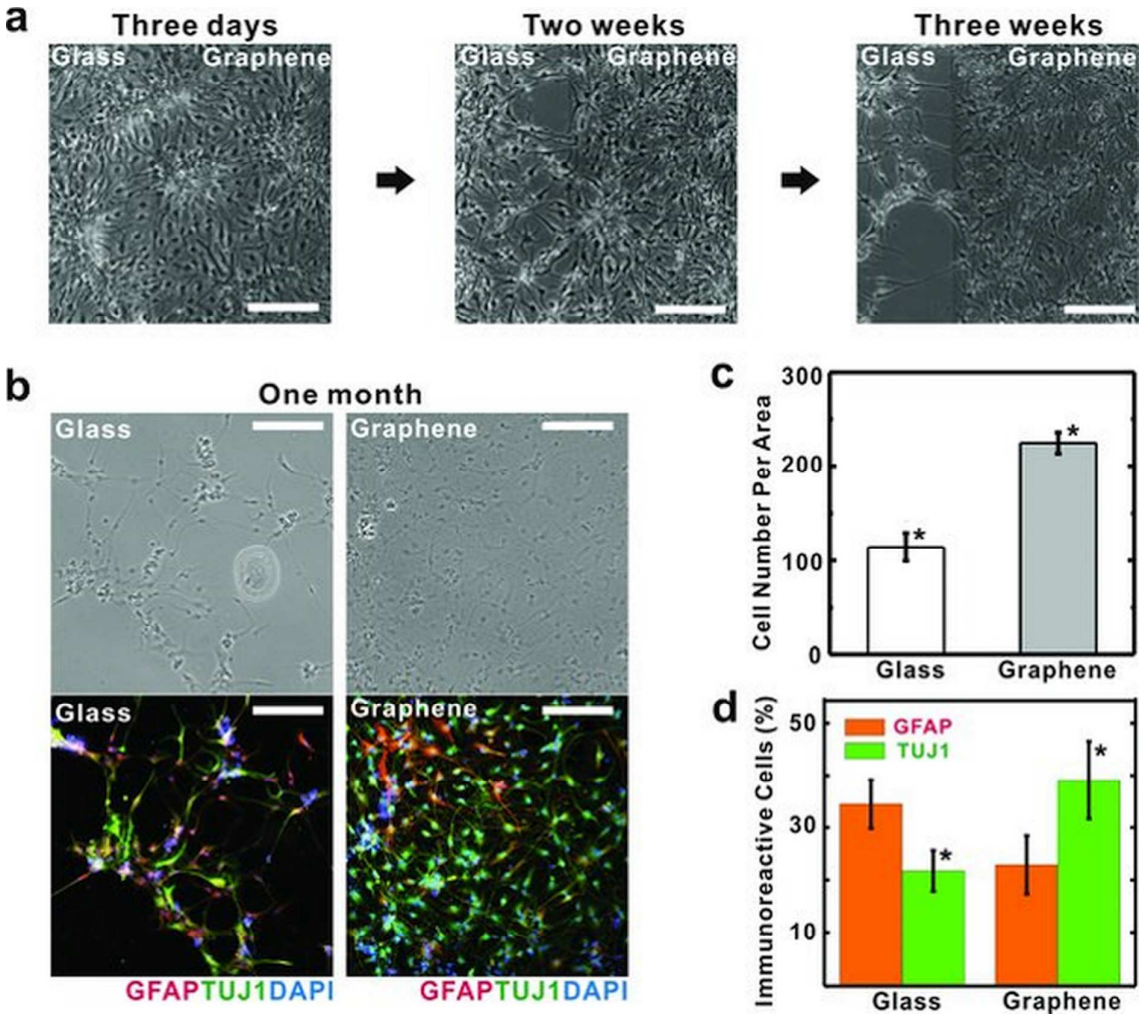

Figure 6. Enhanced neural-differentiation of hNSCs on graphene films. All scale bars represent 200 μm(a) Bright-fi eld images of the hNSCs differentiated for three days (left), two weeks (middle), and three weeks (right). Note that the hNSCs on glass were gradually retracted and detached after two weeks, while those on graphene remained stable even after three weeks of differentiation. b) Bright-field (top row) and fluorescence (bottom row) images of hNSCs differentiated on glass (left) and graphene (right) after one month differentiation. The differentiated hNSCs were immunostained with GFAP (red) for astroglial cells, TUJ1 (green) for neural cells, and DAPI (blue) for nuclei. Note that more hNSCs were adhered to graphene than to glass. c) Cell counting per area (0.64 mm2) on graphene and glass regions after one-month differentiation. Note that much more cells were observed on

graphene in comparison to the glass regions (n = 5, p < 0.001). d) Percentage of immunoreactive cells for GFAP (red) and TUJ1 (green) on glass and graphene. Note that glass regions show more GFAP-positive cells (glia) than TUJ1-positive ones (neurons), while graphene regions have more TUJ1-positive ones (neurons) than GFAP-positive ones (glia) (n = 5, p < 0.05). Reproduced with permission from ref [114]. Copyright 2011 Wiley.

Chen et al. also exhibited the differentiation of induced pluripotent stem (iPSC) cells in presence of graphene and graphene oxide. They found similar behaviour of iPSC towards glass substrate and graphene with respect to cell adhesion and differentiation whereas GO showed better adhesion and differentiation compared to that of bare graphene[115]. Beside hydrophobicity, physical dimensions of the graphene based nanomaterials especially size and number of graphitic layers also play a crucial role to determine their cytocompatibility. The correlation of cytocompatibility with size was further observed by Haynes and co-workers. They synthesized different size of graphene and graphene oxide followed by observation their biological effects on human erythrocytes and skin fibroblasts[111]. They found the hemolytic activity of human erythrocyte cells by both graphene and GO in a dose-dependent manner. Interestingly, it was found that smaller sized GO sheets showed very high hemolytic activity compared to that of large sized GO sheets. When compared between graphene and graphene oxide sheets, GO sheets are dispersed much better than due to its functional groups, whereas graphene tend to aggregate and showed much lower amount of haemolytic activity. In a recent study by Chen and co-workers, they demonstrated that the cell capture capability of the functionalized graphene oxide nanosheets can be enhanced by 54 to 92% through oxygen clustering[116]. More specifically, their system is highly sensitive towards Class II MHC-positive cells from murine whole blood at room temperature, which is almost double the efficiency offered by other devices made directly using as-synthesized GO. In addition to that, clustering of oxygen during the phase transformation of GO improves substance

adherence properties which ultimately results in enhanced stem cell differentiation[117]. Size is another crucial factor which determine the cytotoxicity of nanomaterials. In this context, Yue et al. demonstrated that the role of the lateral dimension (i.e., 350 nm and 2μm) of GO in terms of cellular responses and cell viability[118]. They examined, the ability to internalize GO in six different cell lines and found that only two phagocytic cell lines are capable to internalize both two types of GO. In comparison with size independent uptake, the intercellular phenomenon and cytokine profiles were significantly affected by lateral dimension, specifically micro size GO induced much stronger inflammation responses than nano sized GO in other words nanosized GO demonstrated more cytocompatibility than microsized GO. Fan and co-workers studied the uptake mechanism and cytocompatibility of GQDs on human neural stem cells (hNSCs)[119]. From their result they concluded that the GQDs were internalized in to the hNSCs through endocytosis pathway although the cellular uptake was concentration and time dependent. Additionally they found no significant change in the cell viability, differentiation, metabolic activity and proliferation of hNSCs after treatment with GQDs.

4. Biocompatibility of graphene nanomaterials *in vivo*:- In order to access the full potential of graphene based nanomaterials for biomedical applications, it is necessary to know its biocompatibility *in vivo*. At present, very few number of studies have been highlighted on the *in vivo* biocompatibility by graphene nanomaterials. Similar to cytocompatibility, *in vivo* biocompatibity of graphene nanomaterials also depends upon physicochemical properties (e.g. includes size, surface functionalization), concentration biodegradation and another very important parameter which does not present in case of *in vitro*, that is route of administration.

Girish et al. addressed for the first time the crucial issue of biodegradability of pristine graphene by help of confocal Raman imaging, which is very important criteria for any invivo biological applications of graphene[120]. Their study revealed that, time-bound spectral

alterations such as increase in I_D/I_G ratio, formation of defective D′ band and widening of D and G bands of graphene, embedded in different organs such as liver, kidney over a time of 8-90 days. This is due to increase of structural disorders in graphene phagocytosed by macrophages. In case of spleen bound samples most enhanced amount of disorder was observed which leads to complete amorphization after 3 months of intravenous injection. Their findings suggests that the possible biodegradability of graphene *in vivo* may have greater impact on the practical applications of graphene in the field of biology and medicine. *In vivo* toxicity study of graphene oxide (GO) showed that the intravenous GO administration increased the accumulation of GO largely in lung and liver for longer time although it was dose-dependent[121]. The accumulation may be occurred due to instability and nonspecific binding of GO with different proteins. After injection, the blood flows to the lung initially and hence results more accumulation of GO in lung compared to other body organ. Singh et al. used GO and rGO to analyse the effect on blood platelets[122]. They reported for the first time atomically thin GO sheets caused strong aggregatory responses in platelets through activation of family of Src kinases and subsequent release of calcium from intercellular compartments. Furthermore, they noticed that intravenous administration of GO in mice induced extensive pulmonary thromboembolism. This behaviour was linked with the charge distribution on the surface of GO as the aggregation properties were significantly decreased when it is converted to rGO.

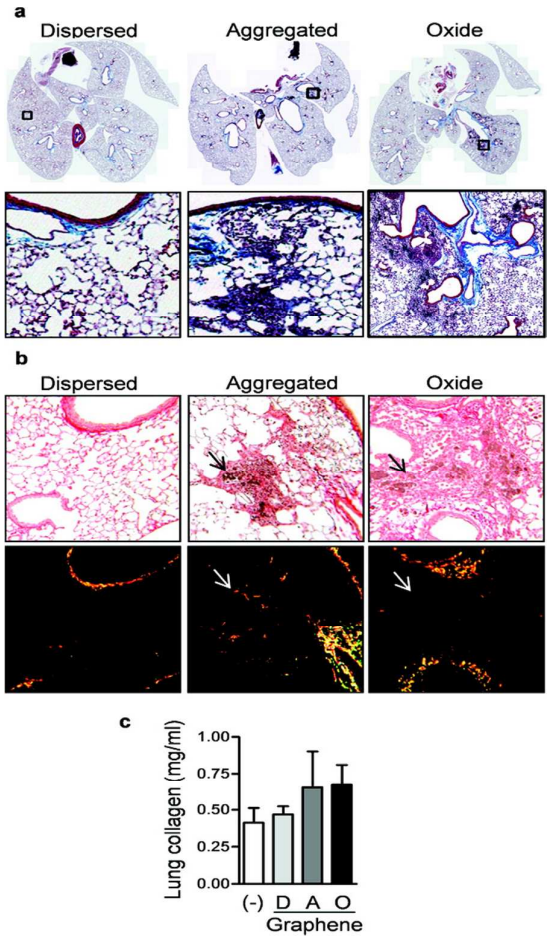

Figure 7. Aggregated graphene induces patchy fibrosis in mice. Mice were treated with highly purified and dispersed preparations of graphene in 2% Pluronic F 108NF (Dispersed), aggregates of graphene in water (Aggregated) or GO in water (Oxide) by intratracheal instillation and 21 days later, the lungs were examined for markers of fibrosis. (a) Trichrome stained lung sections. (b) Sirius Red stained lung sections (bottom panels are photomicrographs obtained using a polarizing filter). (c) Total lung collagen determined by picrosirius red precipitation of whole lung homogenates (GD; dispersed graphene, GA; aggregated graphene, GO; graphene oxide). Representative images from four or more animals per group are shown, N= 8 for picrosirius red precipitation, differences between groups are not significant. Reproduced with permission from ref[123]. Copyright 2011 American Chemical Society.

Toxicity of graphene and graphene oxide can be reduced significantly in case of pristine graphene after liquid phase exfoliation and further decreased when the unoxidized graphene is well-dispersed with the block copolymer Pluronic as shown in Fig 7. Mutlu and co-workers demonstrated that covalent oxidation of graphene play a major role to its pulmonary toxicity and they suggested that dispersion of pristine graphene in Pluronic provides a pathway for the safe handling and potential biomedical applications of graphene nanomaterials[123]. Another *in vivo* biocompatibility study of GO was done by Zhang et al. where they observed compared with other carbon nanomaterials, GO showed long blood circulation time (half-time 5.3 ± 1.2 h), and very little uptake by reticuloendothelial system[124]. Also no pathological changes were observed in major organs when mice were exposed to 1 mg/kg body weight of GO for 14 days. In addition to this, GO exhibited good biocompatibility with red blood cells. Difference in oxidation states of GO also play a crucial role to in-vivo biocompatibility. In this context, Langer and co-workers evaluated the biocompatibility of GO with two different oxidation states followed by implantation in subcutaneous and intraperitoneal tissue sites[125]. They suggested that GO is moderately biocompatible *in vivo* in both tissue sites, with the inflammatory reaction in feedback to implantation consistent with a typical foreign body reaction. Notably reduction in the degree of oxidation resulted in easier immune cell infiltration, uptake and clearance following the both tissues implantation. Furthermore, the toxicity of graphene nanomaterials can be reduced effectively through functionalization of GO by nontoxic biomolecules and or varying the size of GO during the synthesis steps. Additionally, degree of oxidation also play an important role to determine the toxicity of GO. In this concern, Liu and co-workers showed that, *in vivo* toxicity of GO can be modulated through chemical modification[126]. For example, PEGylation of GO reduces toxic effect in mice. In another study they observed the effect of long term biodistribution of ^{125}I labelled nanographene sheets functionalized with polyethylene glycol and systematically examined

the toxicity over time. They found that, PEGylated NGS mainly accumulate in the reticuloendothelial system including liver and spleen after intravenous injection and gradually released by both renal and fecal excretion. PEGylated NGS do not cause any significant toxicity at a dose of 20 mg/kg to the treated mice in a period of 3 months as verified by haematological analysis, blood biochemistry and histological experiment. Researchers also explored the mechanism of stress induced toxicity of graphene oxide, modified with PEGylated poly-L-lysine on C. elegans as an *in vivo* model[127]. Based on their result they proposed multiple mechanistic pathways for the toxicity. When the nematode treated with a concentration range of between 5-20 μg/ml no changes were observed in means of longevity, impairment of locomotion, cell wall damage and reproducibility but polymer factionalized GO significantly affect the resistance of nematode. More specifically under oxidative or heat stress conditions and leading to death. The excessive amount of ROS generation diminished the inherent antioxidant defence system, thus provoking dramatic toxic effect on C. elegans under pathophysiological condition. In conclusion, the toxicity of graphene based nanomaterials in *in vivo* is mainly dependent on the size, dose, exposure duration as well as numbers of graphene sheets. More significantly the surface properties of graphene based nanomaterials such as functionalization/chemical structure play an important role to determine its toxicity; as well as size, shapes, synthesis method, biodegradation and route of administration also play a very crucial role to determine biocompatibility of graphene nanomaterials.

5. Biomedical applications of graphene nanomaterials:-

5.1. Biosensor:- Due to unique properties of graphene family nanomaterials, they are extensively used as biosensors. Recently, a numerous number of electrochemical, fluorescence and field effect transistor biosensor have been developed based on the graphene nanomaterials by various research groups as discussed below.

5.1.1. Electrochemical biosensor:- In the last few decade, high specificity and sensitivity of graphene material make it tremendous attractive compound as electrochemical biosensors among other biosensors. The specificity of electrochemical biosensor lies on the fact that different molecules oxidize or reduce at different potential window. In case of graphene based electrochemical biosensor, electron transfer for oxidation or reduction processes occurs between the graphene and analyte molecules and this heterogeneous electron transfer process happens at the edges and corners of the graphene or at the defect sites of basal plane[128]. The large surface area of graphene provides enormous number of corners edges and defects which can act as superior electroactive sites[129]. Graphene has been extensively used for glucose sensors because presently diabetes has become world-wide public health threat. For glucose sensing, Glucose Oxidase (GOx) enzyme (acts as an oxidizing agent) is used as a bio-recognition element where it oxidizes glucose to gluconic acid and transfer electrons to oxygen which is dissolved in the solution and then converts into hydrogen peroxide which can easily be detected by electrochemically. However there are several examples where direct electron transfer can take place from enzyme without need of O_2 as an electron acceptor[130]. Generally ultrathin multilayer graphene nanosheets have been employed as a transducing material for the biosensing of glucose[131]. There are several reported examples where direct electron transfer occurs from glucose oxidase. GO has also been used for the recognition of glucose. Its biocompatibility with GOx led to formation of a stable glucose sensor with a sensitivity of 8.045 mA cm^{-2} M^{-1} [132]. In another work, Niu and his co-workers discovered a novel glucose biosensor based on direct electron transfer process in graphene/ionic liquid/glucose oxidase system[133]. Their system showed a linear response upto 14 mM. Incorporation of CdS nanocrystal with graphene system provide very low detection limit of 0.7 mM with a linear response between 2 to 16 mM[134]. Razmi and his co-workers made a simple low cost electrochemical glucose biosensor based on GOx-GQD|Carbon Ceramic

Electrode (CCE)[135]. To fabricate the biosensor at first they simply coated the GQDs on carbon ceramic electrode by drop casting method. Then the GQD modified carbon ceramic electrode (CCE) was activated and coated with GOx to form the sensor. Their electrochemical biosensor responds efficiently between 5-1270 µM glucose concentrations with the detection limit of 1.73 µM and sensitivity of 0.085 $mAcm^{-2}M^{-1}$. Excellent performance of the biosensor attributed to large surface to volume ratio, excellent biocompatibility of GQDs, porosity of the GQD|CCE, abundance of the hydrophilic edges as well as hydrophobic surface in GQD which enhances the enzyme absorption on the electrode surface.

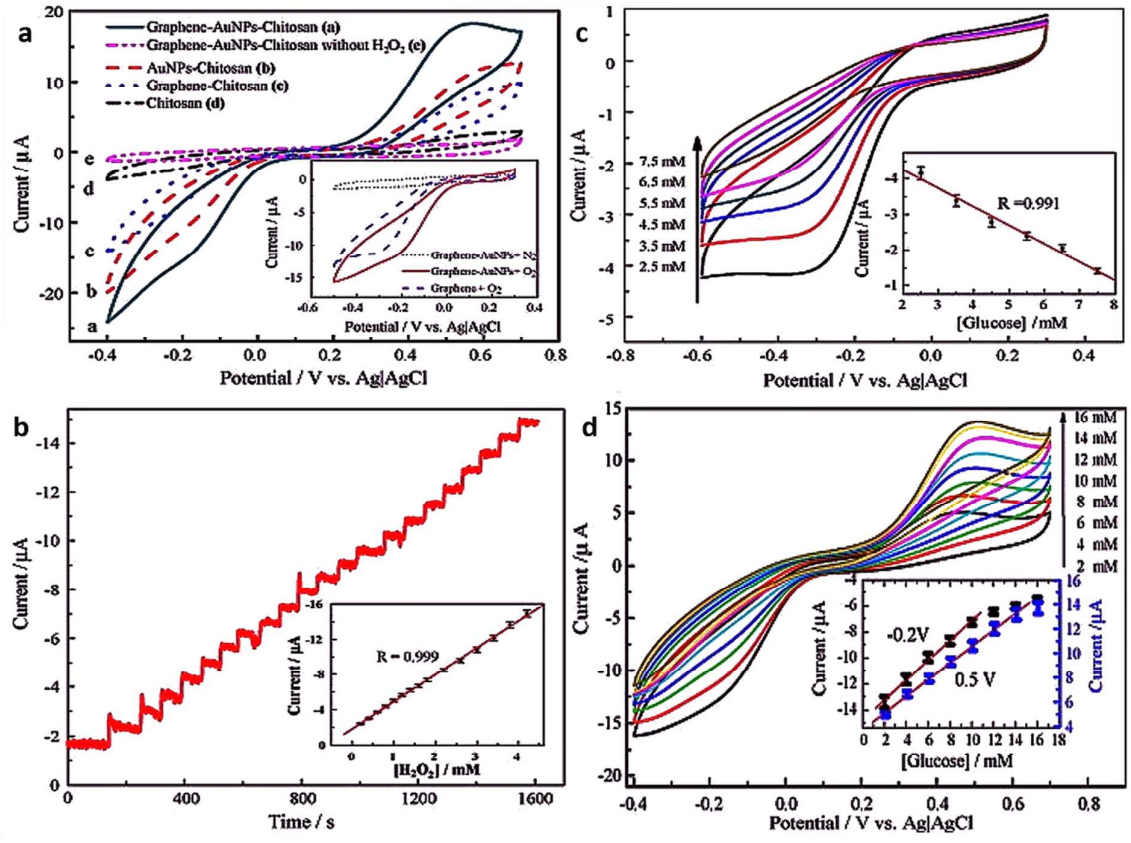

Figure 8. (a) Cyclic voltammograms of different components with graphene and without graphene (b) Chronoamperometric response of graphene/AuNPs/chitosan-modified electrode in N_2-saturated phosphate buffer on injecting the concentration of H_2O_2 in 0.2 mM steps at

working potential of -0.2 V. The inset is amperometric response to H_2O_2 concentration. Error bars = ±standard deviation (c) Cyclic voltammograms at graphene/AuNPs/GOD/chitosan-modified electrode in real blood sample and PBS mixing solutions containing 2.5, 3.5, 4.5, 5.5, 6.5 and 7.5 mM glucose from down to up. Inset is the calibration curve corresponding to amperometric responses. Scan rate: 0.05 V s-1. Error bar = ±standard deviation (d) Cyclic voltammetric measurements at graphene/AuNPs/chitosan-modified electrode in O_2-saturated phosphate buffer containing various concentrations of glucose: 2, 4, 6, 8, 10, 12, 14 and 16 mM from down to up. The inset is the calibration curves corresponding to amperometric responses at -0.2 and 0.5 V. Scan rate: 0.05 V s^{-1}. Error bars= ±standard deviation. Reproduced with permission from ref[136]. Copyright 2010 Elsevier.

There are also some other enzymatic detection methods which have been reported based on graphene/Gold nanoparticles(AuNPs)/chitosan composite[136]. As depicted in Fig 8, the modified graphene/AuNP/chitosan showed electrode good cyclic voltammograms response, chronoamperometric response and amperometric response with good linearity. Not only glucose biosensor there are several other biologically important molecules/macromolecules such as nicotinamide adenine dinucleotide (NADH), DNA, haemoglobin, cholesterol, catechol, hydrogen peroxide, ascorbic acid, uric acid, dopamine etc. which can also be measured by graphene based electrochemical biosensor. A brief details about these sensors have been described below.

NADH is a very essential coenzyme that participate in more than 300 types of dehydrogenase enzymatic reactions[137]. Electro-catalytic oxidation of NADH has been studied as part of the development of dehydrogenase based biodevices. However its electrooxidation at bare glassy carbon (GC) electrodes in neutral solutions occurs at a high over potential (ca. 0.5 V) because of electrode fouling and slow electron transfer kinetics[138]. So the effective oxidation of NADH at low potentials would lead to the path of development of NADH-based biosensors.

Li and his co-workers studied the electrochemical behaviour of NADH on reduced graphene sheet films. They showed increased electron transfer kinetics and excellent electro-catalytic activity compared with normal GC electrodes. They observed that the oxidation of NADH occurs on bare GC electrode at 0.75 V and the required voltage becomes significantly low to the 0.42V using the reduced graphene sheet films/glassy carbon (rGSF/GC) electrode[139]. Zhang and his group also prepared a NADH biosensor based on non-covalent functionalized graphene with water soluble electro-active methylene green (MG)[137]. The oxidation of NADH at bare GC electrode occurs at +0.55 V. However, the voltage changes to +0.40 V and +0.14 V for chemically reduced graphene (CRG) and CRG functionalized with MG electrodes, respectively. Shan et al. reported low potential electrochemical detection of NADH as well as ethanol with the help of the ionic liquid-functionalized graphene (IL-graphene) modified electrode. The IL-CS–GR modified electrode displayed good linearity from 0.25 to 2 mM and a high sensitivity of 37.43 $\mu AmM^{-1}cm^{-2}$ [140].

For the treatment of genetic diseases especially at its initial stage, it is very important to recognize the mismatched DNA base pairs as it is an important parameter for the diagnosis of these diseases. Recently, electrochemical sensors have gained enormous attention to the researchers because of its potential to recognize the defected DNA specifically with elevated signal to noise ratio[141]. Recognition of DNA is possible directly through oxidative signals of DNA bases or by using electro-active labels[142]. Direct detection of DNA is a simple and label free, but its sensitivity is very poor than label free DNA assays. In addition to that conventional carbon materials, such as glassy carbon and graphite give analytically useful signals with adenine (A) and guanine (G) bases while provide poor signals with cytosine (C) and thymine (T). It is reported by Zhou et al. that the chemically reduced graphene oxide provide far better electrochemical activity than glassy carbon and graphite for all four A, G, C, T bases[143]. In a similar type of work Loh and his team exhibited direct voltammetric

detection of DNA on an epitaxial graphene. In fact they discovered that an anodized epitaxial graphene voltammetric sensor can simultaneously detect all four DNA bases in double stranded DNA (dsDNA) without any pre-hydrolysis steps and it can also differentiate single stranded DNA (ssDNA) from dsDNA. Their result revealed that graphene with high edge plane defects leads to a significantly higher response than pristine graphene[144]. So it was suggested that electrochemically oxidized graphene or graphene with large amounts of defects could be an efficient platform for highly sensitive electrochemical sensing. Pumera and his group also proved that large number of defects on graphene surface, beneficial for the electrochemical detection of DNA using stacked graphene platelet nanofibers[145]. Just like graphene, GQDs also possess excellent conductivity due to its excellent graphitic like structure. Based on this property, Li et al. fabricated a simple but efficient electrochemical platform to detect specific sequence of ssDNA by using GQD-modified electrode. The ssDNA inhibited electron transfer between electrochemically active species Ferricyanide/Ferrocyanide ($[Fe(CN)_6]^{3-/4-}$) and the electrode after the probe molecules were strongly adhered to the surface of the modified electrode via their interaction with GQDs. The obtained signal currents of $[Fe(CN)_6]^{3-/4-}$ increased significantly with the target molecules thus various electrochemical sensor can be developed based on this model platform[146].

Haemoglobin (Hb) is the most significant part of blood as it is the carrier of O_2 throughout the circulatory system in animal body. Change of Hb concentration in blood can cause several major diseases and even death. Therefore, precise determination of Hb content in human blood is medically very essential. In 2010 Chen and his co-workers used a chitosan(CS)-graphene(GR) composite electrode for the electro-analysis of Hb[147]. The cyclic voltammogram of Hb at the CS–GR/GC electrode exhibited a well-resolved redox peak compared with a bare CS/GC electrode. The current response of Hb at the GR modified

CS/GC electrode amplified linearly with scan rate from 30 to 150 mVs^{-1} signifying a well surface-controlled electrochemical process. Wang et al. reported an ionic liquid-modified graphene electrochemical sensor for the detection of Bovine haemoglobin (BHb)[148]. They optimized the conditions for the detection of BHb successfully at very low detection value of 3.09×10^{-11} g/L and a wide range from 1.0×10^{-10} to 1.0×10^{-3} g/L (R=0.998). In another work, Luo and his team used novel graphene-molecular imprinted polymers composite (GR-MIP) as recognition element for selective and sensitive detection of BHb[149]. They revealed that under optimized experimental conditions the electrochemical sensor can detect BHb in a concentration range of 1.0×10^{-9} mg mL^{-1} to 1.0×10^{-1} mg mL^{-1} with detection limit of 2.0×10^{-10} mg mL^{-1}.

Accurate determination of H_2O_2 is very important in the field of chemistry, biology, clinical control and for environmental safety[150]. Electrochemical methods are more precise and convenient for this than other conventional methods[138]. Zeng et al. reported Sodium Dodecyl Benzene Sulphonate (SDBS)-GR/Horse Radish Peroxidase(HRP) modified electrode for the recognition of H_2O_2[151]. The biosensor exhibited high electro-catalytic activity to H_2O_2 with high sensitivity, selectivity, low detection limit, wide linear and fast response. The reaction mechanism of the catalytic process is summarized below.

$$\text{HRP(Red)} + H_2O_2 \rightarrow \text{HRP(Ox)} + H_2O$$

$$\text{HRP(Ox)} + \text{Hydroquinone} \rightarrow \text{HRP(Red)} + \text{Benzoquinone}$$

$$\text{Benzoquinone} + 2e^- + 2H^+ \rightarrow \text{Hydroquinone}$$

Zhu and his co-workers synthesized a novel H_2O_2 biosensor based on Au-graphene-HRP chitosan composites which remained stable after 30 measurement without significant loss of sensitivity[150]. The range of detection was 5×10^{-6} to 5.13×10^{-3} M, with a detection limit of 1.7×10^{-6} M (S/N = 3). Ganesh and co-workers in another work developed a HRP

immobilized GQD based platform for the detection of H_2O_2[152]. Their electrochemical sensor showed an excellent selectivity values of 0.905 and 7.057 μA/mM with detection limit of 530 nM and 2.16 μM along with a fast response time of 2-3 s.

Cholesterol and its ester are very crucial constituents of all animal body. Increased level of cholesterol in human body can cause life threatening coronary heart diseases artherosclerosis and cerebral thrombosis as shown in Fig 9. Therefore pinpoint accurate detection of cholesterol level is clinically very important[153].

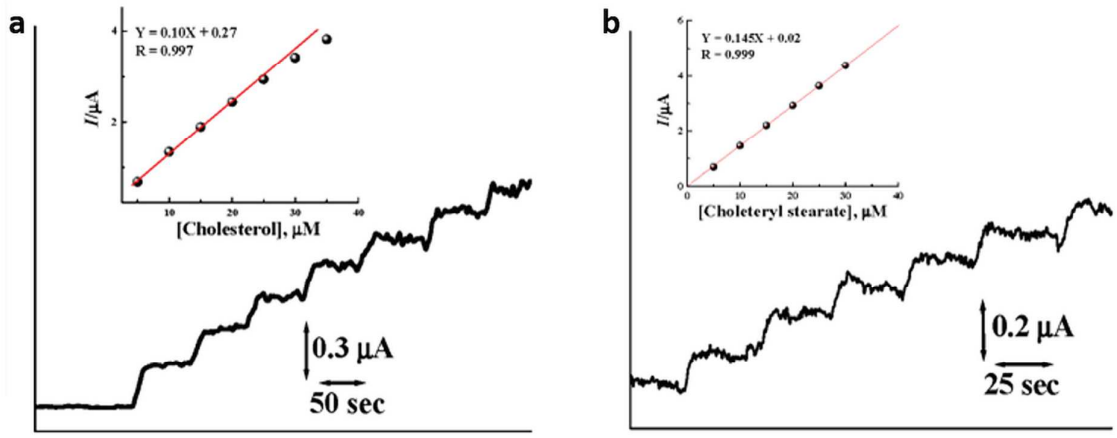

Figure 9. Amperometric response of the cholesterol with the GNS-nPt electrode (a) and cholesterol ester (b) biosensors. An aliquot of H_2O_2 was injected into the stirred supporting electrolyte (PBS, pH 7.2) as indicated by the arrow. The potential of the electrode was held at 400 mV. Reproduced with permission from ref[153]. Copyright 2010 American Chemical Society.

Raj and his co-workers developed a highly sensitive amperometric biosensor based on a hybrid material derived from nanoscale Pt (nPt) and graphene for the recognition of H_2O_2 and cholesterol. The biosensing platform was developed by immobilizing cholesterol oxidase and cholesterol esterase on the surface of the GR/nPt hybrid material. In case of H2O2 the detection limit is 0.5nM with a linear range upto 12mM [Fig10]. The detection limit and

sensitivity of the electrode towards cholesterol ester were 0.2μM and 2.07 ± 0.1μA/μM/cm^2, respectively[153]. In another work Chailapakul and his group developed a novel paper based cholesterol biosensor using graphene/polyvinylpyrrolidone/polyaniline nanocomposite. Under optimum conditions their biosensor can detect up to 1μM cholesterol with a liner range from 50 μM to 10 mM[154].

Uric acid (UA) one of the major end product of purine metabolism in body fluids such as blood serum and urine participants in many vital biological process. High concentration of UA in human body can cause many diseases like renal failure, Lesch-Nyhan Syndrome, gout and so on[155]. So it is very important to measure the UA acid concentration in terms of clinical disease diagnosis. Wang and his group made an electrode based on manganese (III) porphyrin- graphene oxide composite materials which is capable to detect UA with high sensitivity and stability. The sensor showed a linear response between 0.5-500μM and can detect up to 0.30μM[156]. Liang et al. reported an ultrasensitive uric acid sensor constructed by gold micro cluster/sulfonate functionalized graphene modified GC electrode having minimum detection value of 0.12 μM and a range from 0.2μM to 50μM[157].

Not only biologically important molecule, even, with proper modifications of graphene, it can detect cancer cells. In this regard, Qu and his co-workers developed a label free electrochemical aptasensor for detection of cancer cells based on functionalized graphene[158] through conjugation of AS1411 aptamer due to its specific target towards nucleolion as it is overexpressed on cancer cell surface. The aptasensor sensed specifically the cancer cells compared to normal cell using very low number of cells. In another work Qu group reported a graphene based peptide electrochemical sensor for early stage diagnosis of cyclin-A2 in cancer cells[159]. Castillo-Leon and co-workers also made a peptide nanotube-folic acid modified graphene electrode for selective detection of cancer cells[160]. They found the limit of detection is 250 HeLa cells per mL with an incubation time of only 10 min.

Apart from these, graphene has also been used for electrochemical immunosensing. Generally it is not possible to detect antibody-antigen direct electrochemically for this cause electrochemically active labels must be used. Mainly there are two strategies in which graphene can be used for immunosensing. In the first case, graphene can be used as an electrode surface for selective and sensitive detection of electroactive labels[161]. This strategy was applied for the graphene-enhanced recognition of α-fetoprotein, which is a cancer biomarker. Graphene sheets were modified by functionalized carbon nanospheres labelled with horseradish peroxidase-secondary antibodies[161]. In the second strategy, graphene was used as a label bearing nanocarrier[162]. Using this second strategy Lin and co-workers developed an ultrasensitive immunosensor which can detect phosphorylated protein p53. In details, they used functionalized GO linked with HRP and $p53^{392}$ signal antibody ($p53^{392}Ab_2$) at a high ratio of HRP/ $p53^{392}Ab_2$. After a sandwitch type immunoraction the HRP-$p53^{392}Ab_2$-GO captured onto the electrode surface and produced amplified electrocatalytic response due to the reduction of enzymatically oxidized thiamine in presence of H_2O_2which is far better than other traditional sandwich type electrochemical sensor[162].

5.1.2. Fluorescence biosensor:- Fluorescence spectroscopy provide us a very sensitive platform for biomolecular detection. Graphene can be employed in various ways as a substrate in fluorescence detection systems. For an example, the fluorescence quenching principle was employed for the aptamer based detection of thrombin[163]. Zhang et al. reported a graphene based fluorogenic biosensor which can detect sugar ligands and glycoprotein on cancer cells[164]. Vaish and his group developed a label free estriol biosensor based on graphene oxide[165]. Estriol is one of the estrogens, which has been considered medically important. Presence of estriol in urine or plasma is not only used to determine the pregnancy but also used as an important diagnostic marker for various diseases including, insulin resistance, osteoporosis and even breast cancer. The sensor can detect up to 1.3nM

concentration of estriol under physiological condition. Here GO act as a fluorescence quencher and quenched efficiently estriol through fluorescence resonance energy transfer (FRET) mechanism. Fan and his group used graphene oxide as a platform for multicolour fluorescent sensing of DNA[166] [Fig 10]. Because of the extraordinarily high quenching efficacy of GO, the fluorescent ssDNA probe exhibits negligible background fluorescence, while strong emission is noticed when it forms a double helix with the specific targets, leading to a high signal-to-background ratio. More importantly due to large surface area of GO, it allows simultaneous quenching of multiple DNA probes labelled with different dye which leads to detection of multiple DNA targets in the same solution. Liu and his group developed a fluorogenic glucose biosensor platform depending upon FRET from up-converting nanocrystal to graphene oxide[167]. The sensor showed a linear response between 0.56-2 μM with a detection limit of 0.025 μM. From the series of graphene nanomaterials, GQDs are most often used as a fluorescent sensor due to its excellent photoluminescent properties.

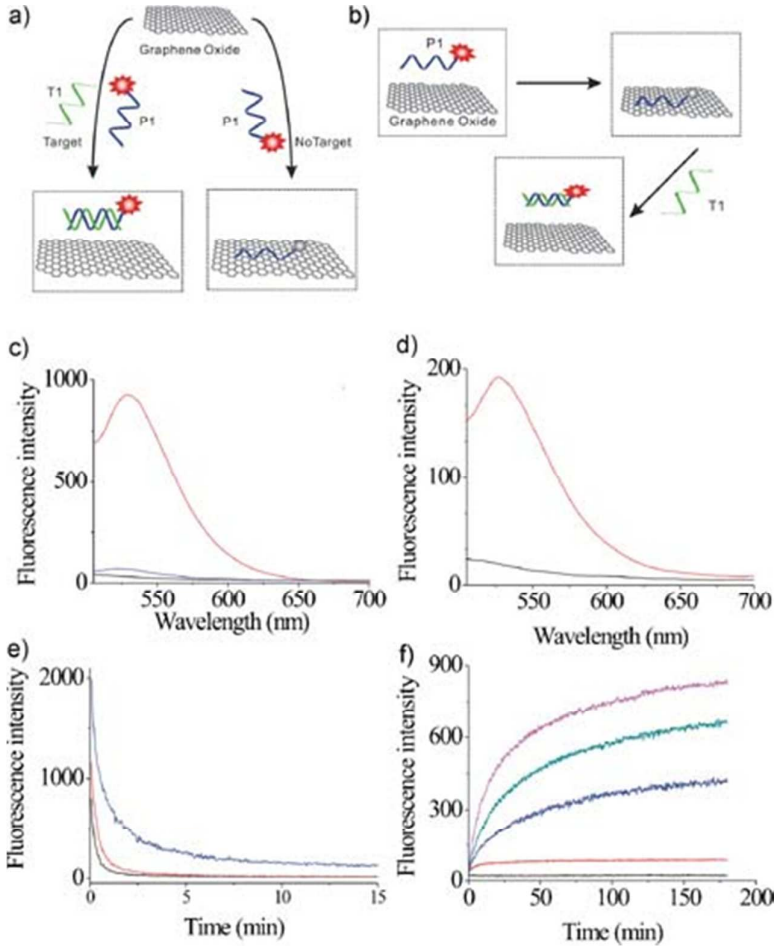

Figure 10. (a) Scheme for the fluorescent DNA detection based on the ssDNA/dsDNA discrimination ability of GO. (b) Scheme for the target hybridization-induced probe liberation from GO. (c) GO-based fluorescence DNA assay. Fluorescence spectra of P1 in the absence (black) and presence of the complementary target T1 of 50 nM (red), and random sequence R1 of 50 nM (blue). (d) Fluorescence spectra for P1 in the presence of GO before (black) and after (red) incubation with T1.(e) Kinetic study for the fluorescence change of the FAM-tagged probes (20 nM) with different lengths in the presence of GO: 17 base pairs (bp; black); 34 bp (red); 51 bp (blue). (f) Kinetic study for the fluorescence change of the GO-bound P1 in the presence of T1 of various amounts (10, 20, 30, 40, 50 pmol). The excitation and the emission wavelengths are 494 and 526 nm, respectively. Reproduced with permission from ref[166]. Copyright 2010 Willey.

Similar to Fan and co-workers, Lu et al. also demonstrated that, GO based system can be a very efficient platform for sensitive and selective detection of DNA and proteins[168]. In case of their system, the sensing mechanism relies on the interaction between GO and dye□ labelled single□stranded DNA which leads to quenching of the dye fluorescence. When a target DNA binds with the dye labelled DNA, the labelled DNA detached from GO surface and consequently restores the dyes fluorescence which confirms the DNA quantification. Yang and co-workers designed NGO with molecular bacon (MB) which can specifically detect surviving transcript, which has received significant attention due to its use in cancer diagnosis[169]. In details, they observed that NGO can absorb MB and quenched the background fluorescence of MB while in presence of target DNA fluorescence intensity increased significantly. The result suggested that, the target DNA efficiently bind with MB on NGO surface and subsequently release of MB from NGO. Zhang et al. reported graphene quantum dot based a universal fluorescence biosensor for detection of microRNAs (mRNAs)[170]. The sensing mechanism relies upon the excellent fluorescence performance of GQDs, and instinct base pairing specificity of molecular bacon probes and exclusive FRET from GQD to fluorescent dyes labelled on pyrine-molecular bacon probes to realize qualitative and quantitative detection of miRNAs. The biosensor platform exhibited excellent selectivity, good stability and a wide detection range from 0.1 nM to 200 nM with a detection limit of 100 pM. Pang's group fabricated a highly selective and sensitive aptasensor for detection of Mucin1 (MUC1) which is a well-known tumour biomarker[171]. In their work, graphene oxide quenched the fluorescence intensity of single stranded fluorescently labelled MUC1 specifically, while the quenched fluorescence is restored significantly upon the addition of MUC1. Their aptamer sensor can sense a wide range from 0.04 to 10 mM of MUC1 having lowest detection concentration of 28 nM. On the other hand, Seo and his team made a graphene oxide based immune-biosensor array for pathogen sensing, where a

rotavirus-specific primary antibody was chemically conjugated through amide linkage with graphene oxide[172]. After capturing the rotavirus, the detection of pathogen was carried out using fluorescence resonance energy transfer (FRET) between graphene oxide sheets and gold nanoparticles. Here graphene oxide act as energy donor. Their pathogen sensor with high specificity, sensitivity (1000 pfu ml) and very rapid detection time serve as a promising alternative probe to the conventional time consuming laborious pathogen detection methods. Ran et al. reported a novel quick method for the detection of Ag^{+} ion and biological thiols such as cysteine, homocysteine and glutathione selectively with the help of GQDs decorated by Ag nanoparticles[173]. Their GQD based sensing platform can detect up to 3.5 nM concentration of Ag^{+} ions, 6.2 nM of cysteine, 4.5 nM of homocysteine and 4.1nM of glutathione. The detection of biological thiols is very important because they play a major role in biological processes and are also responsible for causing many diseases like cancer, AIDS, cardiovascular diseases etc. In another study, Wang and his group produced a fluorescent blood glucose sensing system based on hemin functionalized graphene quantum dots[174]. The noncovalent interaction between hemin and GQDs made H_2O_2 to destroy GQDs passivated surface and consequently quenched the fluorescence intensity of GQDs. Under the optimized conditions, it can detect up to 0.1 μM glucose with a range of detection from 9-300 μM. Qiu group developed a simple but very efficient photoluminescent GQDs based platform for protein kinase sensing[175]. They used aggregation behaviour of phosphorylated peptide−GQD conjugates in presence of Zr^{4+} ion. The sensing mechanism relies on the fact that when substrate peptide was phosphorylated by CK2, the introduced Zr^{4+} ion serve as a linkage between the phosphorylated sites of phosphopeptides *via* the multicoordinative interactions between Zr^{4+} and phosphate groups. Which results in extensive aggregation of the GQDs and effective PL quenching, thus the activity of protein kinase could be facilely monitored with detection limit of 0.03 unit/mL. Qiu group also developed a boron doped

graphene quantum dot (BGQD) (structure as shown in Fig 11a) for the detection of glucose selectively with high sensitivity using the abnormal aggregation induced photoluminescence enhancement property of BGQD[176]. The sensing mechanism relies on the formation of a rigid five membered ring BGQDs−glucose aggregates through the reaction between cis-diol units of glucose and two boronic acid groups of BGQDs surfaces, and thus resulting in a great boost in the PL intensity as shown schematically in Fig 11a. The sensor demonstrated a relatively wider linear range (0.05− 10 mM) with detection limit of 0.01 mM at pH 10 phosphate buffer.

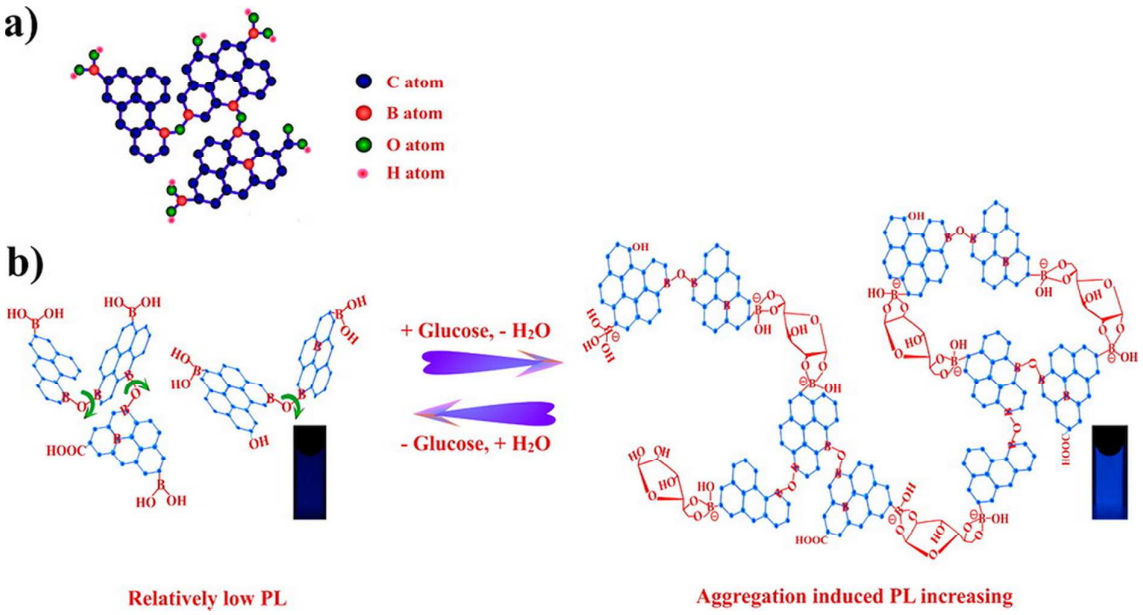

Figure 11. (a) Schematic Representation of the Boron-Doped Graphene Quantum Dots (BGQDs). (b) Proposed "Aggregation-Induced PL Increasing" Mechanism for the Glucose-Specific Sensing by BGQDs. Reproduced with permission from ref[176]. Copyright 2014 American Chemical Society.

A universal immunosensing platform was demonstrated by Zhao and his group depending upon the interaction between graphene and functionalized graphene quantum dots[177]. The sensing mechanism relies upon the fact, when graphene was added to the mouse anti-human

immunoglobulin G –conjugated-GQDs (mIgG-GQDs) solution, both the π-π stacking interaction between graphene and GQDs and the nonspecific binding interaction between mIgG and the graphene surface brought graphene and GQDs into LRET (luminescence resonance energy transfer) proximity to facilitate the PL quenching of GQDs. The addition of human IgG would bind the mIgG due to the specific antibody-antigen interaction, which successively increased the distance between mIgG-GQDs and graphene interface, thus hampering the LRET process and then producing a restoration of PL. Qian et al. constructed a DNA nanosensor based on GQDs and carbon nanotubes[178]. Due to the FRET process between GQDs-labelled probe and oxidized carbon nanotubes is simply achieved by self-assembly through π–π interaction. The nanosensor can discriminate complementary and mismatched DNA sequences with high sensitivity and good reproducibility with an ultralow detection limit of 0.4 nM. From the above discussion we can say that, due to the efficient acceptor characteristics in FRET process by graphene, GO, RGO enormously used in biosensor fabrication, as well as due to excellent photoluminescent characteristics of GQDs, it is also extensively used to develop fluorescence biosensor.

5.1.3. Bio-field effect transistor:- Recently field effect transistors (FET) have received a great attention in the field of biosensing as they can offer fully automated electronic detection that is completely integrated with the electronic chips produced by semiconductor companies. So, it is not only academia that is fascinated by these devices, but there is a growing interest (and investment) from industry as well[128]. FET based biosensors relies upon bioconjugation phenomenon between analyte molecules at the gate of the FET[179]. Upon bioconjugation between the probe and analyte biomolecules, the electric charge distribution alters the charge carrier density at the bioconjugation layer and the conductivity of the channel between the source and drain[128] which ultimately leads to sensing signals. Graphene is an ideal material for the fabrication of FET biosensors due to its semiconductor nature with zero band gap

although the band gap can be tuned according to requirement by surface modification[180]. As discussed above FET transistor is ideal for the detection of charged molecules, so graphene based FETs can be perfect for DNA sensing due to its charged phosphate backbone[181]. Li and co-workers showed CVD grown graphene sheets can be used for DNA hybridization[182]. The change in gate voltage was enough for the detection even at very low concentration of 10 nM of single stranded DNA (ssDNA). To increase the sensitivity of the probe, they decorated gold nanoparticles on the graphene surface which led to linear increase in the response to 500 nM. Their results suggests that the high sensitivity as well as linear response of the FET sensor due to the complementary DNA which is present in FET sensor. In another work Stine et al. developed a FET biosensor based on rGO modified with DNA for real time detection of ssDNA with 10nM detection limit[183].

It is quite possible that by modifying graphene sheets with metal nanoparticles to increase the number of probe biomolecules at the FET gate. It is advantageous in terms of the linearity of the response. Such an approach is not only used for DNA detection but also used for immunosensing. Chen and co-workers designed a FET biosensor which can detect specific protein[184]. They used thermally reduce GO sheets decorated with AuNP-antibody (anti-immunoglobulin G) conjugates to construct the sensor. This functions act as a specific recognition site for the detection of immunoglobulin G (IgG). When a bioconjugation event occurs, a substantial changes occur in the electrical characteristics of the FET, which are used as an analytical signal. Ohno group constructed a label free biosensor based on aptamer-modified graphene FET[185]. The analyte protein is immunoglobulin-E (IgE) which is an antibody subclass found in mammals. Although the amount of IgE in human serum is normally very less (several nM), it significantly increases in individual with atopic dermatitis, allergic asthma, and other immune deficiency diseases. The mechanism is that when IgE proteins are attached with aptamer-modified graphene surface, there is a significant alteration

in electrical characteristics of the FET. Their fabricated sensor specifically detect IgE protein whereas other proteins are not detected. Pak and his co-workers developed a silk fibroin-encapsulated graphene FET enzymatic biosensor that utilizes silk protein as both device substrate and enzyme immobilization material for glucose sensing[186]. Their fabricated biosensor showed a wide linear range of glucose detection from 0.1-10 mM which covers the reference range of medical examinations of diabetes diagnostics. So from the above discussion it can say that graphene nanomaterials can be effectively employed for the fabrication of FET biosensor. **Table 2** summarises the graphene based materials for biosensing application.

Table 2. List of various types biosensors based on graphene nanomaterials

Sensing element	Sensor type	Sensor platform	Limit of Detection (μM)	Linear range (mM)	References
Glucose	Electrochemical	GOx/AgNPs/PAMAM/rGO/GCE	4.5	0.03-1.89	[187]
Glucose	Electrochemical	GOx/AuNCs/HS-graphene SH/Au	100	0.3-0.8	[188]
Glucose	Electrochemical	Cu_2O NCs/rGO/GCE	20.8	0.3-3	[189]
Glucose	Electrochemical	Cu_2O-PtNCs/rGO/GCE	0.01	0.0005-12	[190]
Glucose	Electrochemical	Ionic liquid doped screen-printed electrode (IL-SPE)/ER-GO/GOx-BSA mixture/GA	1	0.05-12	[191]
Glucose	Electrochemical	GCE/graphene/GOx	10±2	0.0001-10	[192]
Glucose	Electrochemical	GCE/ER-GO-MWCNT)/GOx	4.7	0.01-6.5	[193]
Glucose	Electrochemical	GCE/ERGO/Gold-palladium bimetallic nanoparticles (AuPdNPs) /GOx	6.9	0.0069-3.5	[194]
Glucose	Electrochemical	GCE/Gaphene-CdS nanocomposite/GOx	700	2-16	[134]
Glucose	Electrochemical	GCE/poly(1-vinyl-3-	267	0.8-20	[195]

		butylimidazolium bromide)-Graphene (poly(ViBulm+Br-)-Gr)/ GOx			
Glucose	Electrochemical	GCE/[amine terminated ionic liquid (IL-NH2)-sulfonic acid (SO_3^-) functionalized graphene (S-RGO)]/ GOx/Nafion	3.33	0.01-0.5	[196]
Glucose	Electrochemical	GCE/Graphene-(3-Aminopropyl) triethoxysilane (APTES)/ GOx/Nafion	-	1.4-27.9	[197]
Glucose	Electrochemical	GCE/Graphene/AuNPs/GOx/Nafion	1	0.001-30	[198]
Glucose	Electrochemical	GCE/CS-ferrocene/GO/GOx nanocomposite	7.6	0.02-6.7	[199]
Glucose	Electrochemical	GCE/CS functionalized graphene platelet-GOx (GP-GOx)	20	2-22	[200]
Glucose	Electrochemical	GCE/functional SiO2-coated GO/ AgNP/GOx	310	2-12	[201]
Glucose	Electrochemical	GCE/rGO-titanium dioxide nanocluster (TDN)/GOx/CS	4.8	0.032-1.6	[202]
Glucose	Electrochemical	GCE/NiO composites/Graphene	1	0.005-2.8	[203]
Glucose	Electrochemical	GCE/nickel nanoparticles/Graphene	1.85	0.005-0.55	[204]
Glucose	Photoelectrochemical	ITO/Gaphene-Cd QDs	7	0.1-4	[205]
Glucose	Electrochemical	CuO-Graphene	1	0.001-8	[206]
Glucose	Electrochemical	CuNPs/graphene	0.5	0.005-4.5	[207]
Glucose	Electrochemical	Polypyrrole/Graphene/GOx	3±0.5	0.002-0.04	[208]
NADH	Electrochemical	rGO/GC	0.33	0.01-0.6	[209]
NADH	Electrochemical	Graphene-Au nanorod	1.5	0.005-0.337	[210]
NADH	Electrochemical	Au-TiO_2/graphene	0.2	0.01-0.24	[211]
NADH	Photoelectrochemical	Graphene-TiO_2 nanohybrids	0.003	0.00001-2	[212]
NADH	Electrochemical	AuNPs-rGO	0.00113	0.00005-0.5	[213]
NADH	Electrochemical	ADH/IL-graphene/chitosan-modified electrode	5	0.25-2	[140]
NADH	Electrochemical	rGO-AuNPs-PAH-screen printed electrode	3.5	0.01-0.2 0.2-5	[214]
NADH	Electrochemical	PLM–PNR–MWCNT–GO	0.0133	0.0000133-0.195 0.208-0.581	[215]

NADH	Electrochemical	DMF exfoliated graphene	1.9	0.05-0.36	[216]
DNA	Electrochemical	GCE-Graphene/cDNA1/tDNA/Au-cDNA2	0.000072	0.0002-0.5	[217]
DNA	Electrochemical	Chitosan-Graphene/AuNPs/CILE	$3.33*10^{-8}$	$1*10^{-10}$-$1*10^{-3}$	[218]
DNA	Electrochemical	Polyaniline/Graphene	$1*10^{-8}$	$1*10^{-10}$-$1*10^{-3}$	[219]
DNA	Electrochemical	3D-N-doped Graphene/Fe_3O_4 nanoparticles	$3.63*10^{-9}$	$1*10^{-8}$-1	[220]
DNA	Electrochemical	Graphene/Polyaniline nanowire	$3.25*10^{-7}$	$2.12*10^{-9}$-$2.12*10^{-3}$	[221]
DNA	Electrochemical	GCE/Graphene/cDNA|tDNA|rDNA.AuNPs	$1*10^{-9}$	-	[222]
Hemoglobin	Electrochemical	MIPs/IL Graphene/GCE	3.09×10^{-11} g/L	1.0×10^{-10} - 1.0×10^{-3} g/L	[223]
Hemoglobin	Electrochemical	Graphene- -molecular imprinted polymers	2.0×10^{-13} g/L	1.0×10^{-12} - 1.0×10^{-4} g/L	[149]
H_2O_2	Electrochemical	Cyt c/GO-MWCNT/Au NP	27.7×10^{-6}	1.0×10^{-8} - 1.4×10^{-7}	[224]
H_2O_2	Electrochemical	rGO-MWCNT-Pt/Myoglobin	6×10^{-6}	1.0×10^{-8} - 1.9×10^{-7}	[225]
H_2O_2	Electrochemical	rGO-carboxymethyl cellulose/Hb	0.08	0.000083-0.01394	[226]
H_2O_2	Electrochemical	Hb/Au/GR-CS	0.35	0.002-0.935	[227]
H_2O_2	Electrochemical	rGO-PMS@AuNPs	0.06	0.0005-50	[228]
H_2O_2	Electrochemical	Graphene/MnO_2	0.8	0.005-0.6	[229]
H_2O_2	Electrochemical	HRP-functionalized graphene-Ag	5	0.025-19.35	[230]
H_2O_2	Electrochemical	HRP/CeO_2-rGO	0.021	0.0001-0.5	[231]
H_2O_2	Electrochemical	HRP-MoS_2-Graphene	0.049	0.0002-1.103	[232]
H_2O_2	Electrochemical	Au-PEI/GO	0.2	0.0005-1.68	[233]
H_2O_2	Electrochemical	AuNPs-N-GQDs	0.12	0.00025-13.327	[234]
H_2O_2	Electrochemical	Cu_2O/N doped graphene/Nafion modified GCE	0.8	0.005-3.5	[235]
H_2O_2	Electrochemical	rGO-Cu_2O nanocomposite	0.37	0.001-1.47	[236]

H_2O_2	Electrochemical	rGO/Ag-Pd/GCE	1.1	0.005- 14.65	[237]
Cholesterol	Electrochemical	Graphene/polyvinylpyrrolidone/ polyaniline nanocomposite	1	0.05-10	[154]
Cholesterol	Electrochemical	Graphene-CHOD-CHER-PtNPs	0.2	0.005-0.035	[153]
Uric Acid	Electrochemical	N-doped Graphene	0.045	0.0001-0.02	[238]
Uric Acid	Electrochemical	Nafion-AgNPs-rGO	8.2	0.01-0.8	[239]
Uric Acid	Electrochemical	Pt-rGO	0.45	0.01-0.13	[240]
Uric Acid	Electrochemical	Graphene modified carbon fiber electrode	0.132	0.000194-0.04968	[241]
Cancer cells	Electrochemical	Functionalized graphene aptasensor	794 cells/ml	$1*10^3$-$1*10^6$ cells/mL	[158]
Cancer cells	Electrochemical	Graphene-peptide nanotube-folic acid	250 cells/ml	-	[160]
Thrombin	Fluorescence	Aptamer labelled graphene	0.0000313	$6.25*10^{-8}$ - $1.875*10^{-7}$	[163]
Glycoprotein receptor	Fluorescence	N□acetyl glycosaminyl rhodamine coupled GO	534 cells/ml	50000 -300000 cells/ml	[164]
Estriol	Fluorescence	GO	0.0013	0.0013-0.01	[165]
DNA	Fluorescence	GO-Fluorophore tagged probe	0.00001	-	[166]
Glucose	Fluorescence	GO–CS–ConA–UCP	0.025	0.00056-0.002	[167]
miRNAs	Fluorescence	GQDs- Py-MBs	0.000	$1*10^{-7}$ - $2*10^{-4}$	[242]
Mucin 1 (MUC 1)	Fluorescence	GO-MUC 1 specific aptamer	0.028	0.00004-0.01	[171]
Glucose	Fluorescence	Hemin functionalized-GQDs	0.1	0.009-0.3	[174]
Protein Kinase	Fluorescence	Phosphorylated peptide–graphene quantum dot (GQD)-Zr^{4+}	0.03 unit mL^{-1}	0.1 - 1.0 unit mL^{-1}	[175]
Glucose	Fluorescence	Boron doped GQDs	10	0.05-10	[176]
Immunoglobulin-G	Fluorescence	Graphene-mIgG-GQDs	10 ng/ml	0.2 -12 µg/ml	[177]
DNA	Fluorescence	GQDs-cDNA-CNTs	0.0004	0.0000015-0.000133	[178]
Carcinoembryonic antigen	FET	Graphene-Anti CEA	100pg/ml	-	[243]
DNA	FET	Single crystal graphene domain-PBASE-Probe DNA	0.000001	$2.5*10^{-7}$ - $1*10^{-5}$	[244]
Glucose	FET	Graphite oxide- Cu/AgNPs	1	0.001-30	[245]

Urea	FET	rGO-PEI-Urease	1	0.001-1	[246]

GOx-Glucose Oxidase, AgNPs- Silver Nanoparticles, PAMAM- Polyamidoamine, AuNCs- Gold nanocubes, NCs-Nanocubes, PtNCs-Platinum Nanocubes, PPy-Polypyrrole, AgNPs-Silver Nanoparticles, QDs-Quantum Dots, ADH-Alcohol Dehydrogenase, IL Graphene-Ionic liquid Functionalized Graphene, PAH-Poly(allylamine hydrochloride), PLM- poly(luminol), PNR- poly(neutral red), GCE- Glassy Carbon Electrode, cDNA-captured probe, rDNA- receptor probe, tDNA- target DNA, CILE-Carbon ionic liquid electrode, MIP-Molecular imprinted polymer, MWCNT- Multiwalled carbon nanotube, PMS-Mesoporous silica, HRP-Horseradish peroxidase, CHER- Cholesterol esterase, CHOD-Cholesterol oxidase, SPE-Screen printed electrode, CS-Chitosan, ConA-Concanavalin A, UCP-Up Converting Phosphor, Py-MBs-Pyrene Functionalized Molecular Bacons, mIgG- Mouse anti-human immunoglobulin G, CNTs-Carbon Nanotubes, CEA- Carcinoembryonic antigen, PBASE-1-pyrenebutanoic acid succinimidyl ester, PEI-Polyethylenimine

5.2. Tissue engineering:- Tissue engineering is an emerging field of research that involves the expertise from medicine to biology, from chemistry to engineering for the development of artificial tissue construct which may solve the shortage of organ damaged through various diseases or accidents globally[247-249]. Biomaterials can act as a mimic of extracellular matrix (ECM) for cellular support followed by proliferation and differentiation, cellular functions, and modulate cell–cell interactions[250-251]. Owing to the different mechanical, physical, electrical, and biological properties of the tissues presented in our body, the extraordinary mechanical, electrical and physical properties of graphene based nanomaterials have inspired many researchers to use them in the field of tissue regeneration[252]. The applications of graphene nanomaterials in the field of tissue engineering have been discussed briefly in next section.

5.2.1. Cardiac tissue engineering and regeneration:- Over the last few decades, myocardial infarction or coronary artery diseases cause the major death globally. The blockage in coronary arteries results the less blood supply is myocardium and simultaneously arise various heart functional problems, which is also known as cardiac ischemia. In case of

cardiac ischemia, the patient feels severe chest pain due to release of toxin from the cardiomyocyte cells death through either by necrosis or apoptosis processes. Since the regeneration of cardiac tissues are limited, the damage or injury is almost permanent[253]. Cardiac tissue possesses exceptional mechanical properties and systematized contractile properties due to its properly arranged anisotropicity as well as its electrical conductivity having 0.005 S/m and 0.1 S/m in transverse and longitudinal direction, respectively. The presence of aligned collagen nanofibers with a diameter in between 10-100 nm results the high mechanical properties of the myocardium [254-255]. It is already reported that stem cells can be applicable for the regeneration of injured myocardium in presence of micro-environmental signals. Previous report showed that graphene and graphene family nanomaterials can regulate the differentiation lineage of stem cells *in vivo* through morphological signals and electrical conductivity due to the presence of conjugated pyrene ring in graphene structure[256]. In a latest study done by Kim and co-workers, where they showed that, graphene can stimulate the cardiomyogenic differentiation of mesenchymal stem cells (MSCs) even in absence of cardiomyogenic differentiation inducers[257]. In presence of GO flakes, the survival rate of MSCs was enhanced drastically as shown in Fig 12 and it may be explained by the fact that GO protected the cells from the generation of reactive oxygen species (ROS) in *in vivo* [258] . Not only that, they also showed that after implantation of MSC- GO, it increased the cardiac repairing process drastically. Ahn and co-workers reported that, incorporation of rGO within the MSCs spheroids enhances cardiac repair into infarcted hearts compared to the injection of rGO flakes or MSC spheroids only[259]. They also proposed that the high conductivity nature of rGO flakes might increase the affinity towards fibronectin and improved cardiac repair in MSCs spheroids. One of the major advantage of such type of composite delivery systems is that, cells and nanoparticles can be precisely placed at the injured tissue site in a more accurate, systematic and sustainable manner. In this

concern Khademhosseini group developed a 3D cardiac tissue mimics through layer by layer assembly technique using cells and functionalized graphene [260]. The GO sheets serve as an adhesive layer which facilitates the formation of multi array with interlayer connectivity. In another study Khademhosseini and his co-workers synthesized a highly elastic hydrogel using GO and methacryloyl-substituted recombinant human tropoelastin (MeTro)[261]. The synergistic effect of these two materials significantly increased ultimate strain, reversible rotation and the fracture energy. In addition to that, developed composite material carry electrical current which can be effectively used for cardiac tissue engineering.

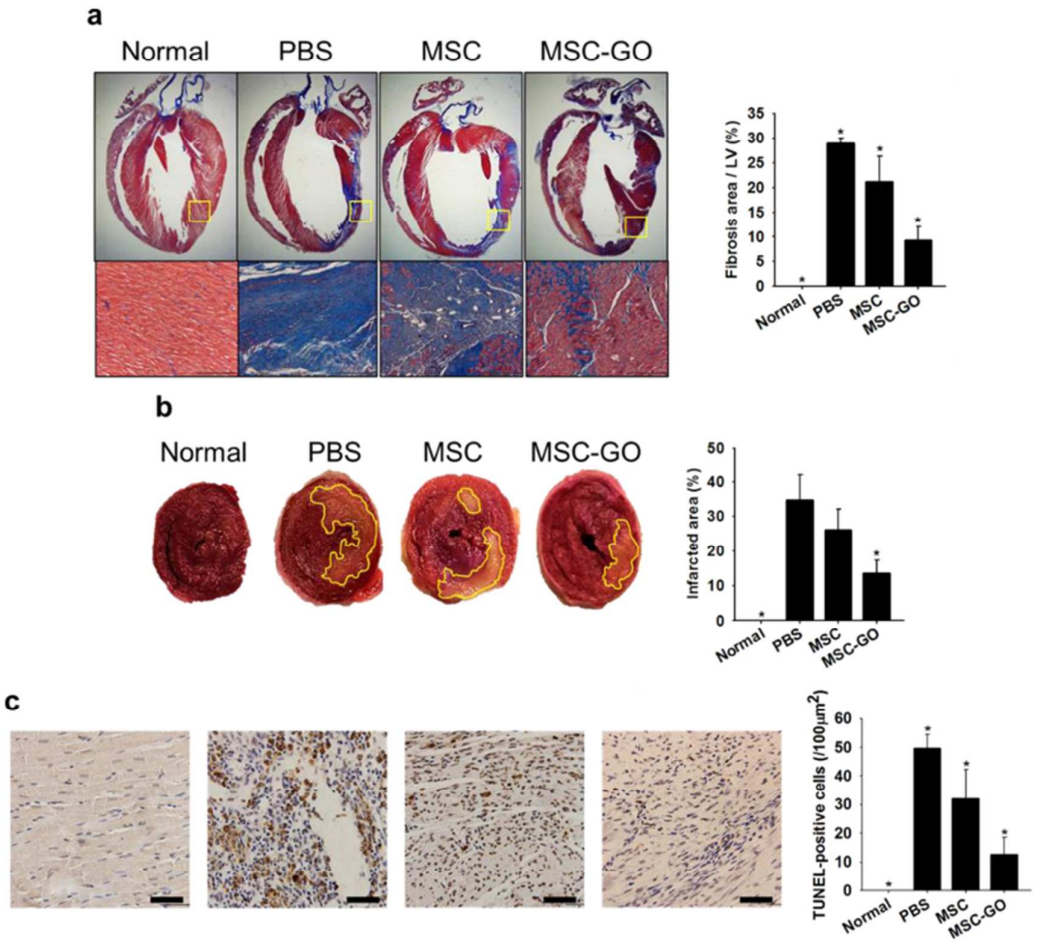

Figure 12. Enhanced cardiac repair by MSC-GO implantation (14 days after implantation). (a) Fibrosis evaluated based on a histological analysis with Masson's trichrome staining. Blue indicates fibrosis. (b) Infarcted area evaluated based on the TTC staining of heart sections. The infarcted area is marked with a yellow line. (c) Tissue apoptosis in the infarcted zone as evaluated by TUNEL staining (brown). Scale bars, 50 μm. *p < 0.05 compared to any group. Reproduced with permission from ref[258]. Copyright 2015 American Chemical Society.

In summary, we can say that graphene based nanomaterials can hold great promise for cardiac tissue engineering application due to its unique properties. Most of the polymeric hydrogels which are used in cardiac tissue engineering applications, their mechanical properties are much weaker than desired value but incorporation of graphene nanomaterials (except GQDs) in those hydrogels may increase both mechanical properties as well as surface functionality by various ways. Furthermore the cell signalling property of hydrogel is increased due to the presence of electrical conductivity of graphene nanomaterials and consequently enhance the signal propagation which are very essential in cardiac tissue regeneration. Therefore, graphene nanomaterials are quite appropriate for cardiac tissue engineering applications but the biodegradation and biocompatibility needs to be improved in near future.

5.2.2. Bone tissue engineering and regeneration:- Graphene nanomaterials have been widely used without or in a composite material as bone implants or scaffolds to enhance the propagation rate of bone tissue repair and regeneration as it enhance the cellular adherence, proliferation, and osteoblast differentiation[262]. It is already well established that graphene-based materials can differentiate of human mesenchymal stem cells (hMSCs) into osteogenic lineage even in absence of any external osteogenic stimuli such as[262] insulin-like growth factor 1 (IGF-1)[263]. It is observed that the presence of graphene enhance the osteogenic differentiation through increase the local concentration of dexamethasone via π- π interaction

between the basal plane of graphene and the aromatic rings that are present in biomolecules[264].

The scaffold containing graphene or its derivatives can increase osteoconductivity through inherent π conjugation and resulted cellular osteogenic differentiation followed by biomineralization for bone regeneration. But, the presence of calcium carbonate known as biominerals synergistically enhance the biomineralizatio in conjugation with graphene and GO sheets[265]. In a recent study done by Zou and co-workers synthesized a self-supporting graphene hydrogel (SGH) film with excellent cell adhesion, spreading and proliferation[266]. In addition to that when it was implanted in a rat, the SGH film exhibited minimal fibrous capsule formation, a mild host tissue response and no obvious toxicity was observed indicating the biocompatibility and nontoxicity of the film. Rosa and his team reported high elastic modulus of graphene based materials can be a driving force for spontaneous osteoblastic differentiation[267]. Lee and his co-workers showed when rGO was combined with hydroxyapatite (HAP) it enhanced osteogenic differentiation of MC3T3-E1 cells[268] . Surface functionalization of GO with different compounds such as carrageenan, can also accelerate the nucleation of hydroxyapatite and results the enhancement of biomineralization[269]. Previous study showed that carrageenan functionalized GO (GO-Car) not only increased the cell adhesion and proliferation of MC3T3- E1 cells but also improved osteogenic differentiation. *In vitro* studies clearly showed that GO-Car composite effectively enhanced HAP mineralization. Xie et al. reported a simple method to synthesize free standing graphene/hydroxyapatite hydrogel based on colloidal synthesis method with unexpected homogeneity in their 3D structure[270]. The hydrogel showed excellent mechanical properties, high electrical conductivity, high specific surface area, and good cell compatibility. In another study Han group showed that the reduced graphene oxide-coated hydroxyapatite composites can stimulate spontaneous osteogenic differentiation of hMSCs which was

confirmed by alkaline phosphatase activity and osteoblastic differentiation markers[271]. They suggested that rGO coated-HAP composites can be successfully utilized as a dental and orthopaedic bone fillers. In a recent study, Chatterjee and his co-workers fabricated strontium decorated graphene/polycaprolactone (RGO-Sr/PCL) composite for bone regeneration[272]. They discovered that osteoblast proliferation and differentiation significantly increased in presence of RGO-Sr nanoparticles. The improved bone tissue formation in the scaffolds was due to release of strontium ions in the culture medium from the scaffolds containing the hybrid nanoparticles. In another study, they synthesized PCL/polyethyleneimine functionalized GO (PCL/GO_PEI) composite for bone formation[22]. From *in vitro* studies they confirmed that incorporation of PEI functionalized GO in PCL not only enhanced focal adhesions and proliferation of hMSCs with the composite but also induced osteogenesis and mineralization as shown in Fig 13. This type of cellular response was attributed to the multiple free amine and oxygen containing functional groups presented in PCL/GO_PEI composite along with increased nanosized roughness on the surface. The amine and oxygen containing polar functional groups of the GO_PEI further promotes the adsorption of osteogenic factors for improved differentiation. Liane and co-workers discovered that the incorporation of calcium silicate ($CaSiO_3$) in graphene enhanced the osteoblastic differentiation synergistically compared to that of bare calcium silicate ceramics[273].

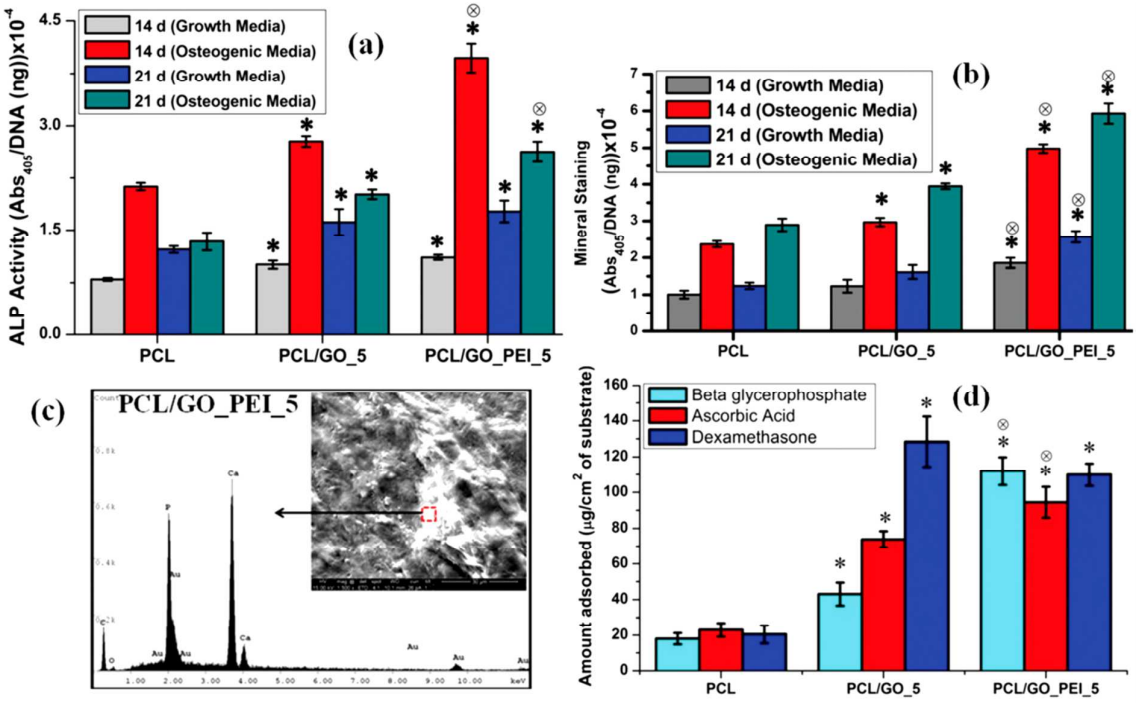

Figure 13. Evaluation of osteogenic differentiation of hMSCs: (a) ALP activity of hMSCs on PCL, PCL/GO_5 and PCL/GO_PEI_5 films in growth and osteogenic supplement media at day 14 and 21; (b) mineral quantification at day 14 and 21 using ARS dye, (c) EDAX spectra with the inset showing SEM micrographs of mineral deposited PCL/GO_PEI_5 and (d) adsorption of osteogenic factors on PCL, PCL/GO_5 and PCL/GO_PEI_5. Statistically significant differences ($p < 0.05$) compared to PCL, PCL/GO_1, PCL/GO_3, PCL/GO_5, PCL/GO_PEI_1 and PCL/GO_PEI_3 are indicated by *, ◆, ●, ⊗, ∅ and Φ respectively. Reproduced with permission from ref[22]. Copyright 2016 Royal Society of Chemistry.

Apart from these, the mechanical properties of biological grade ceramics, glasses, polymeric hydrogels can be improved by incorporation of graphene based nanomaterials without hampering their structures or biocompatibilities[274]. Suhai and co-workers reported on the improvement in mechanical properties of nano-58S bioactive glass through incorporation of graphene for bone repair and regeneration. The optimum compressive strength and fracture toughness reached 48.65 ± 3.19 MPa and 1.94 ± 0.10 MPa·$m^{1/2}$, respectively in presence

of graphene content of only 0.5 wt%[274]. Some other study revealed that, self-supporting graphene hydrogel posses with much higher tensile strength of 69 ± 5 MPa[266] while conventional polymer hydrogels were reported to have very less tensile strength with range between 0.01 to 10 kPa[275]. In addition of GO not only increase the mechanical properties but also enhance the crosslinking density of the scaffold system. In this context, Kolanthai et al. demonstrated that, incorporation of GO in a scaffolds made with alginate, chitosan, collagen enhanced both mechanical strength as well as crosslinking density of the scaffold system which ultimately leads to the improvement of osteoblast cell attachment and proliferation[276]. Therefore, graphene nanomaterials may be a promising nanomaterial in the field of bone tissue engineering.

5.2.3. Cartilage tissue engineering and regeneration:- The main component of human cartilage is extracellular matrix (ECM) having various proteins including glycosaminoglycan (GAG), collagens, proteoglycans, and noncollagenous proteins. It is a resilient elastic tissue and the chondrocytes cells are embedded within the ECM in highly ordered manner[277]. The main role of articular cartilage is not only for frictionless movement with the help of synovial fluid but also to withstand our body weight. Due to avascular and acellular nature of cartilage tissue, it is also unable to regenerate itself once it becomes damage or injure[256]. To overcome this problem, MSC based cellular therapy has gained tremendous attention in hospitals/clinic centre to regenerate cartilage tissues. To introduce the cellular repairing process, graphene nanomaterials have been used as a scaffold material for the stem cell therapy of cartilage tissue regeneration, based on its stimulation effects on cell growth, differentiation, proliferation and outstanding mechanical properties.

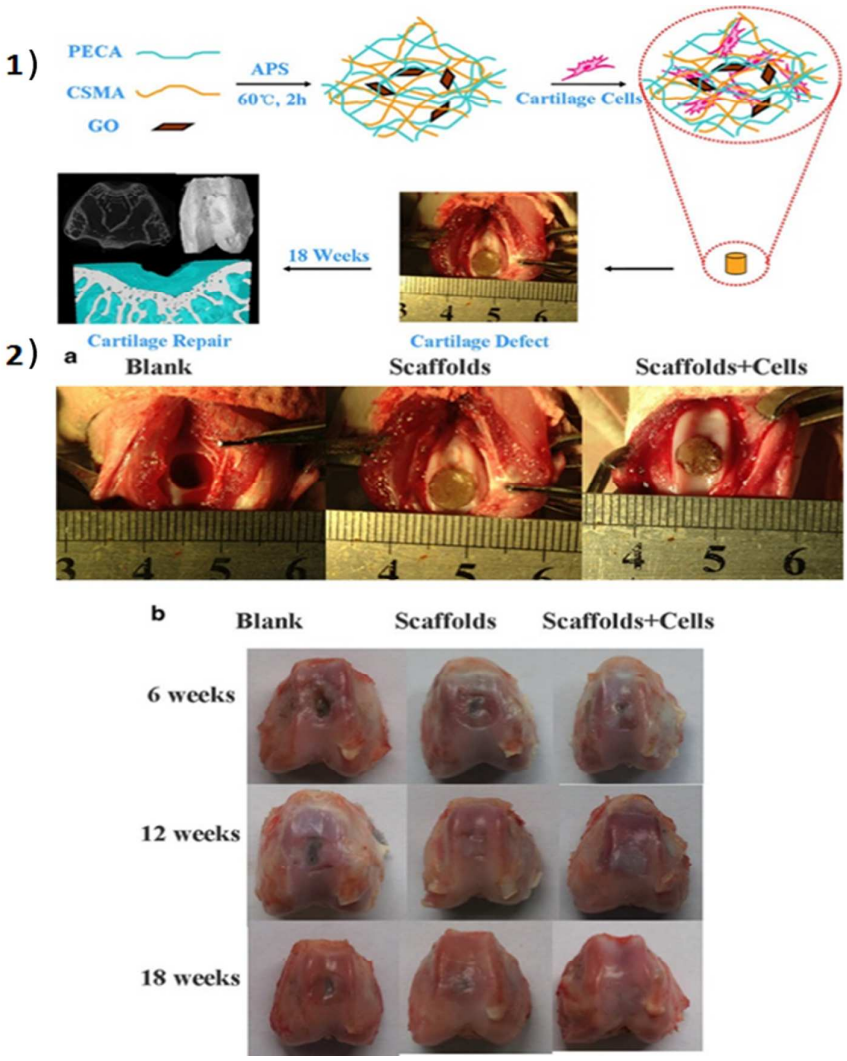

Figure 14. 1) Schematic diagram of hybrid scaffold prepared from CSMA/PECA/GO for cartilage tissue regeneration 2) Photographs of the knee joint in different groups (**a**) at operation and (**b**) post-operation for 6, 12 and 18 weeks. Reproduced with permission from ref[278]. Copyright 2015 Nature.

For cartilage tissue regeneration, graphene was not only used as biocomposites but also showed activity like growth factor and resulted enhanced cell and protein activity toward MSCs[278-279]. In this context, Qian group synthesized a novel GO reinforced 3D porous scaffold by free radical copolymerization of methacrylated chondroitin sulphate (CSMA) and poly(ethylene glycol) methyl ether-ε-caprolactone-acrylate (PECA) in presence of GO

for cartilage tissue regeneration[278]. The obtained pore size, porosity, swelling capability, compression modulus and conductivity of the scaffold were showed perfect mimic to natural extracellular matrix (ECM) of cartilage. After implantation the scaffold in knee defect of rabbit, the cartilage defect was completely repaired after 18 weeks in presence of GO based scaffold compared to without GO scaffold as shown in Fig 14. In another work, Kim and his team showed that graphene oxide can be utilized as both a cell adhesion substrate and a protein such as growth factor delivery system for chondrogenic differentiation of adult stem cells. They utilized GO sheets (0.5-1 μm) to absorb fibronectin (FN, a cell-adhesion protein) and protein transforming growth factor-β3 (TGF-β3) followed by formation of pellets with human adipose-derived stem cells (hASCs) suspension using hanging-drop method. The hybrid pellets of hASC-GO showed elevated chondrogenic differentiation of hASCs compared to only cell pellet[279]. Graphene based materials not only improve mechanical properties but also increase electrical conductivity through its inherent pπ-pπ conjugation. In a recent study, Lee et al. showed that graphene-cell biocomposites can be used as a source of pre-concentrate growth factors for chondrogenic differentiation[280]. They assembled bone marrow derived mesenchymal stem cells (MSCs) with GO solution to form graphene-cell biocomposites. They also found that the increasing concentration of GO significantly accelerated the extent of differentiation. Although beyond a certain concentration of GO, it dropped down the chondrogenesis due to increased diffusional barrier and cytotoxic effects.

5.2.4. Neural tissue engineering and regeneration:- The nervous system is one of the very crucial part in our body which plays one of the most important role in our body as it transmits signals to synchronise between brain and other parts of the body. At cellular level the nervous system is defined by presence of a distinctive type of electrically sensitive cells called neurons. Neurones are act in such a manner that they sustain a certain

voltage difference across their membranes through ion pumps that produce a concentration gradient of ions such as sodium, potassium, chloride, calcium etc[256]. In details, neurons, transfer signals in the form of electrochemical waves travelling along very tinny fibers often called axons, by utilizing different chemical neurotransmitters such as acetylcholine via a specific synapse structure[281]. In this context, the inherent electrical conductivity of graphene as well as its tunable biocompatibility make it an essential carbon material to mimic the complex signalling processes which are related to our nervous system.

Interestingly, embryonic stem cells (ESCs) showed the ability to differentiate into neurons in presence of graphene nanomaterials[282]. In this concern, Le and co-workers made a thorough investigation on the differentiation of mouse ESCs to dopamine neurons in presence of graphene and GO[282]. They observed that ESCs differentiated into neurons, on the GO sheets more than two times faster than that differentiated of graphene. In addition to that, they found that the differentiation of ESCs into dopamine neurons increased in a dose dependent manner of GO. More specifically, the total number of differentiated dopaminergic neurons at the minimum treated concentration of GO (1μg/ml) was improved three times when it was treated with a concentration of GO (100μg/ml).

Hong and co-workers discovered for the first time the fundamental aspects of graphene nanomaterials on the human neural stem cells (hNSCs)[114]. In details, they cultured hNSCs in a medium containing both 2D graphene film and growth factors, where the hNSCs showed enhanced differentiation compared with the control group. The graphene served as an excellent cell-adhesion layer during the long-term differentiation process and induced the differentiation of hNSCs more toward neurons than glial cells. Wang research group studied how surface charge of graphene oxide can affect the neuronal outgrowth and branching[283]. In details they modified graphene oxide by primary amine (-NH_2) or sulfonic acid- (–SO_3H), or methoxyl- (–OCH_3) terminated functional groups. Subsequently they used the resulting

graphene oxide as substrates for culturing for primary rat hippocampal neurons to examine neurite outgrowth and branching. The result demonstrates that positively charged graphene oxide (primary amine terminated) to be more beneficial for neurite outgrowth and branching than neutral (methoxy terminated) and negatively (sulfonic acid terminated) charged graphene oxide. In another work Wang and co-workers showed biomimetic choline-graphene oxide composites can be used for neurite outgrowth and branching[284]. They constructed biomimetic graphene oxide composites by covalently binding an acetylcholine- like unit (dimethylaminoethyl methacrylate, DMAEMA) or phosphorylcholine-like unit (2-methacryloyloxyehtyl phosphorylcholine, MPC) with GO surfaces to enhance neurite outgrowth and branching. The number of neurites and average neurite length on GO-DMAEMA and GO-MPC composites were significantly improved compared to GO itself as shown in Fig 15. In addition to that, analysis of growth-associate protein-43(GAP-43) by western blot showed that GAP-43 expression was significantly enhanced in biomimetic GO composite groups compared to GO groups, which promote neurite outgrowth and branching. Weaver et al. synthesized a nanocomposite composed of conducting polymer poly(3,4-ethylenedioxythiophene) (PEDOT) and graphene oxide (GO) nanosheets[285]. The GO/PEDOT material is nontoxic and enhanced Neural Stem Cells (NSCs) differentiation towards neuronal lineage. Researchers also observed that, aligned graphene substrate not only has the ability to enhance neuronal differentiation but also enhance neurite outgrowth to form a well-organized interconnected neuronal network[286-287]. Lee and co-workers found that GO-coated silica nanoparticle monolayer can improve human neural stem cells (hNSCs) differentiation as well as can induce outstanding axonal alignment[287]. In another work, they established a new concept that is, by changing combinatorial patterns of GO we can control differentiation of the human adipose-derived mesenchymal stem cells (hADMSCs)[288]. Specifically by generating GO grid patterns, they showed the highly efficient conversion of mesodermal stem

cells to ectodermal neuronal cells with 30% conversion efficiency, due to the ability of the grid patterns to mimic interconnected/elongated neuronal networks. Similarly, in another work Akhavan group demonstrated that graphene nanorigids on a SiO_2 matrix containing TiO_2 nanoparticles (NPs) can be used as a photocatalytic stimulator in the accelerated differentiation of human neural stem cells (hNSCs) into two dimensional neural networks[289]. The number of two dimensional neural networks on reduced graphene oxide nanoribbon (rGONR) grid/TiO2 NPs/SiO2 increased ~5.9 and 26.8 fold under dark and photo stimulation, respectively compared to the number of cells on quartz substrates after three weeks of differentiation. In addition to that, graphene based materials not only promotes the differentiation of neural cells, graphene based materials can be used also in neural interface preparation and electrical recording due to their exceptional electrical properties[290]. Therefore researchers have developed graphene based multichannel neural probe using a facile one-step electrochemical method through an ion (Cl^-)-induced process. The design of probe includes a neural-chemical interface with close electrostatic interaction between the positively charged Au^{3+} and negatively charged GO sheets. The rGO/Au_2O_3 nanohybrid deliver very fast electron transferring on tissue/electrode interfaces by tuning different deposition scan rates[291].

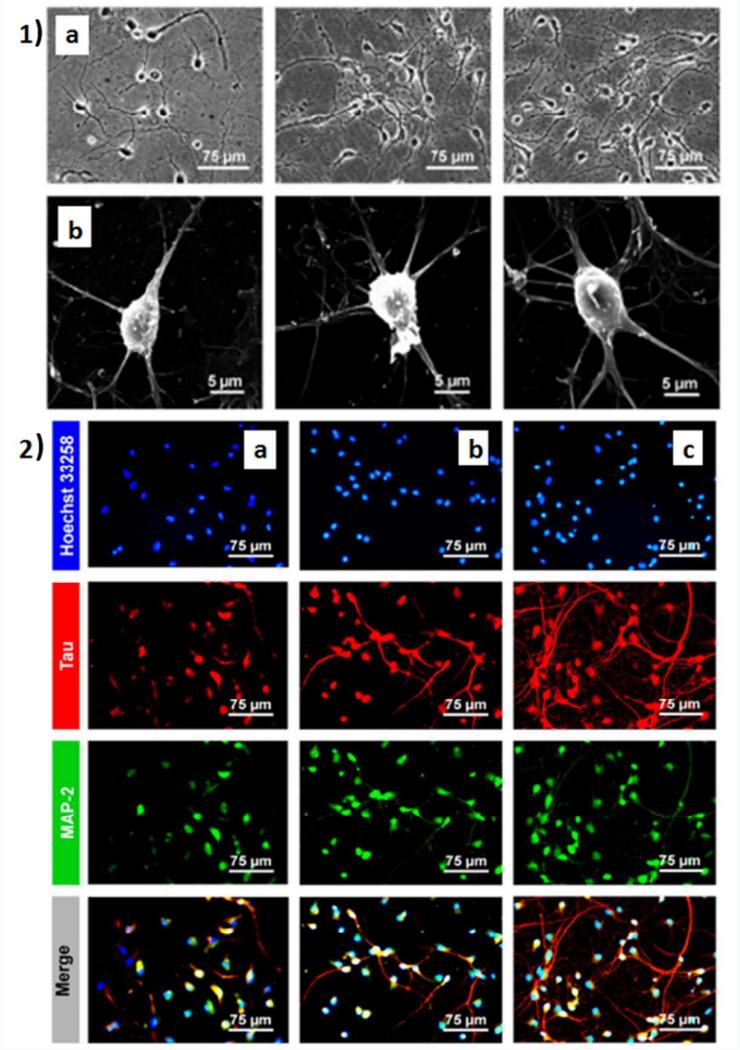

Figure 15. 1)(a) Optical images (400× magnification) of neurons after a 7 day culture on GO, GO-MPC, and GO-DMAEMA films (from left toright) and (b) SEM images (2000× magnification) of neurons after a 7 day culture on GO, GO-MPC, and GO-DMAEMA films (from left to right). (2) Immunochemistry staining fluorescent hippocampal neuron images (400×magnification) after a 7 day culture on GO (a), GO-MPC (b), and GO-DMAEMA (c) films. Reproduced with permission from ref[284]. Copyright 2013 American Chemical Society.

Although graphene based platform widely utilized to fabricate 3D scaffolds[292] or films[291] still there is huge scope in order to improve the flexibility and functionality of graphene and graphene based nanomaterials for neural tissue engineering applications. The positive impact

of graphene based materials have been confirmed in electrical stimulation of neural cells for the development of new neural cells, growth and differentiation. In addition to these facts, the tunable electrical and surface properties of graphene based materials are suitable for regeneration of neuronal tissue-like structures in order to align the arrangement of neurons. So from the above properties of graphene based materials, graphene based materials might have enormous possibilities for neural tissue engineering applications.

5.2.5. Skeletal muscle and skin tissue engineering:- Skeletal muscle is one of the major muscle types including cardiac muscle and smooth muscle. Like neural tissues, skeletal muscle tissues also have insufficient regeneration capabilities, so the loss is almost permanent if they are severely injured. For skeletal tissue engineering, nowadays stem cell based treatments are frequently used in presence of suitable scaffold materials for better cell growth and differentiation. In this context, graphene based materials can serve as excellent platform for skeletal tissue engineering due to its excellent flexibility, very high electrical conductivity, outstanding mechanical properties with ultralow density[293]. Lu and his co-workers designed a new generation three dimensional porous carbon material which consist of carbon nanotube, nanofiber and graphene sheets. This next generation carbon nanomaterial is capable of substantial shape deformation. Even after 1000 compressions, the nanohybrid can still fully recover to its original volume and retain 70% of the maximum stress value[293].

Graphene family nanomaterials showed enhanced adhesion, differentiation, and myogenesis of skeletal muscle cells[294]. Khademhosseini and his group demonstrated that C2C12 myoblasts cells showed enhanced cell adhesion and growth on ultrathin thermally reduced graphene (TR-Graphene) films compared to those on graphene oxide (GO) and glass slide substrates[294].

Patterned graphene substrate can also increase cellular alignment which resulted in increased contractile power of skeletal muscle tissues[295]. Bajaj et al. reported that C2C12 cells efficiently differentiate on graphene and this differentiation potential of C2C12 cells was further improved by the addition of IGF-1 as shown in Fig 16[295]. They showed that by patterning islands on graphene oxide surfaces they can restrict most of the myotubes on the graphene surfaces. This phenomenon leads to spontaneous alignment of the myotubes. They also established that the myotubes formed on these graphene surfaces were highly functionalized and responded efficiently to electrical pulse stimulations. Their cumulative findings suggest that graphene can be applied for the development of artificially engineered functional skeletal muscles.

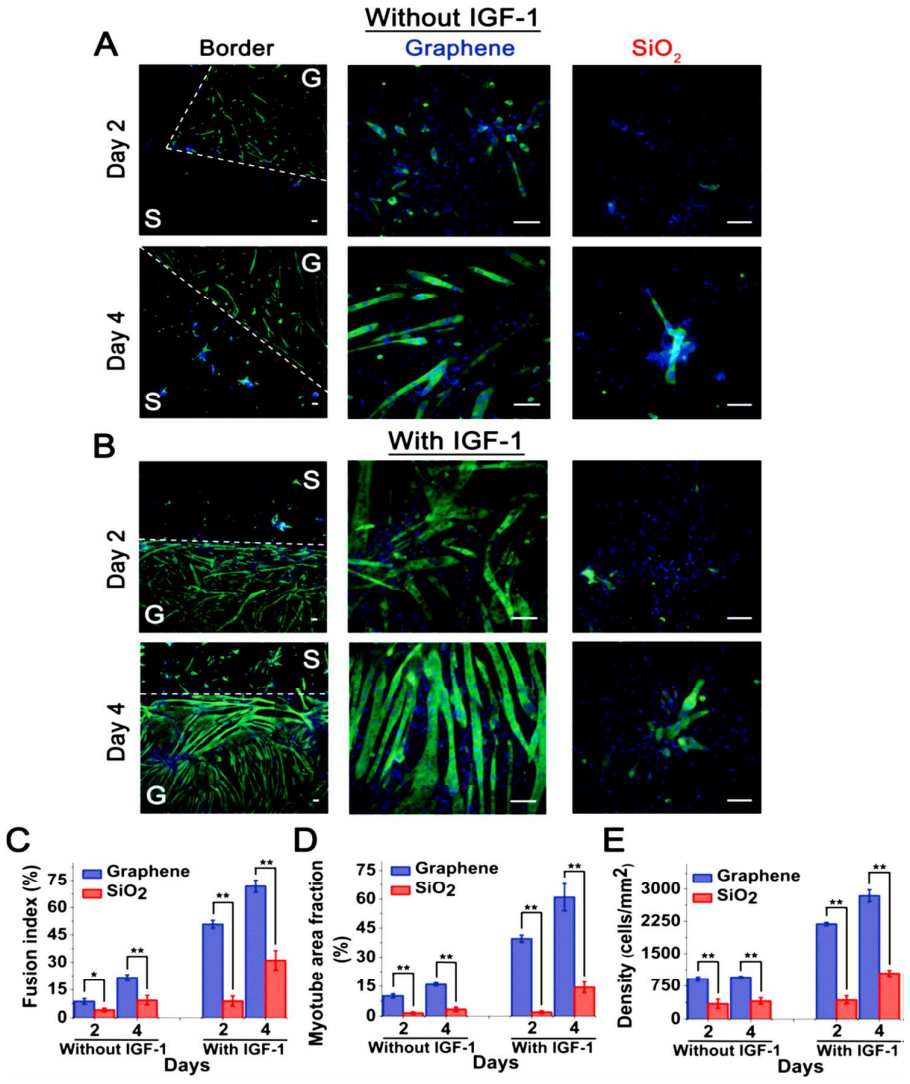

Figure 16. C2C12 cells on graphene (G)/SiO_2 (S) chips in DM with and without IGF-1. A) Without IGF-1. Fluorescent images of the C2C12 cells on graphene and SiO_2. Column 1 shows the cells on the border of graphene and SiO_2 regions of the chip for days 2 and 4. Column 2 shows the cells on graphene and column 3 shows the cells on SiO_2. Row 1 shows the C2C12 cells on day 2, while row 2 shows the cells on day 4. Cells were stained for anti-MHC (green) and nucleus (blue) and these were used for the calculation of the fusion index. The dashed white bar in column one is the border of SiO_2 and graphene surfaces on the chip. Scale bar is 100 μ m. B) With IGF-1. Quantifi cation of C) fusion index, D) myotube area fraction, and E) cell density for C2C12 cells on graphene and SiO_2. Significance: ** $p < 0.01$

and * $p < 0.05$. Data are represented as mean ±SE ($n = 5$). Reproduced with permission from ref[295]. Copyright 2014 Willey.

Skin tissue engineering are complicated, because of complicated wound structure, excretion of sweat and formation of extracellular matrix (ECM) of the skin tissue. Materials that contains micro pore and high surface to volume ratios are considered for skin tissue engineering[296]. Owing to high surface to volume ratio and protein adsorption properties, grapheme based materials would be a promising material in this field. In this context, researchers already showed that GO decorated hybrid fiber sheets composed of both poly(lactic-co-glycolic acid) (PLGA) and collagen (GO-PLGA/col) can offer good hydrophilicity as well as surface tension which can stimulate the cell attachment behaviour and proliferation of human dermal fibroblasts (HDFs) on the scaffold. The use of collagen and GO enhanced the hydrophilicity of the scaffold as well as biochemical interactions with the HDFs compared to integrin-ECM interaction. Their result suggested that GO-PLGA/Col hybrid fiber sheets can be used successfully as a suitable scaffold for skin tissue regeneration[296]. In summary we would hypothesize that graphene based nanomaterials would offer one of the most promising platform for of tissue engineering and regeneration applications. **Table 3** summarizes the graphene based nanomaterials towards tissue engineering applications.

Table 3: List of various graphene nanomaterial based platform for tissue engineering applications

Platform	Cell type	Commitment towards tissue engineering/tissue regeneration	Results	References
Graphene	MSCs	Cardiac	Graphene promotes cardiomyogenic	[257]

			differentiation without any cytotoxicity	
Graphene oxide	MSCs	Cardiac	Prevention of reactive oxygen species mediated death of implanted MSCs for cardiac repair	[258]
Reduced graphene oxide	MSCs	Cardiac	Improves myocardial repair efficacy of MSCs by stimulating angiogenic growth factors and gap junction protiens	[259]
Graphene oxide-GelMA hydrogel-PLL	Cardiomyocytes/ Cardiac fibroblasts	Cardiac	Layer by layer assembly of cardiac tissues in presence of graphene with very good spontaneous beating behaviour, improved mechanical integrity and programmable pumping properties	[260]
MeTro-Graphene oxide hybrid hydrogel	Cardiomyocytes/muscle tissues	Cardiac/muscle	Improved electrical signal propagation and subsequent contraction of the muscles connected by hydrogels	[261]
Graphene oxide	ESCs	Neuronal	Enhanced dopamine neural differentiation of ESCs in presence of GO	[282]
Micro-nano patterned Graphene oxide-Polyethylene glycol scaffolds	Cardiac cells	Cardiac	Due to the presence of patterned graphene oxide surface, the anisotropic electroconductivity and topographic cues resulted in property enhancement in myofibrils and sarcomeres, and showed substantial improvement in the expression of cell–cell coupling and calcium handling proteins, as well as in action potential duration and peak calcium release	[297]
Graphene foam	HL1	Cardiac	The graphene foam supports electrogenic cells to grow and attach to the graphene foam which can be used for real-time recording electrical activity of the cells and also idle for cardiac tissue engineering	[298]
Graphene	HNSCs	Neuronal	Enhanced stem cells differentiation into neurons	[114]

Poly-D-Lysine coated with single layer graphene	Primary embryonic hippocampal neurons	Neuronal	An ordered neuron patterning observed	[286]
Graphene oxide nanogrid/TiO_2NPs/SiO_2	HNSCs	Neuronal	~5.9 and 26.8 fold increase in cell numbers compared with quartz substrate	[289]
Graphene film	NSCs	Neuronal	Supports the growth of functional neural circuits, improved neural performance and electrical signalling of the network	[299]
Graphene film on glass	PC-12 cells	Neuronal	Graphene coated glass substrate shows a better PC-12 cells proliferation and neuronal differentiation	[300]
Glass slides, PET, PDMS, Si/SiO_2 coated with graphene sheets	MSCs	Osteogenic/ Bone tissue	In presence of an osteogenic medium, graphene coating helps human MSCs to differentiate to osteogenic lineage	[263]
SiO_2 substrate coated with graphene films	MSCs, Osteoblast cells	Bone tissue	Graphene induces osteoblast cell proliferation. It was found that, on graphene coated substrates cells are adhered and proliferated better than SiO_2 substrate	[301]
Titanium(Ti) coated with Graphene oxide sheets	BMMSCs	Osteogenic/ Bone tissue	The osteogenic differentiation of human BMMSCs on Ti/GO substrate is significantly higher compared to bare Ti substrate	[302]
Graphene and Graphene oxide film on PDMS	BMMSCs	Osteogenic/Adipogenic	Graphene and GO demonstrate to be outstanding platform for stem cell growth and differentiation factors. Graphene promotes osteogenic differentiation, whereas GO enhances adipogenic differentiation.	[264]
Graphene oxide film	ADSCs	Osteogenic, Adipogenic	GO film provides a perfect environment for the adhesion, proliferation, and differentiation of human ADSCs. Compared to tissue culture polystyrene, the GO film enhances the	[303]

			differentiation of human ADSCs to osteoblasts and adipocytes	
Reduced graphene oxide nanoribbon (rGONR)	MSCs	Osteogenic	rGONR grid showed enhanced osteogenic differentiation of the hMSCs (a patterned differentiation) in short time of 7 days in which the amount of the osteogenesis was ~2.2 folds greater than the differentiation (a uniform differentiation) on the rGO sheets	[304]
Self-supporting graphene hydrogel film	BMSCs	Osteogenic/ Bone tissue	The self-supporting hydrogel showed good cell adhesion, spreading, and proliferation	[266]
Glass slides coated with two and three-dimensional graphene substrates	PDLSCs	Osteogenic/Bone tissue	All the substrates allowed stem cell survival and proliferation. 2D-graphene substrates and 3D-graphene substrates induced the differentiation of PDLSC into mature osteoblasts at higher levels as compared to glass slides and polystyrene	[267]
Reduced graphene oxide (rGO) and hydroxyapatite (HAp) (rGO/HAp NCs)	MC3T3-E1	Bone tissue	The results suggest that rGO/HAp NCs can be exploited to craft a range of strategies for the development of novel dental and orthopaedic bone grafts to accelerate bone regeneration	[268]
Reduced graphene oxide-coated hydroxyapatite composites	MSCs	Osteogenic/ Bone tissue	Synergistically enhanced spontaneous osteogenic differentiation of hMSCs, without hampering their proliferation	[271]
Carrageenan functionalized graphene oxide	MC3T3-E1 cells	Bone tissue	Carrageenan functionalized graphene oxide promoted hydroxyapatite mineralization and cell differentiation	[269]
Graphene-Hydroxyapatite nanocomposite	MSCs	Bone tissue	Graphene-Hydroxyapatite nanocomposite showed better cell affinity than bare graphene	[270]

PCL/rGO-Sr scaffolds	Osteoblast	Bone tissue	Osteoblast proliferation and differentiation was significantly higher in the PCL scaffolds containing the RGO_Sr particles in contrast to bare PCL and PCL/RGO scaffolds	272
Calcium Silicate–Reduced Graphene oxide Composites	Osteoblast cells	Bone tissue	Proliferation rate and alkaline phosphatase (ALP) activity of cells on the CS/rGO composites were improved compared with the pure CS ceramic	273
Chitosan-Gelatin-Graphene oxide	MSCs	Bone tissue	Chitosan-Gelatin-Graphene oxide scaffolds were cyto-friendly to osteoprogenitor cells, and promoted differentiation of mouse mesenchymal stem cells into osteoblasts.	305
Graphene oxide-hyaluronic acid–chitosan with simvastatin	MC3T3 cells	Bone tissue	Scaffolds are biocompatible and osteoinductive in nature with enhanced mineralization activity	306
Graphene oxide	ADSCs	Chondrogenic	Graphene oxide act as a cell□adhesion substrate as well as it served as a carrier for growth factor protein□ delivery carrier for chondrogenic differentiation of adult stem cells	279
CSMA/PECA/Graphene oxide porous hybrid scaffold	Cartilage cells	Cartilage	CSMA/PECA/Graphene oxide scaffold was cytocompatible as well as biocompatible and had a favourable degradation rate. *In-vitro* and *in-vivo* both results suggested that the scaffolds are very useful for cartilage tissue engineering	307
Growth factor loaded Graphene/Graphene oxide/ Porous graphene oxide	MSCs	Chondrogenic	Their findings suggest that both graphene and porous graphene oxide could serve as effective pre-concentration platforms for the construction of tissue-engineered cartilage and suspension-based cultures in vitro	280
Thermally	C2C12	Skeletal muscle	Electrical stimulation on	294

reduced graphene films	myoblast cells	tissue	graphene films significantly enhanced myoblast cells differentiation	
Graphene films	C2C12 muscle cells	Skeletal muscle tissue	C2C12 cells efficiently differentiate on graphene films and this differentiation potential of C2C12 cells can be further enhanced by the addition of growth factors in addition to that it was observed that, by patterning graphene islands on silicon oxide surfaces, majority of the myotubes are constricted on the graphene surfaces which leads to spontaneous alignment of the myotubes	[295]
Graphene oxide-PLGA-Collagen	Human dermal fibroblasts	Skin tissue	In-vitro results suggested that, Graphene oxide-PLGA-Collagen scaffold could be a potential candidate for skin tissue engineering applications	[296]
3D-Graphene foam	MSCs	Skin tissue	Graphene foam guided the wound healing process in a faster way with reduced scarring effect	[308]

MSCs-Mesenchymal stem cells, PLL-Poly-L-Lysine, GelMA-Gelatin methacryloyl, MeTro-Methacryloyl□substituted recombinant human tropoelastin, ESCs-Embryotic stem cells, HNSCs-Human neural stem cells, TiO_2NPs-Titanium dioxide nanoparticles, SiO_2-Silicon dioxide, BMMSCs- Bone marrow derived mesenchymal stem cells, PDMS–Polydimethylsiloxane, ADSCs-Adipose derived stem cells, BMSCs-Bone marrow stromal stem cells, PDLSCs-Periodontal ligament stem cells, PCL-Poly(ε-caprolactone), Sr-Strontium, CSMA-Methacrylated chondroitin sulfate, PECA-poly(ethylene glycol) methyl ether-ε-caprolactone-acryloyl chloride, PLGA-Poly(lactic-co-glycolic acid), HDFs-Human dermal fibroblasts

5.3. Drug/gene delivery:- The delivery of drug and biomacromolecules (e.g- protein, peptide and genes) to specific cells or interest tissues is a primary concern in modern medicinal research. With respect to the traditional old methods of drug delivery such as oral

administration or intravenous injection, nowadays substantial effort has been done to fabricate smart theranostics system with enhanced biocompatibility to achieve targeted drug/gene delivery at the site of interest, to solubilize drugs/biomacromolecules more efficiently with greater loading capacity and to protect them from enzymatic degradation[309]. In this context graphene based targeted delivery systems have come up with new opportunities and providing benefits from the effective triggered as well as targeted delivery of drugs/genes to imaging and real time monitoring viewpoints.

Since the discovery of graphene in 2004, applications of graphene nanomaterials increasing rapidly for drug/gene delivery because of graphene's high surface to volume ratio and multiple modes of complex formation such as π-π stacking, electrostatic interactions, and hydrophobic interactions[310]. In the last few years, a significant effort has been done by researchers for appropriate modifications of graphene based nanomaterials in order to improve their efficacy for both *in vitro* cancer cell assays as well as *in vivo* chemotherapy applications. For example Zhang and co-workers prepared a functional nanoscale graphene oxide (NGO) for the loading and targeted delivery of anticancer drugs[311]. The NGO was functionalized with sulfonic acid groups to stabilize it under physiological solutions followed by covalent binding of folic acid (FA) for targeted delivery to cancer cells. Furthermore they loaded two anticancer drugs doxorubicin (DOX) and camptothecin (CPT) onto the FA conjugated NGO (FA-NGO) via π-π stacking and hydrophobic interactions. They got much better therapeutic efficacy dual drugs delivery compared to single drug. In another work, Yang et al. reported GO-Fe_3O_4 nanohybrid for DOX delivery[312]. The nanohybrid can uptake the drug as high as 1.08 mg/mg of nanohybrid. Dai and co-workers synthesized PEGylated nanographene oxide to deliver water soluble anticancer drug SN38 to colon cancer cells[313]. They studied MTS assay and found that NGO-PEG-SN38 nanocomposite is highly effective for colon cancer cell killing. They also noticed that NGO-PEG nanocomposites are not

cytotoxic by themselves. Depan et al. reported a novel graphene mediated drug delivery system for controlled and targeted drug release[314]. The nanocarrier system was prepared by attaching doxorubicin to graphene oxide with folic acid conjugated chitosan. The π–π stacking interaction, simplified as a non-covalent type of functionalization, allows high drug loading and subsequent controlled release of the drug. The encapsulated graphene oxide improved the stability of the nanocarrier system in aqueous medium due to the hydrophilicity and cationic nature of chitosan. The loading and triggered release of DOX indicated strong pH dependence and hydrogen bonding interaction between DOX and graphene oxide. Li and his group developed a covalently functionalized graphene sheets (GS) by grafting a well-defined thermos-responsive poly(N-isopropylacrylamide)(PNIPAM) via *click* chemistry[315]. Due to the π–π stacking and hydrophobic interaction between PANIPAM-GS was able to load an anticancer drug camptothecin (CPT) with a superior loading capacity of 15.6 wt%. The PNIPAM-GS-CPT nanocomposite showed a strong potency towards *in vitro* cancer cell killing. More significantly, the PANIPAM-GS does not exhibit any toxicity to the cell line. Shi and co-workers developed a redox responsive PEGylated nanographene oxide (NGO-SS-mPEG) for intercellular drug delivery[316]. The PEGylated nanographene oxide with redox responsive detachable PEG shell can rapidly release an encapsulated payload at tumour-relevant glutathione levels. The surface engineered structures accelerated almost 1.55 times faster release of DOX from NGO-SS-mPEG in presence of GSH. While attaining sufficient drug loading capacity, targeted delivery of the nanocarrier at the site of interest is equally important factor to achieve successful therapeutic effect. In this regard, Wang et al. reported a nanohybrid made of gold nanocluster and reduced graphene oxide loaded with DOX for targeted delivery to cancer (hepatocarcinoma) cells[317]. Fan et al. prepared a graphene-carbon nanotube-iron oxide (GN–CNT–Fe_3O_4) nanohybrid to investigate the anticancer effect through the delivery of 5-fluorouracil (5-FU) (anticancer drug) into liver cancer cells[318]. The

nanocomposite can efficiently bind the anticancer drug 5-FU with a loading capacity of up to 0.27mg mg^{-1} and showed pH dependent drug release profile. The presence of CNT in the nanocomposite enhanced transportation of the graphene-CNT-Fe_3O_4 hybrid across the cell membrane. TEM image revealed that GN-CNT-Fe_3O_4 accumulated more in the cell cytoplasm but only graphene-Fe_3O_4 was outside of the cell. To achieve more specific targeted delivery of drugs, researchers have developed quantum dots-graphene-based hybrid nanocomposite functionalized with transferrin (Trf) ligand[319]. Trf are iron binding blood plasma glycoproteins with high affinity to the overexpressed Trf receptors presented on the plasma membrane of several kinds of cancerous cells[320]. Wang and his team members developed a new kind of nanohybrid system consists of SiO_2-coated quantum dot conjugated graphene for targeted cancer fluorescent imaging, tracking, and monitoring drug delivery, as well as cancer therapy[319]. Their nanocomposite showed enhanced toxicity towards Trf positive Hela cells when compared with Trf negative HEK293 cells, however the nanocomposite without Trf ligand and with Trf ligand exhibited a same type of results on Trf negative HEK293 cell viability. Furthermore with targeted therapies, nowadays triggered drug delivery also have become very prevalent among researchers due to the fact, that triggered drug delivery systems can provide control over drug doses and adjust dosing regimens on-demand, depending upon user's physiological response[106, 321]. In this context, Wang and co-workers designed a remote controlled drug delivery system by immobilizing a commercially available photoacid generator (PAG) into graphene oxide conjugated with mesoporous silica system for delivering drug payloads to cancer cells via photoinduced pH jump activation[322] as shown in Fig 17. In details they immobilized PAG molecules on the pore wall of mesoporous silica nanopaticles which are conjugated with boronic acid via strong physical adsorption and then they capped the nanoparticles with GO sheets by an acid labile GO sheets, which formed a nanogate type assembly.

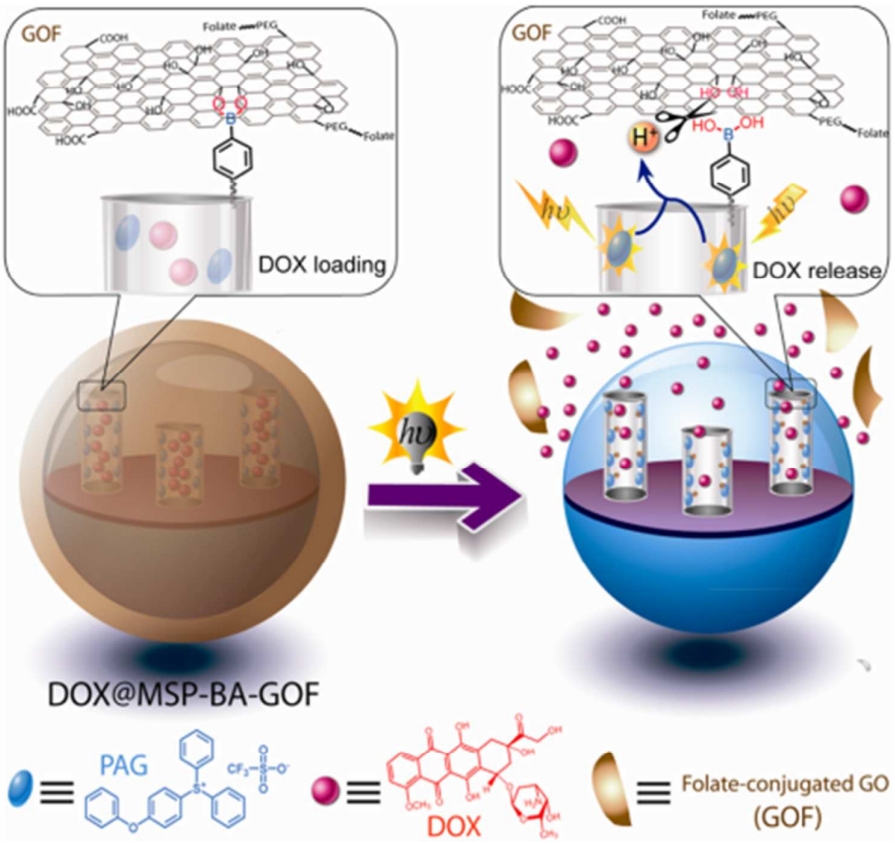

Figure 17. Schematic Illustration of DOX@MSP-BA-GOF as a Drug Delivery System for Remote Light Control of Drug Release. Reproduced with permission from ref [322]. Copyright 2014 American Chemical Society.

More specifically, PAG can produce strong acid in presence of UV or near-UV light[323]. Their system works in such a manner, that in presence of UV light PAG molecules generate a sudden pH change which resulted in cleavage of the boroester bonds and open up the pore gates and release the loaded DOX. Furthermore they conjugated the nanocomposite with folic acid for targeted delivery of drugs to cancerous cells. DOX-loaded nanocomposites showed selective toxicity toward cells, with almost 80% in case of HeLa cells (high expression of Folate Receptors), while a very slight change in cell viability was observed in the case of L02 cells (low expression of Folate Receptors)[322]. One more example of graphene based nanomaterials for drug delivery system through polyethylene glycol (PEG) and branched

polyethyleneimine (BPEI) functionalized rGO (PEG-BPEI-rGO); which can be triggered photothermally. Kim and co-workers found that, PEG-BPEI-rGO has the ability to load a greater amount of doxorubicin (DOX) than unreduced PEG-BPEI-GO via π-π and hydrophobic interactions with high water stability and in presence of NIR light, PEG-BPEI-rGO/DOX complex can easily escape from endosome after cellular uptake by photothermally induced endosomal disruption and the proton sponge effect, followed by glutathione-induced DOX release into the cytosol. Their system showed very high cancer cell killing efficiency in presence of NIR irradiation than compared with no NIR irradiation which again proved that phototriggered delivery of the DOX[324]. Huang and co-workers reported that graphene family nanomaterials can perform multiple tasks at a time[325]. In details they showed ligand modified graphene quantum dots can facilitate the simultaneous operation of multiple tasks at a time without need of any external tracking dyes. These tasks include selected cell labelling, targeted drug delivery and real time monitoring of cellular uptake. They conjugated folic acid with GQDs, which can discriminate between cancer cells and normal cells and loaded the nano-assembly with DOX. The inherent stable fluorescence of GQDs allow the real-time monitoring of the cellular uptake of the DOX–GQD–FA nanoassembly and the consequent release of drugs in cancer cells. *In vitro* toxicity results suggest that the DOX-GQD-FA nanoassembly can target cancer cells (Hela cells) specifically while exhibiting significantly reduced cytotoxicity to non-cancer cells.

In a similar type of work, Iannazzo et al. synthesized GQDs from multi wall carbon nanotube and then they covalently linked a tumour targeting module biotin (BTN), which are able to recognize overexpressed biotin receptors on cancer cells and subsequently loaded the GQD-BTN nanocomposite with DOX. They performed the biological test on A549 cancer cell line[326]. The carrier showed very low toxicity in case of carrier system (GQDs and GQDs-BTN) but after loading of DOX it showed the strong cytotoxicity to the cancer cells (A549).

The triggered drug detachment from the nanosystem is controlled by the acidic environment of the cancer cells. Chen et al. reported a unique GQDs based FRET platform for nucleus targeted and real time monitoring system of drug delivery[327]. Their system consists of GQDs which serve as a drug carrier at the same time it act as a donor of FRET pair, peptide TAT (YGRKKRRQRRR) which aids to transport the delivery system to the nucleus and an anticancer drug DOX. The study established the fact that the conjugated TAT as well as the small size of GQDs helps in nucleus targeting which in terms exhibit an improved result in intranuclear accumulation of drugs. They demonstrated that both the conjugated TAT and small size of GQDs contribute to targeting nucleus which results in improved intranuclear accumulation of drugs, as well as due to extremely sensitive FRET signal of the system, it can capable of real time monitoring of the separation process of drugs. They synthesized GQDs by hydrothermal method from graphene oxide followed by PEGlyation of the synthesized GQDs. Then they conjugated the PEGlyated GQDs with TAT peptide followed by loading of DOX. MTT assay showed that the GQD-TAT-DOX system is highly efficient to kill cancer cells (Hela) with a percentage of 62.5%. In a similar type of study Zhu and co-workers reported a smart nanocarrier for ATP triggered drug delivery and real time monitoring of drug release[328]. They synthesized aptamer functionalized mesoporous silica nanoparticles, which was further conjugated with GQDs through π-π interaction followed by drug loading. Their nanocarrier possesses various attractive properties like dual target of AS1411 and ATP aptamer, the FRET nanocarrier could release the drug more specifically in the cytoplasm of the cancer cells, the aptamer/GQD nanocomposite act as a gatekeepers to completely encapsulate the drugs in the nanocarriers as well as electron acceptors to quench the fluorescence of FMSNs and most importantly the drug release was directly reflected by the recovery of the FMSNs along with the dissociation of GQDs. Nigam and co-workers synthesized graphene quantum dots conjugated albumin nanoparticles for targeted drug

delivery to the pancreatic cancer cells[329]. They used gemcitabine, the most preferred drug for pancreatic cancer treatment. Due to presence of hyaluronic acid (HA) in the nanocarrier system they can target selectively overexpressed HA receptor at the cancer cells. The superior nanoformulation not only attained sustained release of drug but also showed a notable effect on bioavailability of gem to cancer cells *in vitro* as exhibited by MTT assay as well as overcome the rapid metabolism and short half-life of gemcitabine. Wang et al. established that, GQD can act as efficient drug delivery vehicle as well as it can boost the anticancer activity of the DOX without any modification due to their exceptional structural properties[330]. Briefly they showed that, GQDs are capable of effectively deliver DOX to the nucleus through DOX/GQDs conjugates, due to the different cellular and nucleus internalization process of DOX/GQDs conjugates comparing to free DOX and also improve the DNA cleavage activity of the DOX remarkably.

Although the delivery of small molecule drugs has been extensively studied using graphene nanomaterials, there is a few number of studies focused on graphene as a gene carrier. Since the discovery of genetic code and increasing knowledge of genetic etiology of various ailments together with significant advances in molecular biology to biochemistry to bio-nanotechnology has opened up a new therapeutic approach for many incurable diseases. Till now viral vectors are most efficient carriers to deliver genetic payload and almost 70 percent of all gene therapy medical trials were performed by viral vectors[331]. However random genomic integration, severe immunogenicity, limited capacity to accommodate very long nucleic acid as well its elevated production cost are the prime challenges for clinical use of viral vectors[332].

In contrast, the development of non-viral vectors that are safer and more adoptable than viral vectors, but poor transfection efficiency and gene expression efficacy are the major drawbacks. Despite, the development of several non-viral vectors including cationic

polymers, polysaccharides, dendrimers[333] etc, efficient and safe nonviral vectors are still remain undiscovered[334]. In this context graphene based nanomaterials have gained tremendous attention as nonviral vectors due to its remarkable physicochemical, optical and photothermal properties[333]. Graphene nanomaterials can offer strong covalent binding sites through carbon rehybridization from sp^2 to sp^3 hybrid orbital state[335]. More specifically presence of epoxides, carbonyls and hydroxyl groups on the GO, RGO and GQDs surface offer further modification through amidation or esterification. In addition to that graphene nanomaterials can act as an electron donating ligand to establish π-π stacking as well as electron acceptor in the case of physisorption which normally occurs via electrostatic interaction, Van der Waals force or through hydrogen bonding[336]. Due to these reasons graphene nanomaterials can offer numerous possibilities of functionalization to enhance pharmacokinetic properties and biocompatibility, engraft cationic molecules to increase nucleic acid loading efficacy, incorporate water insoluble drugs that are subject to drug-resistance mechanisms and to integrate imaging agents.

Incorporation of cationic polymer such as PEI (polyethylenimine) to the graphene nanomaterial surface has been studied as a strategy to enhance gene transfection efficiency. Presence of PEI induces a cloud of positive charges around the graphene material which favours the complexation with negatively charged DNA and cellular internalization through electrostatic interactions with DNA and cell membrane, respectively. Apart from this, the positive charges of PEI also facilitate the release of the cargo from the endosome through "proton sponge" effect[333]. As discussed on above, the most common approach for PEI conjugation with GO, rGO or GQD surface is via carbodiimide chemistry[23, 337]. Already PEI has been well established as a nonviral gene delivery vector on its own, however compromised by its cytotoxicity, especially at high molecular weight 25kDa[338]. Like PEI another polymeric material Polyethylene Glycol(PEG) have been extensively studied for

biomedical applications such as increase blood circulation in vivo, enhance stability of the gene delivery vehicle under physiological conditions and biocompatibility[339]. Exploiting these properties Feng et al and Yin et al developed similar type of GO nanoplatforms integrated with both PEG and PEI which are able to load EGFP-coding plasmid DNA (pDNA)34 and plasmid-based stat3 siRNA[340-341]. Chatterjee and his group synthesized a very efficient gene delivery vehicle based on dendron conjugated GO. They conjugated polyamidoamine (PAMAM) dendron with nano graphene oxide (nGO) through *click* chemistry to improve both DNA complexation capability as well as the transfection efficiency as shown in Fig 18[23]. They observed that transfection efficiency of the dendron conjugated GO dramatically increased compared to that of naked nGO. Although the transfection efficiency was dependent on PAMAM generation and highest transfection efficiency was obtained with generation 3.0 PAMAM Dendron conjugated nGO in HeLa cells (51%) and the efficiency surpassed the efficiency obtained by "gold standard" branched polyethyleneimine (bPEI, 25 kDa) (27%) and lipofectamine 2000 (47% efficiency). Dong et al. reported a multifunctional nanocomposite made of poly(L-lactide) (PLA) and PEG grafted GQDs for simultaneous intracellular microRNA (miRNA) imaging and gene therapy. The large surface area of GQDs provide simultaneous adsorption of miRNA-21 and surviving, respectively. The combined action of miRNA-21 and survivin targeting agents induced better inhibition of cancer cell growth and enhanced apoptosis of cancer cells compared with miRNA-21 or survivin targeting agents alone[337]. In another study, Zhang et al. developed a PEGylated reduced graphene oxide nanovector for efficient delivery of single stranded ribonucleic acid (ssRNA). They showed that the PEG-rGO exhibits superior ssRNA loading and delivery capability compared to the PEGylated graphene oxide[342]. Li and co-workers designed chitosan-functionalized graphene oxide as a nanocarrier for both drug and gene delivery. Chitosan imparts good aqueous solubility and biocompatibility to the system. The

nanocarrier system can load the water insoluble anticancer drug Camptothecin (CPT) as well as plasmid DNA, which exhibit reasonable transfection efficacy in Hela Cells at certain nitrogen to phosphate ratios[343]. Chitosan itself is a well-known alternative gene transfection vehicle due to its low cytotoxicity than PEI[344-345].

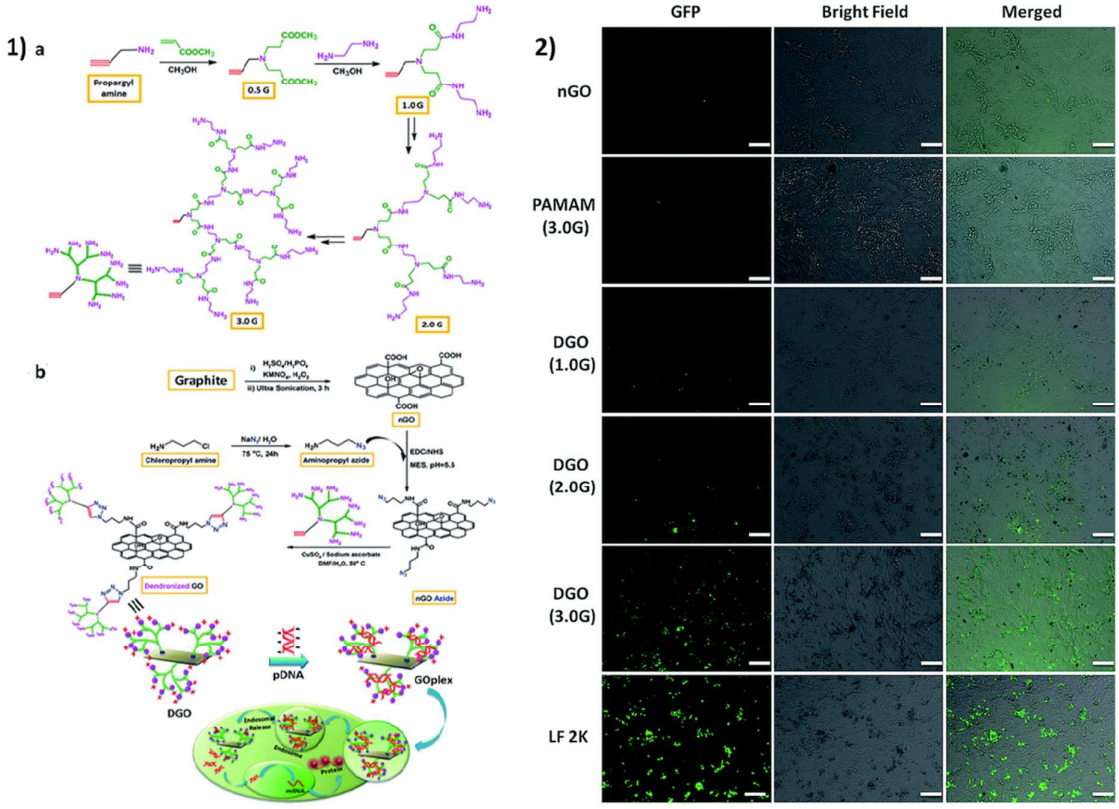

Figure 18. 1) Schematic diagram for (a) synthesis of focal point PAMAM dendrimer and (b) synthesis of DGO by "click" chemistry and cellular uptake of dendronized GO/pDNA complex (2) Fluorescence micrographs of transfected HeLa cell by nGO/pDNA, PAMAM (3.0G)/pDNA, DGO (1.0, 2.0 and 3.0G)/pDNA complexes at weight ratios of 30:1 and LF 2K/pDNA complex containing 1 mg of pDNA in each formulation. The scale bar is 10 mm. Reproduced with permission from ref[23]. Copyright 2015 Royal Society of Chemistry.

Xu et al. reported a hybrid nonviral vector composed of gold nanoparticles (AuNPs), gold nanorods (AuNRs) and GO. The electrostatic self-assembly between AuNPs, AuNRs and GO

stabilize the nanocomposite. The surface functionalization on AuNPs and AuNRs with cetyl trimethylammonium bromide (CTAB) provide further functionalization with PEI. The PEI functionalized GO encapsulating AuNPs were exhibited very high transfection efficiency of 65% while retaining 90% viability on Hela cells[346]. Imani et al. investigated the applicability of octaarginine (R8) functionalized graphene oxide (GO) as a nanocarrier for gene delivery. In order to increase cellular uptake they engrafted cationic cell penetrating peptide octaarginine with GO flakes[347]. In another strategy, Yang and co-workers synthesized a biocleavable organic inorganic hybrid materials by decorating GO with poly(2-dimethylamino)ethyl methacrylate (PDMAEMA) via atom transfer radical polymerization. This chemical modification enable the system, tumour specific targeting and release of drug and genes. The cleavable disulphide bond between GO and PDMAEMA facilitate release of pDNA under reducible conditions[348]. Not only delivery of the drug/genes on the targeted site, graphene nanomaterials can protect oligonucleotides from enzymatic degradation. Lu et al. proved that functionalized nanoscale graphene oxide can protect oligonucleotides from enzymatic cleavage and efficiently deliver oligonucleotides into cells[169]. Liu and co-workers fabricated patterned substrates on nanographene oxide demonstrating highly localized and efficient gene delivery to multiple cell lines. The GO substrate served as a platform to preconcentrate PEI/pDNA complexes and then gradual release for a sustainable period of time. Their strategy offers spatial control over gene transfer and therefore could be very useful in the preparation of genetically different cell populations for the investigation of cell-cell interactions[349]. Tripathi et al. used PEI grafted GO for the delivery of GFP-encoding pDNA and later silence its expression by the delivery of an anti-GFP siRNA with the same vector. Under optimum condition it supressed 70% of the target gene as measured by fluorescence intensity[350]. Feng et al. synthesized PEG and PEI dual functionalized nGO via amide bond. The nGO-PEG-PEI exhibits remarkably high gene transfection efficacy without

influence of serum, in addition to that it exhibited minimal cytotoxicity. Using the NIR optical absorbance property of nGO, they showed that the cellular uptake of nGO-PEG-PEI can be improved upon a low power NIR laser irradiation, due to the trivial photothermal heating which increases the cell membrane permeability without significantly destroing cells[340]. A different strategy has been taken up by Zhi et al. to increase cytotoxicity against cancer cells by combining both gene therapy and drug delivery. They designed multifunctional nanographene oxide composed of polyethylenimine (PEI)/poly(sodium 4-styrenesulfonates) (PSS)/graphene oxide (GO) for delivery of miR21 targeted siRNA and the anticancer drug Adriamycin. They discovered that when adryamicin-resistant MCF7 cells were exposed to the drug delivered by the designed vector, their viability was decreased significantly but when the drug delivered alone it was not effective at all, which confirmed the ability of the carrier to overcome drug resistance property developed by malignant cells. Most importantly significant reduction in cell viability was achieved when drug and siRNA were codelivered, which highlights the overwhelming possibilities of combined therapies[293]. Kim and his group developed a photothermally controlled targeted gene delivery carrier by conjugating low molecular weight branched polyethylenimine, polyethylene glycol and reduced graphene oxide. This PEG–BPEI–rGO nanocomposite forms a stable nano-sized complex with pDNA. *In vitro* gene transfection assay confirmed that the nanocarrier has a higher transfection efficacy without obvious cytotoxicity than unmodified ones in PC-3 and NIH/3T3 cells. In addition to that PEG–BPEI–rGO nanocomposite exhibits an enhanced gene transfection efficacy upon NIR irradiation, which is attributed to accelerated endosomal escape of polyplexes improved by locally induced heat[351]. Zhang et al. showed that chemotherapy efficiency can be increased by sequential delivery of siRNA and anticancer drug. They found the synergistic effect of anticancer drug DOX and Bcl-2-targeted siRNA by codelivery and sequential delivery of DOX and the siRNA to HeLa cells by the PEI-GO

nanovector. Under optimum conditions PEI-GO/Bcl-2-targeted siRNA complex inhibited ~70% of the Bcl-2 expression level, without showing much cytotoxicity. Whereas in absence of PEI-GO/DOX the relative cellular viability was 92.5%[352]. Khademhosseini and his co-workers developed a unique graphene oxide/hydrogel based angiogenic gene delivery system for vasculogenesis and cardiac repair. In details they synthesized a biocompatible hydrogel which can efficiently deliver nanocomplex of graphene oxide and vascular endothelial growth factor-165 pro angiogenic gene for myocardial therapy. To evaluate the effectiveness of the system, they used a rat model with acute myocardial infection and injected the therapeutic hydrogels intramyocardially in the peri-infarct regions. The growth factor-165 from *in vitro* cardiomyocytes exhibited profound mitotic activities on endothelial cells. A significant increase in myocardial capillary density at the peri-infarct regions is observed as well as reduction of the scar area noticed in the infarcted heart as shown in Fig 19[353].

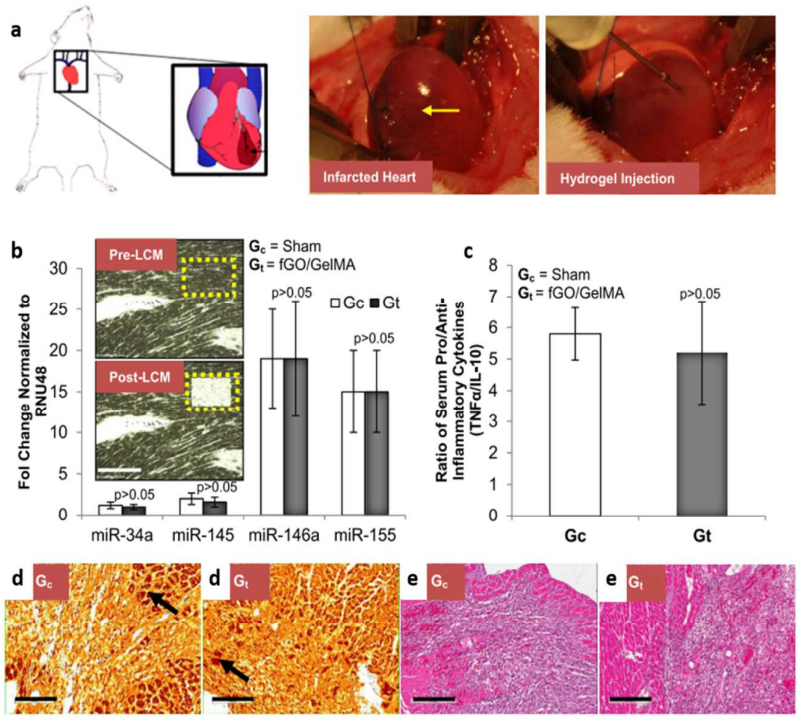

Figure 19. *In vivo* delivery and biocompatibility of injectable PEI functionalized GO carrying low-modulus methacrylated gelatin (GelMA) hydrogel. (a) Schematic of rat heart with AMI. Photograph (infarcted heart) represents a myocardially infarcted rat heart after causing myocardial infarction by ligation of left anterior descending artery. Arrows indicate the damaged area in the left ventricular region. Photograph (hydrogel injection) shows the route of administration via direct intramyocardial delivery of injectable fGO/GelMA hydrogel to the periinfarct zones. (b) Representative pictures of peri-infarct region of ventricular tissues 7 days post injection, pre- and postlaser capture microdissection (LCM) (scale bar: 100 μm). Post-LCM tissue capture and RNA extraction and qPCR based miRNA expression assays were performed to compare the inflammatory marker-specific miRNA levels in Sham and fGO/GelMA hydrogel treated groups. The data in graph represents fold change in expression levels of inflammation-specific miRNAs, miR-34a, miR-145, miR-146a and miR-155, between the two groups normalized to RNU48, an abundant and stable human small nuclear RNAs (snRNAs). No significant differences were found between the two groups confirming the in vivo biocompatibility of the injected hydrogels. (c) Quantification of blood plasma TNFα and IL10 represented as a ratio of pro and antiinflammatory cytokines analyzed by ELISA assay ($P < 0.05$ = statistically significant, $n = 3$). (d and e) fGO/GelMA hydrogel does not invoke any significant difference in pro-inflammatory TNFα expression or white blood cell accumulation in the infarcted heart compared to sham control. The tissues were either immunostained with TNFα antibody to trace myocardial TNFα expression (d) or counterstained with H&E (e) to demonstrate histological morphology of orderly arranged myocardial cells.The TNFα immunoreactive cells were stained as dark brown colour. Data are expressed as mean value ±SD. Scale bar: 200 μm. Reproduced with permission from ref [353]. Copyright 2014 American Chemical Society.

In summary, despite the development of graphene nanomaterials based gene/drug delivery system with enhanced gene loading efficiency and *in vitro* intercellular delivery, lots of in vivo study should be carried out to validate the *in vitro* study to go ahead towards the clinical applications in future. **Table 4** summarises the graphene based nanomaterials for drug/gene delivery applications.

Table 4. List of graphene based nanocarriers for drug/gene delivery

Carrier	Delivered drugs/genes	Results and uses	References
Folic acid conjugated nano graphene oxide	DOX, CPT	Targeted delivery of DOX and CPT to MCF-7 cells with enhanced toxicity than single DOX or CPT	311
Superparamagnetic graphene oxide-Fe_3O_4 nanoparticles	DXR	The nanohybrid showed a pH-triggered controlled magnetic behaviour which makes this material a promising candidate for controlled targeted drug delivery	312
Functionalized nano graphene oxide with branched polyethylene glycol	SN38	The NGO-PEG-SN38 exhibited high potency with IC50 values of ~6 nM towards HCT-116 cells	313
Graphene oxide nanohybrid with folic acid conjugated chitosan	DOX	pH sensitive drug release mechanism was observed which makes it a suitable drug carrier for nanomedicine applications	314
Poly(N isopropylacrylamide)–graphene sheets nanoconjugate (PNIPAM-GS)	CPT	The in vitro drug release experiment showed that 16.9% and 19.4% CPT were released after 72 h at 37°C in water and PBS, respectively. In addition to that, PNIPAM-GS showed very good in vitro cancer cell killing efficacy, verified by the MTT assay	315
PEGylated nano graphene oxide	DXR	Redox responsive drug detachment was observed. Furthermore, inhibition of cell proliferation is directly correlated with increased intracellular GSH concentrations due to rapid DXR release	316
Graphene-carbon nanotube-Fe_3O_4 hybrid	5-FU	*In vitro* cytotoxicity tests suggested that the obtained nanohybrid is nontoxic for Chang liver cells, even at the high concentration of 80 μg	318

		mL^{-1}, however, the 5-FU-loaded GN–CNT–Fe_3O_4 hybrid showed significant cytotoxicity effects towards HepG2 cells.	
Graphene-SiO2 quoted quantum dots (HQDs) with Transferrin	DOX	The hybrid system efficiently deliver DOX to the targeted cancer cells. The hybrid system also enable us to monitor the intracellular DOX release	[319]
Folic acid conjugated graphene oxide-capped boroester linked mesoporous silica (MSP-BA-GOF)	DOX	DOX loaded MSP-BA-GOF showed selective cell internalization via receptor-mediated endocytosis and subsequent release of DOX by the remote illumination. In addition to that, the DOX loaded MSP-BA-GOF demonstrated very good anticancer activity upon remote illumination with a viability ~20%	[322]
Reduced graphene oxide functionalized with polyethylene glycol and branched polyethyleneimine (PEG-BPEI-rGO)	DOX	Much greater cancer cell death efficacy was observed in PEG-BPEI-rGO/DOX complex-treated cells with NIR irradiation than those with no irradiation	[324]
Folic acid conjugated graphene quantum dots	DOX	The nanoassembly can clearly discriminate between cancer cells from normal cells and efficiently deliver the drug to targeted cells. The inherent stable fluorescence of GQDs also enable us the real-time monitoring of the cellular uptake of the DOX–GQD–FA nanoassembly and the consequent release of drugs.	[325]
Biotin conjugated graphene quantum dots	DOX	The nanocarrier showed very good cytocompatibility towards normal cells while it showed enhanced toxicity towards cancer cells by targeted delivery of drugs	[326]
Peptide (TAT) conjugated PEGylated graphene quantum dots (GQDs)	DOX	TAT conjugated GQDs showed nucleus targeted delivery of DOX with enhanced intranuclear accumulation and increased toxicity towards Hela Cells than free DOX	[327]
Aptamer/graphene quantum dots nanocomposite capped fluorescent mesoporous silica nanoparticles	DOX	The nanocarrier showed selective drug release behaviour in the cytoplasm of the cancer cells with enhanced toxicity	[328]
Hyaluronic acid	GMC	Targeted delivery of GMC was	[329]

functionalized graphene quantum dot conjugated albumin nanoparticles		observed with sustained release behaviour. In addition to that very good toxicity was showed by GMC loaded nanocarrier system towards pancreatic cancer cells	
Graphene quantum dots (GQDs)	DOX	DOX/GQDs conjugate demonstrated increase nuclear uptake efficacy and cytotoxicity of DOX towards drug-resistant cancer cells	[330]
PAMAM and Oleic acid functionalized graphene oxide	pDNA	Expression of exogenous genes EGFP	[354]
Graphene oxide	Oligonucleotides	Molecular sensing	[169]
Graphene oxide	DNA aptamer	Molecular sensing	[355]
Chitosan functionalized graphene oxide	CPT, pDNA	Enhanced toxicity was observed in HepG2 and Hela cells compared to free CPT. pDNA was used to express endogenous gene luciferase	[343]
Polyethyleneimine functionalized graphene oxide	pDNA	Expression of endogenous genes EGFP	[356]
Polyethyleneimine functionalized graphene oxide	pDNA	Expression of exogenous genes EGFP	[357]
Octaarginine functionalized graphene oxide	pDNA	Expression of exogenous genes EGFP	[347]
PDMAEMA functionalized graphene oxide	pDNA, CPT	The nanocarrier showed very high potency of killing cancer cell *in vitro*. In addition to that pDNA was used to express endogenous gene luciferase	[348]
Polyethylene glycol and polyethylenimine dual□functionalized nano□graphene oxide	pDNA, siRNA	Photothermally controlled expression of exogenous gene (EGFP) and gene silencing (Plk-1)	[340]
Polyethylene glycol and polyethylenimine functionalized graphene oxide	Plasmid - siRNA	Gene silencing (Stat3)	[341]

Polyethylenimine functionalized graphene oxide	siRNA	Gene silencing (CXCR4)	[358]
Polyethylenimine /poly(sodium 4-styrenesulfonates/graphene oxide	Adriamycin, siRNA	The dual therapy of drug and gene overcome the multidrug resistivity of cancer cells *in vitro*	[293]
Branched polyethylenimine polyethylene glycol functionalized reduced graphene oxide	pDNA	Photothermally controlled expression of exogenous gene (luciferase)	[351]
Phospholipid-based amphiphilic polymer and cell penetrating peptide functionalized reduced graphene oxide	siRNA	Gene silencing (cell death siRNA)	[359]
Gold nanoparticles/nanorods encapsulated with graphene oxide functionalized with polyethyleneimine	pDNA	Expression of exogenous genes	[346]
PEGylated graphene/Au composites	siRNA	Gene silencing *(Bcl-2)*	[360]
Poly(amidoamine) dendrimer-grafted gadolinium-functionalized nano graphene oxide	EPI, miRNA	In presence of miRNA the IC_{50} value of EPI reduces dramatically than bare EPI for cancer cell killing.	[361]
Chitosan-supermagnetic iron oxide-graphene nanocomplex	DOX, pDNA	The nanocarrier effectively deliver DOX to lung cancer cells with very low IC_{50} value of 2 μM than free DOX 4 μM. The nanocarrier also effectively deliver pDNA to cancer cells which supports its use as a nonviral vector also	[362]
Poly(l-lactide)–polyethylene Glycol-grafted graphene quantum dots	miRNA	Gene silencing (miR-21, survivin)	[337]
Dendron conjugated graphene oxide	pDNA	Expression of endogenous genes EGFP	[23]
Polyethylenimine	pDNA	Expression of endogenous genes	[363]

graphene oxide/poly(D,L-lactic-co-glycolic acid)		EGFP	
Polyethylene glycol-engrafted graphene oxide	PNA	Gene silencing EGFR	[364]

DOX-Doxorubicin, CPT-Camptothecin, DXR-Doxorubicin hydrochloride, SN38-Camptothecin analogue hydrophobic molecule, 5-FU-5-Flurouracil, GMC-Gemcitabine, pDNA-plasmid DNA, EGFP-Enhanced green fluorescence protein, siRNA- Small interfering RNA, miRNA-Micro RNA, PNA- Peptide nucleic acid, EGFR- Epidermal growth factor receptor gene

5.4. Bioimaging:- For better understanding of simple to complex biological processes which occurs within living cells, tissues and whole organisms in our body has raised the necessity to develop new bioimaging tools, techniques and materials. In addition to this, bioimaging can help us to identify abnormal processes which are related with cancer and other diseases, thus underscoring its importance in medicine. At the primary stages of bioimaging includes tools and techniques to see biological processes in living cells, tissues, organs of animals/human using specialized imaging probes. However in case of medicinal applications, it is limited due to its poor sensitivity, specificity and targeting of bioimaging probes or bioimaging materials. So there is a continuous need to improve the performance of existing bioimaging probes/agents as well as to develop new advanced and specialized bioimaging probes/imaging agents and imaging modalities. Till now there are mainly three types of imaging techniques based on graphene nanomaterials, which are based on Raman spectroscopy fluorescence imaging and photoacoustic imaging. Details about these three techniques are discussed below.

5.4.1. Raman spectroscopy:- Raman spectroscopy relies upon the inelastic scattering of photon and has been extensively used as an analytical tool in wide range of applications. Recently Raman spectroscopy has been also used in the biomedical sectors including cancer

diagnosis to bioimaging as it can offer a brief information on chemical composition of cells and tissues[365]. In this context Raman spectroscopy extensively used to characterize graphene based nanomaterials (Graphene, GO, rGO, GQDs) due to its characteristic bands in the Raman spectra. As graphene is Raman active material it opened up a new route of bioimaging which completely depends upon the intrinsic structure and properties of graphene nanomaterials.

Incorporation of noble metal nanoparticles, such as gold nanoparticles or silver nanoparticles on the graphene nanomaterials surface further increase surface enhanced Raman scattering (SERS) which can be used to increase the Raman intensity and sensitivity in comparison with bare graphene nanomaterials[366]. As a result, a number of studies have been carried out to utilize this feature as imaging probes in biological cells.

As an example, Li and co-workers demonstrated that GO decorated with gold nanoparticles (AuNPs) can enhance Raman intensity of GO remarkably by the surface enhancement effect. They further used this Au/GO hybrids for Raman imaging in Hela229 cells as shown in Fig 20. They also studied cell internalization mechanism of GO and Au/GO hybrids using Raman imaging. An endocytosis pathway was proposed from the results[367]. Liu et al. made a graphene oxide and silver nanoparticle based Surface Enhanced Raman Scattering (SERS) probe for cancer cell imaging. By changing the weight ratio between $AgNO_3$ and GO, an optimum Raman enhancement was found with a ratio of 192. Under optimum conditions a very fast SERS imaging of cancer cells is obtained with a very short integration time of about 0.06s per pixel[368]. Zhang et al. also reported that GO/AuNPs/pATP hybrids are highly efficient for cell imaging. The characteristic G band of the GO at 1595 cm^{-1} is used to directly probe the GO and image the live cells. In presence of AuNPs, enhancement in the Raman intensity was observed which offers better cell imaging than GO alone[369].

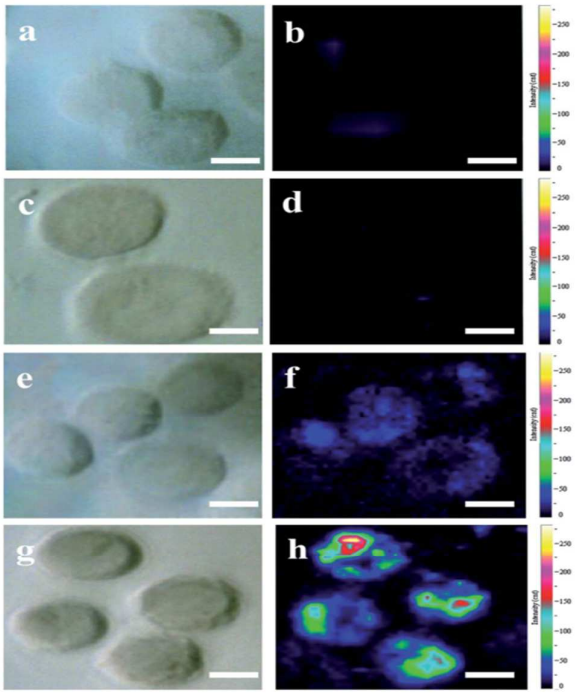

Figure 20. Optical (a, c, e and g) and Raman (b, d, f and h) images of Hela229 cells. Cells were incubated with GO (e and f) and Au/GO hybrids (gand h) at 37 C for 24 h before imaging. Cells incubated in medium without GO (a and b) and in medium with Au nanoparticles (c and d) are shown as control (scale bar: 10 mm). Reproduced with permission from ref [367]. Copyright 2012 Royal Society of Chemistry.

5.4.2. Fluorescence imaging:- Fluorescence based imaging techniques are extensively used in biology for bioimaging and diagnosis. Though fluorescence based imaging techniques have few drawbacks like photobleaching, photoblinking, degradation of the dye compound and background noise due to autofluorescence from tissue and cells[370]. However, a number of studies showed that graphene based nanomaterials are very effective for bioimaging applications. Based on intrinsic photoluminescence properties of nGO, Dai and his co-workers reported for the first time, B-cell specific antibody Rituxan conjugated and polyethylene glycol modified GO for Raj B-cells targeted fluorescence imaging using 658 nm

laser excitation[371]. But their system cannot be applied for *in vivo* system due to low quantum yield. Liu group synthesized a NIR Dye, Cy7 conjugated with nanographene sheets-polyethylene glycol (NGS-PEG) for *in vivo* fluorescence imaging of xenografted mice, which demonstrated high tumour accumulation of NGS-PEG-Cy7 based on the enhanced permeability and retention effect of cancerous tumours[372]. He and co-workers demonstrated in their work, receptor targeted imaging and theranostics using a graphene oxide based supramolecular glycocomposite. Their synthesized glycocomposite showed very good imaging ability to the cancer cells due to overexpression of glycoprotein receptor compared to control cells[373]. Chen et al. synthesized a new type of fluorescent probe based on graphene-QDs. Generally graphene quenches the fluorescence of the QDs. But they showed that the reduced graphene oxide (rGO) conjugated with QDs via a bridge bovine serum albumin can provide highly fluorescent nanoprobe for intercellular imaging[317]. Zhang et al. synthesized water soluble highly fluorescent GQDs for biological label of stem cells. Their synthesized GQDs demonstrated direct and easy cell penetration proliferation or differentiation capacity with strong photoluminescence (QY- 14%), good photostability and low cytotoxicity[374]. In a similar type of work, Yang and co-workers also reported strongly green fluorescent GQDs for bioimaging applications. The synthesized GQDs had a quantum yield of 11.4% with excellent biocompatibility. They used GQDs for imaging of MG-63 cells[92]. Wu and co-workers also used 1.5-5 nm sized green fluorescent GQDs for imaging of Hela cells [Fig 21][375].

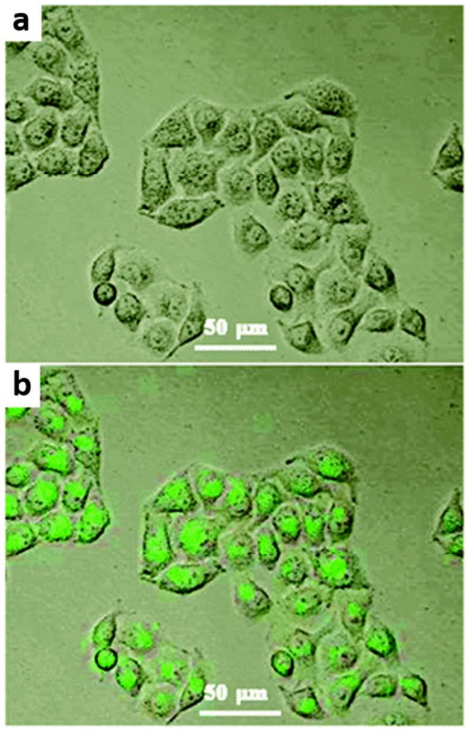

Figure 21. HeLa cells treated with the GQD suspension: (a) bright-field image, (b) confocal fluorescence photomicrograph taken with an excitation wavelength of 405 nm and the detection wavelength in the 420–520 nm range. Reproduced with permission from ref [375]. Copyright 2012 Royal Society of Chemistry.

Zhao and his team fabricated GQDs with a quantum yield of 54.5% from L-glutamic acid for *in vitro* and *in vivo* imaging. They showed that the GQDs can emit strong fluorescence in the green to red range for *in vitro* fluorescence imaging in MH-S cells. For *in vivo* imaging they used solution of GQDs of 25 mg ml^{-1} and injected to nude mice and applied various excitations (430, 465, 500, 535 and 605 nm). Under optimum conditions GQDs showed very good fluorescence signal in both visible and IR regions[103]. Nahain et al. synthesized a photoresponsive fluorescent rGO nanocomposite for *in vivo* imaging. The functionalized rGO nanocomposite can efficiently accumulate to tumour tissue in *in vivo* model and can be used as a fluorescent probe[376].

5.4.3. Photoacoustic imaging:- Photoacoustic imaging technique is an alternative method of non-invasive imaging which offers functional structural and molecular imaging. The imaging method relies upon photoacoustic phenomenon which admits conversion between light and acoustic waves due to the absorption of electromagnetic waves and localized thermal excitation. Recently, graphene nanomaterials have been extensively used as photoacoustic imaging agent due to its high NIR optical absorbance which enables greater spatial resolution than purely optical imaging especially in deep organ tissue while simultaneously overcoming the drawbacks of ultrasonic imaging technique regarding both biochemical contrast and speckle articrafts[377].

Liu and co-workers designed for the first time a novel probe based on rGO and iron oxide nanoparticle (IONP) functionalized with PEG for photoacoustic tomography[378]. Another study performed by Patel et al. where they reported microwave-enabled low oxygen graphene (ME-LOGr) can exhibit strong and wavelength independent visible and NIR absorption. They found that the absorption of ME-LOGr (with a coefficient of 22.7 L/g.cm at 808 nm) can exceed one of the best NIR fluorophores indocyane green (absorption coefficient of 13.9 L/g.cm at 808 nm) and provides clearer cellular background. The difference in NIR absorption and endogenous background resulted in excellent optical limiting photoacoustic imaging applications in addition to that as graphene nanosheets are non-luminescent, so that all the optical energy absorbed by graphene nanosheets would transformed into heat which can be used for acoustic wave generation. In contrast to GO ME-LOGr nanosheets exhibited remarkably strong photoacoustic signals at same concentration (0.04 mg/ml) under the wavelength independent NIR laser irradiation as shown in Figure 22 which is very different from other photoacoustic imaging agents like Au nanorods and Ag nanoplates[377].

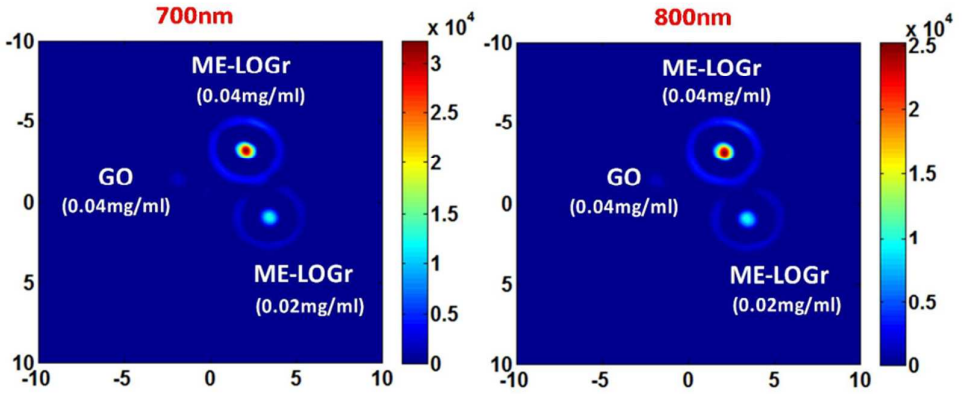

Fig-22: Photoacoustic (PA) signal of GO and graphene nanosheets of different concentrations,

illuminated with 700nm and 800nm laser. The colour coded vertical bar represents the strength of the photoacoustic signal generated. Reproduced with permission from ref[377]. Copyright 2013 American Chemical Society.

Lalwani et al. investigated the role of graphene nanoribbons as photoacoustic and imaging agent. In details they observed that single or multiwalled graphene oxide nanoribbons can enhance the photoacoustic signals 5-10 folds in comparison to blood at the wavelength of 755 nm[379]. Lim and co-workers also synthesized a hybrid nanomaterial based on rGO and gold nanorods (rGO-AuNRs) for photoacoustic imaging. The efficiency of the hybrid system relies upon excellent NIR absorption properties of rGO. Their hybrid system have much higher photoacoustic amplitudes than bare AuNRs or nonreduced graphene oxide-AuNRs (GO-AuNRs) or silica coated gold nanorods in both *in vitro* and *in vivo* systems. Using a 755 nm laser irradiation and varying laser powers to (4-9 mJ/cm^2) to get photoacoustic images. The rGO-AuNRs exhibited the highest photoacoustic signals in animal model among all the samples (AuNRs: 19.34 ± 0.30, GO-AuNRs: 19.34 ± 1.03, and r-GO-AuNRs: 28.81 ± 0.84; 6.0 mJ/cm2 incident laser power), their finding is also consistent with in-vitro experiments[380]. Sheng et al. also demonstrated nano sized rGO stabilized with BSA can be used as

photoacoustic imaging both *in-vitro* and *in-vivo*[381]. Similar to GO and rGO or hybrid systems containing GO/rGO, pristine graphene also can be used as photoacoustic imaging agent. In a recent work done by Paradossi and co-workers where they showed pristine graphene also can be used as photoacoustic agent *in-vivo*. To use the pristine graphene they interfaced with acoustic contrast poly(vinyl alcohol) (PVA) shelled microbubbles. The assembly between PVA microbubbles and pristine graphene capable to capture the radiation by the graphene sheets in the transparent NIR region between 700-850 nm. Despite very low dose of graphene they got good enhancement in photoacoustic signal in *in-vivo* i.e. 6.6 a.u. with respect to 0.6 a.u. of endogenous background[382]. So from the above discussion we can say that there are enormous possibilities that graphene nanomaterials can be used as a photoacoustic agent for *in-vivo* deep tissue imaging. **Table 5** summarizes the graphene based nanomaterials for bioimaging applications.

Table 5. List of graphene based materials for bioimaging application

Platform	Imaging tool	Use	References
Graphene oxide decorated with gold nanoparticles	Raman	Imaging of Hela cells	[367]
Folic acid conjugated graphene oxide decorated with silver nanoparticles	Raman	Imaging of Hela cells	[368]
Gold nanoparticles/ 2-aminoethanethiol/ graphene oxide/ fluorescein isothiocyanate or Gold nanoparticles/ p-aminothiophenol/ graphene oxide	Fluorescence and Raman bimodal imaging, multifrequency Raman imaging	Imaging of Hela 229 cells	[369]
Polyethylene glycol functionalized nano graphene oxide conjugated with Rituxan	NIR fluorescence	CD20 positive Raji B-cells	[371]

Glycoprobe conjugated graphene oxide	Fluorescence	Imaging of HepG2 cells	[373]
Graphene quantum dots	Fluorescence	Imaging of neurospheres stem cells	[374]
Graphene quantum dots	Fluorescence	Imaging of Hela 229 cells	[375]
Dopamine-spiropyran-hyaluronic acid conjugated graphene oxide	Fluorescence	Imaging of MDCK, A549 cells *in vitro*, as well as *in vivo* imaging of tumor site present in mouse	[376]
Amino-functionalized nitrogen-doped graphene quantum dots	Fluorescence	Imaging of bacteria and KB-50 cancer cells	[383]
Microwave-enabled low oxygen graphene nanosheets	Photoacoustic	The fabricated graphene nanosheets exhibited strong NIR absorption and high photoacoustic conversion efficiencies, which suggests its applicability for deep tissue imaging	[377]
Polyethylene glycol functionalized reduced graphene oxide-iron oxide nanoparticles	Fluorescence, photoacoustic, magnetic resonance imaging	The nanocomposite demonstrated excellent triple modal tumour imaging capability *in vivo* due to the EPR effect	[378]
Oxidized single- and multiwalled graphene oxide nanoribbons	Photoacoustic and thermoacoustic	Very good photoacoustic and thermoacoustic signal observed with laser irradiation which indicates its potential use as photoacoustic and thermoacoustic imaging agent for deep tissue imaging	[379]
Reduced graphene oxide coated gold nanorods (rGO-AuNRs)	Photoacoustic	Very good photoacoustic signal was observed for both *in vitro* and *in vivo* imaging. In case of *in vivo* imaging the rGO-AuNRs showed highest PA signal intensities among all of the samples (AuNRs: 19.34±0.30, GOAuNRs: 19.34±1.03, and r-GO-AuNRs: 28.81± 0.84; 6.0 mJ/cm2 incident laser power)	[380]
Bovine serum albumin functionalized nano graphene oxide	Photoacoustic	Imaging of MCF7 cells *in vitro*	[381]

Graphene-polyvinyl alcohol microbubbles	Photoacoustic	Deep tissue imaging in-vivo	[382]

5.5. Photothermal and photodynamic therapy:- Temperature is an important parameter by which the viability and functionality of biological species including cells, tissues or entire organs are tightly regulated. The increase of temperature above the regular body temperature (37 °C) is the indication of illness/disease. But, the increase of temperature in targeted tissues/organs by controlled way has been reported to have several therapeutic advantages in patients with cancer or other diseases[384]. The therapeutic temperature range between 41-48 ^{O}C has been reported clinically for the thermal treatment of diseases known as hypothermia[385]. Moderate level of hypothermia is adequate for inducing protein denaturation and aggregation and it is quite different from normal cancer treatments by chemotherapy. In contrast, short thermal treatments above 48 ^{O}C even for few minutes can cause severe cell/tissue damage or permanent cells and tissues damages may happen by long exposures through excessive necrosis and ablation[106]. As a consequence, it has become the most important effort to develop smart materials and techniques in advanced thermal therapies where the heating can be localized. In this regard, photothermal therapy (PTT) has gained incredible attention owing to its unique mechanism where the generated heat can be localized by controlled way using optical energy exposure. Graphene nanomaterials catch tremendous consideration among the various number of nanomaterials developed for photothermal therapy due to its strong optical absorption in the NIR range and consequently makes it one of the promising candidate for PTT application. In addition to this, further modification/functionalization of graphene would provide the generation of hybrid/composite materials with better temperature control and greater dynamic range of heating.

In case of, photodynamic therapy (PDT) there is involvement of a laser and a photosensitizing chemical substance which can produce reactive oxygen species (ROS) and

causes cell death. Recently along with PTT graphene nanomaterials also used in PDT to deliver the photosensitizing agent at the therapeutic site. Already it is well established that graphene based nanomaterials are highly efficient to carry the PDT agents and can treat many debilitating disease like cancer[386].

Liu and co-workers demonstrated for the first time *in vivo* behaviour of nanographene sheets with polyethylene glycol (PEG) coating by a florescent labelling methods. Then they used strong optical absorbance of nanographene sheets in the NIR region for *in vivo* photothermal therapy, achieving very efficient tumour ablation after intravenous administration of nanographene sheets (NGS) in the NIR region for *in vivo* photothermal therapy[372] as shown in Fig 23. Yang et al. used PEG functionalized nanographene sheets anchored with magnetic iron nanoparticles for multimodal imaging guided photothermal therapy. Utilizing strong NIR absorbance of graphene and magnetic property of iron nanoparticles, they used RGO-IONP-PEG nanocomposite for *in vivo* triple modal fluorescence, photoacoustic tomography and tumour imaging and photothermal therapy. They observed that upon irradiation of 808 nm NIR laser at a low power density of 0.5W/cm^2, tumours of mice can be treated effectively[378]. Dai and co-workers synthesised ultrasmall reduced graphene oxide sheets with extraordinary NIR absorbance for photothermal therapy. They also used PEG to render stability in biological solutions. Then they attached a target peptide containing Arg-Gly-Asp (RGD) motif for selective cellular uptake in U87MG cancer cells and highly effective photoablation of cells *in vitro*[387]. Tian et al. demonstrated enhanced photodynamic therapy (PDT) by Chlorin e6 loaded PEG functionalized graphene oxide. The synthesized GO-PEG-Ce6 complex showed excellent water solubility and generate cytotoxic singlet oxygen under optical excitation for photothermal therapy[386].

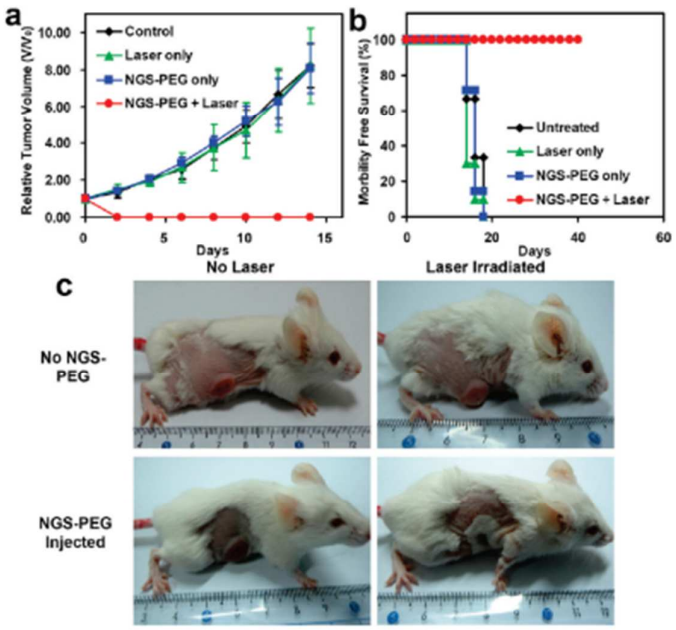

Figure 23. *In vivo* photothermal therapy study using intravenously injected NGS-PEG. (a) Tumor growth curves of different groups after treatment. The tumor volumes were normalized to their initial sizes. There were 6 mice in the untreated, 10 mice in the 'laser only', 7 mice in the 'NGS-PEG only', and 10 mice in the 'NGS-PEG + laser' groups. While injection of NGS-PEG by itself or laser irradiation on uninjected mice did not affect tumor growth, tumors in the treated group were completely eliminated after NGS-PEG injection and the followed NIR laser irradiation. (b) Survival curves of mice bearing 4T1 tumor after various treatments indicated. NGS-PEG injected mice after photothermal therapy survived over 40 days without any single death. (c) Representative photos of tumors on mice after various treatments indicated. The laser irradiated tumor on NGS injected mouse was completely destructed. Error bars in (a) were based on standard deviations. Reproduced with permission from ref[372]. Copyright 2010 American Chemical Society.

They showed that the combination of NIR light triggered mild photothermal heating of graphene and photodynamic therapy using Ce6 delivered by GO-PEG, which enhances the

overall PDT efficiency remarkably. Akhavan and co-workers synthesised reduced graphene oxide nanomesh (rGONM), another promising candidate for photothermal therapy. After synthesising of rGONMs, they functionalized it with polyethylene glycol, a RGD based peptide and cyanine 7 for better targeted therapy of U87MG tumours. The 1μg/ml suspension of rGONM-PEG exhibited around 4.2- and 22.4- fold NIR absorption at 808 nm compared to reduced graphene oxide nanoplatelet- polyethylene glycol and graphene oxide, respectively. The excellent NIR absorbance of rGONM-PEG-Cy7- RGD complex resulted in ultra-efficient photothermal therapy for tumour treatment. They eliminated 100% tumour after 48 h intravenous injection of rGONM-PEG-Cy7-RGD with ultra-low concentration of 10μg/ml followed by irradiation with a low laser power (0.1 Wcm^{-2}) for 7 min[388]. Huang and co-workers reported a method for synergistic photothermal therapy to treat glioma with the help of functionalized mesoporous silica coated graphene nanosheets. They modified the graphene nanosheets with a targeting peptide and coated with silica nanoparticles. The functionalized silica coated graphene nanosheets (GSPI) showed heat responsive, pH sensitive and sustained release properties of drugs. The DOX loaded GSPI system demonstrated the synergistic therapy mediated highest rate of glioma cell death compared to single photothermal therapy or chemotherapy. The photothermal heating effect of GSPI exhibited a concentration dependent and laser power intensity dependent way which is far better than carbon nanotube[389]. Li et al. used high NIR absorbance of graphene oxide for photothermal treatment of Alzheimer's disease. They utilized thioflavin-S (ThS) modified GO for remote and local heating and to dissociate amyloid aggregation upon NIR laser irradiation. The ThS modified GO selectively bind with Aβ aggregates which are the main reason of Alzheimer and form GO–ThS–Aβ complex. After the complex formation, they used strong NIR optical absorption ability of nano GO to generate local heat and destroy the Aβ fibrils followed by low power NIR laser irradiation[390]. Tae and co-workers exhibited graphene oxide mediated delivery of

methylene blue, a photosensitizer for combined photodynamic and photothermal therapy of cancer. The nano GO play a dual role of photothermal therapy as well as a carrier for photosensitizer. The release of the methylene blue from nano GO surface was pH dependent and an acidic condition increased the release rate significantly. The nanocomplex showed enhanced cellular uptake by cancerous HeLa cells in mice rather than normal cells and showed no major toxicity towards the cells in the absence of optical energy. After the NIR light irradiation, mice were observed for 15 days none of mice was died and no drastic change was observed in their body weight[391]. Ge et al. reported GQDs for photodynamic therapy agent with high singlet oxygen generation. Their synthetized GQD based PDT agent can produce $^1O_2$ via a multistate sensitization process resulted highest quantum yield till date among other PDT agents. The performance of the GQDs for *in vivo* PDT was assessed using female BALB/nude mice with subcutaneous breast cancer xenografts as an animal model. GQDs were injected with a concentration of 4 mg/kg then irradiated twice, with white light (400–800 nm) at a power density of 80 mW cm^{-2}on the first and seventh days, for 10 min. The tumours start to decompose after 9 days and were destroyed completely after 17 days, leaving black marks at the original sites, which fell off ~1 week later. No tumour regrowth was detected in the PDT group over the course of 50 days[392]. In a recent study by Srivastava and his co-workers reported multifunctional graphene quantum dots for combined photothermal and photodynamic therapy with cancer cell tracking applications. They showed that upon irradiation of 808 nm laser (0.5W/cm2), a concentration dependent photothermal response were observed with generation of large amount of reactive oxygen species which can kill cancer cells[393]. Guo et al. demonstrated that, ruthenium nitrosyltriphenylphosphonium functionalized GQDs (NGQDs@Ru-NO@TPP) can be used as an efficient nanoplatform for NIR light triggered and mitochondria targeted delivery of nitric oxide combined

photothermal therapy. Upon irradiation of NIR light, it instantly released NO and exhibited photothermal effect for both *in vitro* and *in vivo* tumour model[394]. In another study, Shi et al. used a graphene based magnetic plasmonic nanocomposite for photothermal therapy. They decorated graphene oxide by both iron oxide nanoparticles (IONP) and gold nanoparticles (AuNP) and formed a multifunctional magnetic plasmonic nanocomposite. To investigate the enhanced PTT efficacy of their system, they introduced an 808 nm NIR laser at a power density of 1 W/cm^2 to irradiate PEGylated GO (GO-PEG), PEGylated GO-IONP (GO-IONP-PEG), and GO-IONP-Au-PEG at the same GO concentration of 10 mg/mL for 5 min. The temperature of GO-IONP-Au-PEG increased rapidly from 23 ^{O}C to 40 ^{O}C whereas other solutions showed much less temperature change, consistent with the much stronger NIR absorbance of the former. *In vitro* studies in 4T1 breast cancer cells showed that almost all cancer cells were killed after incubation with the nanocomposite upon exposure of 808 nm laser (2 Wcm^{-2} for 5 min). Mice bearing 4T1 tumours were then intratumorally injected with GO-IONP-Au-PEG at a dose of 50 μg/ml and subjected to an 808 nm laser at 0.75 W cm-2 for 5 min. IR thermal images revealed that the surface temperature of the tumours injected with the nanohybrid increased rapidly to about 55 °C within 5 min of laser irradiation and destroyed the tumour cells[395]. Recently to enhance the therapeutic efficiency of graphene based nanomaterials the combination of both PTT and PDT are used by reseachers. In this context, Taratula and co-workers reported Pthalocyanine (Pc) loaded graphene nanosheets for combinatorial photothermal and photodynamic therapy. In details they developed chemically modified polypropylenimine dendrimers graphene nanosheets loaded with Pc as a photosensitizer. To increase the biocompatibity of the nanoplatform system they combined it with PEG molecule as well as for tumour targeted delivery they conjugated luteinizing hormone-releasing hormone (LHRH) peptide. A low power NIR laser was irradiated for simultaneous heat generation (PTT) and ROS production

(PDT). Their combinatorial phototherapy demonstrated synergistic destruction of ovarian cancer cells with a killing efficacy of 90-95% at low Pc and low oxygen graphene dosages[396]. Another study done by Zhang et al. in which they exhibited that, reduced graphene oxide with ruthenium(II)-polyethylene glycol (Ru(II)-PEG) can be used as a ultra-efficient photodynamic and photothermal therapy agent to kill cancer cells. The release of Ru-PEG from the rGO surface was pH dependent and irradiation of optical energy can increase the release rate. The synergistic effect of PDT and PTT have been studied by cytotoxicity study by serial irradiation of 808 nm and 450 nm laser. A detailed study on mechanism investigation showed that the nanocomplex can induce programmed cell death through generation of reactive oxygen species and cathepsin-initiated apoptotic signalling pathways under light excitation. Further they used rGO-Ru-PEG nanocomposite for *in vivo* photothermal treatment of cancer with irradiation of 808 nm and 450 nm laser[397]. **Table 6** summarizes the graphene based nanomaterials for PTT and PDT therapy.

Table 6. List of graphene based materials for photothermal/photodynamic therapy

Platform	Application	Results	References
Chlorin e6 loaded, polyethylene glycol functionalized graphene oxide	Photothermal and photodynamic therapy	The combination of NIR light-triggered mild photothermal heating of graphene and the photodynamic treatment using Chlorin e6 delivered by the graphene oxide enhances the PDT efficacy remarkably	386
Polyethylene glycol functionalized nano reduced graphene oxide tagged with arginine–glycine–aspartic acid or arginine-alanine-aspartic acid peptide loaded with cyanine 5 dye	Photothermal therapy	6-fold enhancement in NIR absorbance with nano reduced graphene oxide. Selective uptake to cancer cells and photothermal ablation in vitro	387
Polyethylene glycol	Photothermal Therapy	4.2, 22.4 times enhancement in NIR absorption than bare polyethylene	388

functionalized arginine–glycine–aspartic acid peptide conjugated reduced graphene oxide nanomesh loaded with cyanine 7		glycol functionalized reduced graphene oxide and graphene oxide with ultraefficient photothermal therapy (100% tumor elimination 48h after intravenous injection of an ultralow concentration (10 μg mL^{-1}) and ultralow laser power *in vivo*	
Polyethylene glycol functionalized mesoporous silica coated graphene nanosheets conjugated with a cancer cell targeting peptide	Photothermal therapy, Chemotherapy	High absorption in the NIR window and efficient heat transformation for photothermal therapy. In addition to that, a NIR responsive drug release profile and synergistic cancer cell killing efficacy was observed by dual chemo-photothermal therapy	[389]
Thioflavin□S modified graphene oxide	Photothermal therapy	Thioflavin□S modified graphene oxide demonstrated very good photothermal therapy to cure Alzheimer Diseases. It selectively attached to A β aggregates and form the conjugated GO–ThS–A β. The strong NIR optical absorption ability of nano graphene oxide generate local heat which dissociate the A β fibrils in presence of low-power NIR laser	[390]
Nano graphene oxide sheet (nanoGO) functionalized with Pluronic block copolymer loaded with methylene blue	Photothermal and photodynamic therapy	The nanocomplex showed enhanced uptake by cancer cells than normal cells and in absence of light it showed no major toxicity towards the cells. However, when irradiated with selective NIR laser lights, it induced significant cell death. Additionally intravenous injection of the complex into tumor bearing mice showed high tumor accumulation, and when the tumors were exposed to NIR lights, it caused total ablation of tumor tissue through the combined action of photodynamic and photothermal therapy	[391]
Graphene quantum dots	Photodynamic therapy	The PDT agent based on graphene quantum dots produced $^1O_2$ via a multistate sensitization process, which resulted in a quantum yield of ~1.3, the highest reported for PDT agents. Additionally the synthesized graphene quantum dot	[392]

		showed very high efficiency PDT therapy of cancer *in vivo*	
Graphene quantum dots	Photothermal and photodynamic therapy	Upon irradiation with an 808 nm laser (0.5 W cm^{-2}), a concentration-dependent photothermal response and production of reactive oxygen species were observed. Furthermore it showed very good PTT and PDT towards MDA-MB-231 breast cancer cells *in vitro*	[393]
Ruthenium nitrosyl functionalized graphene quantum dots	Photothermal therapy	The nanoplatform demonstrated both in vitro and in vivo anti-tumor efficacy upon irradiation with 808 nm light	[394]
Graphene-iron oxide nanoparticles-gold nanoparticles coated with polyethylene glycol	Photothermal therapy	Remarkably enhanced photothermal cancer ablation effect is observed in comparison with polyethylene glycol functionalized graphene oxide both *in vitro* and *in vivo*	[395]
Polyethylene glycol functionalized phthalocyanine-loaded graphene nanoplatform	Photothermal and photodynamic therapy	The combinatorial phototherapy resulted in an enhanced destruction of ovarian cancer cells, with a killing efficacy of 90%–95% at low phthalocyanine and low-oxygen graphene dosages, which confirmed cytotoxicity to the synergistic effects of generated ROS and mild hyperthermia	[396]
Graphene oxide decorated with ruthenium(II)–polyethylene glycol	Photothermal and photodynamic therapy	The nanohybrid induced apoptosis in cancer cells through generation of reactive oxygen species (ROS) and cathepsin-initiated apoptotic signalling pathways under light excitation	[397]
Palladium nanoparticle-decorated 2-D graphene oxide	Photothermal and photodynamic therapy	Compared to graphene oxide or palladium nanoparticles alone, the nanohybrid showed higher cytotoxic effects in prostate cancer 3 (PC3) cells. In addition to that, irradiation of treated cells with near infrared (NIR) laser demonstrated considerably enhanced apoptosis induced by synergistic photothermal effect and reactive oxygen species (ROS) generation	[397]

6. Conclusion and future perspective:- Since the revolutionary discovery of graphene in the year of 2004, it has gained ever increasing interest from scientific community due to its exceptional properties. Because of its extraordinary properties, graphene nanomaterials already being used in a wide range of applications including optoelectronics, sensing, catalysis and even bioapplications like drug/gene delivery, tissue engineering, biosensors, photothermal therapy, and bioimaging. In this review, we have sought to provide an outlook from the synthesis of graphene based nanomaterials to their end bioapplications.

In terms of synthesis, already there are various synthesis methods for graphene nanomaterials. However the optimal method depends upon its end applications. During the last few years graphene based nanomaterials have been used in wide range of biomedical applications including biosensors, photodynamic and photothermal therapies, tissue engineering and regenerative medicine due to their outstanding physical, chemical and biological properties not only that, the specific arrangements of graphene provide a robust absorbing capability which makes it a novel carrier for gene/drug delivery. In addition to this, graphene and graphene family nanomaterials opened up a new platform for photothermal therapy and bioimaging due to its unique properties. On the other hand, due to the high electrical conductivity of graphene it is employed as various types of biosensor. However, the control over synthesis processes, the lack of reproducibility and the difficult characterization techniques render these materials for clinical applications[398]. Another major problem consist that the nanomaterial changes its characteristics during biological experiments, so its physicochemical characterization should be carried out under same experimental conditions, which makes the tasks more complicated and this problem also applied for graphene based nanomaterials. To overcome these problems, researchers are trying to establish a protocol and some standardized way by comparing different characterization results, where all crucial factors should be considered[399]. In this context, there are some recent efforts done by

researchers on nanoinformatics which are focused on minimal characterization criteria of nanomaterials[400].

There are already some physicochemical characterizations considered very essential before any applications of graphene based nanomaterials, including oxygen content, the size of the graphene flakes and the number of graphene sheet layers[401]. However, there is still no clear idea on the differences in biological behaviour between small and large sheets, single/few/multilayer graphene sheets while the amount of oxygen can also cause undesirable effects. Achieving good aqueous stability of graphene nanomaterials play a crucial role for any biological application as aggregated graphene can cause toxicity, so the colloidal stability is another critical factor should be always taken into account when running any biological experiments, since the interactions of cells with the graphene environment could change whether it is a freshly-prepared suspension or after hours or days or months of preparation. Regarding this, GO and GQDs based nanomaterials have an easier handling in aqueous media while pristine graphene not so much stable in aqueous media and requires external physical processes (such as sonication)/chemical agents (FDA approved biopolymer such as PEG which are already extensively used for functionalization of graphene based polymer to increase both biocompatibility and to make it stable for longer period of time) to get a stable suspension. For any specific applications, it is very important to run a control suspension of graphene based materials in the media of working interest and continuously monitor the process by means of spectroscopic (e.g. DLS, Raman Spectroscopy) or microscopic techniques (e.g. TEM, SEM, AFM)[402].

Apart from these, any medical devices/drugs for clinical applications require permission from special regulatory authorities which is often concerns with the toxicity of the new materials which also applied for graphene based materials also. However, the future prospects of graphene nanomaterials are very bright and optimistic. Combination of graphene

nanomaterials with other material compositions that have good flexibility or wettability make them better candidates for fabrication of multifunctional smart materials.

As a result these graphene nanomaterial composites can become environmental sensitive or self-folding properties or more biocompatible which can extend their biomedical applications but till now most of the graphene based nanomaterials are at research stage, we have to wait few more years to get these nanomaterials for real life clinical applications.

So, for real life clinical applications of graphene nanomaterials it is necessary to focus on-

- The reproducibility during the synthesis graphene nanomaterials, so we can proceed forward without any question.
- Stability of the graphene nanomaterials, aggregation can leads to severe toxicity.
- Proper functionalization so it can be biostable, biocompatible and biodegradable.
- Most importantly to check the biocompatibility of the graphene nanomaterials *in vivo* not only in small animal model such as mouse but also in bigger animal model such as sheep, monkey etc. If we solve these problems there is a huge scope beyond our imagination what graphene nanomaterials can offer in the field of biomedical applications.

Acknowledgement: This work is financially supported by DST-SERB funding agency through two sanctioned projects *EEQ/2016/000712* and *ECR/2016/002018*. K.S. also acknowledge UGC for UGC-BSR Research Start-Up Grant (F.30-363/2017(BSR), Dt-08/08/2017) and CU for UPE-II Nanofabrication project fund (UGC/166/UPE-II, Dt-03/04/2017) for financial support.

References:

1. Mirkin, C. A., The Beginning of a Small Revolution. *Small* **2005,** *1* (1), 14-16. DOI: 10.1002/smll.200400092.
2. Li, X.; Cai, W.; An, J.; Kim, S.; Nah, J.; Yang, D.; Piner, R.; Velamakanni, A.; Jung, I.; Tutuc, E.; Banerjee, S. K.; Colombo, L.; Ruoff, R. S., Large-Area Synthesis of High-Quality and Uniform Graphene Films on Copper Foils. *Science* **2009,** *324* (5932), 1312-1314. DOI: 10.1126/science.1171245.
3. Ranjbartoreh, A. R.; Wang, B.; Shen, X.; Wang, G., Advanced mechanical properties of graphene paper. *Journal of Applied Physics* **2011,** *109* (1), 014306. DOI: 10.1063/1.3528213.
4. Balandin, A. A.; Ghosh, S.; Bao, W.; Calizo, I.; Teweldebrhan, D.; Miao, F.; Lau, C. N., Superior Thermal Conductivity of Single-Layer Graphene. *Nano Letters* **2008,** *8* (3), 902-907. DOI: 10.1021/nl0731872.
5. Wu, Z.-S.; Ren, W.; Gao, L.; Zhao, J.; Chen, Z.; Liu, B.; Tang, D.; Yu, B.; Jiang, C.; Cheng, H.-M., Synthesis of Graphene Sheets with High Electrical Conductivity and Good Thermal Stability by Hydrogen Arc Discharge Exfoliation. *ACS Nano* **2009,** *3* (2), 411-417. DOI: 10.1021/nn900020u.
6. Nair, R. R.; Blake, P.; Grigorenko, A. N.; Novoselov, K. S.; Booth, T. J.; Stauber, T.; Peres, N. M. R.; Geim, A. K., Fine Structure Constant Defines Visual Transparency of Graphene. *Science* **2008,** *320* (5881), 1308-1308. DOI: 10.1126/science.1156965.
7. Novoselov, K. S.; Geim, A. K.; Morozov, S. V.; Jiang, D.; Zhang, Y.; Dubonos, S. V.; Grigorieva, I. V.; Firsov, A. A., Electric field effect in atomically thin carbon films. *science* **2004,** *306* (5696), 666-669.
8. Lee, C.; Wei, X.; Kysar, J. W.; Hone, J., Measurement of the Elastic Properties and Intrinsic Strength of Monolayer Graphene. *Science* **2008,** *321* (5887), 385-388. DOI: 10.1126/science.1157996.
9. Bunch, J. S.; van der Zande, A. M.; Verbridge, S. S.; Frank, I. W.; Tanenbaum, D. M.; Parpia, J. M.; Craighead, H. G.; McEuen, P. L., Electromechanical Resonators from Graphene Sheets. *Science* **2007,** *315* (5811), 490-493. DOI: 10.1126/science.1136836.
10. Bonaccorso, F.; Sun, Z.; Hasan, T.; Ferrari, A. C., Graphene photonics and optoelectronics. *Nature Photonics* **2010,** *4*, 611. DOI: 10.1038/nphoton.2010.186.
11. Novoselov, K. S.; Jiang, Z.; Zhang, Y.; Morozov, S. V.; Stormer, H. L.; Zeitler, U.; Maan, J. C.; Boebinger, G. S.; Kim, P.; Geim, A. K., Room-Temperature Quantum Hall Effect in Graphene. *Science* **2007,** *315* (5817), 1379-1379. DOI: 10.1126/science.1137201.
12. Geim, A. K.; Novoselov, K. S., The rise of graphene. *Nature Materials* **2007,** *6*, 183. DOI: 10.1038/nmat1849.
13. Lu, Y.-H.; Zhou, M.; Zhang, C.; Feng, Y.-P., Metal-Embedded Graphene: A Possible Catalyst with High Activity. *The Journal of Physical Chemistry C* **2009,** *113* (47), 20156-20160. DOI: 10.1021/jp908829m.
14. Wang, B.; Chang, Y.-h.; Zhi, L.-j., High yield production of graphene and its improved property in detecting heavy metal ions. *New Carbon Materials* **2011,** *26* (1), 31-35. DOI: https://doi.org/10.1016/S1872-5805(11)60064-4.
15. Zhao, X.; Hayner, C. M.; Kung, M. C.; Kung, H. H., Flexible Holey Graphene Paper Electrodes with Enhanced Rate Capability for Energy Storage Applications. *ACS Nano* **2011,** *5* (11), 8739-8749. DOI: 10.1021/nn202710s.
16. Liu, K.; Zhang, J.-J.; Cheng, F.-F.; Zheng, T.-T.; Wang, C.; Zhu, J.-J., Green and facile synthesis of highly biocompatible graphene nanosheets and its application for cellular imaging and drug delivery. *Journal of Materials Chemistry* **2011,** *21* (32), 12034-12040. DOI: 10.1039/C1JM10749F.
17. Parlak, O.; Tiwari, A.; Turner, A. P. F.; Tiwari, A., Template-directed hierarchical self-assembly of graphene based hybrid structure for electrochemical biosensing. *Biosensors and Bioelectronics* **2013,** *49*, 53-62. DOI: https://doi.org/10.1016/j.bios.2013.04.004.

18. Lu, Y.; Lyu, H.; Richardson, A. G.; Lucas, T. H.; Kuzum, D., Flexible neural electrode array based-on porous graphene for cortical microstimulation and sensing. *Scientific reports* **2016,** *6*, 33526.
19. Wang, J., Glucose biosensors: 40 years of advances and challenges. *Electroanalysis* **2001,** *13* (12), 983.
20. Wang, J., Electrochemical glucose biosensors. *Chemical reviews* **2008,** *108* (2), 814-825.
21. Sayyar, S.; Murray, E.; Thompson, B. C.; Gambhir, S.; Officer, D. L.; Wallace, G. G., Covalently linked biocompatible graphene/polycaprolactone composites for tissue engineering. *Carbon* **2013,** *52*, 296-304.
22. Kumar, S.; Raj, S.; Sarkar, K.; Chatterjee, K., Engineering a multi-biofunctional composite using poly (ethylenimine) decorated graphene oxide for bone tissue regeneration. *Nanoscale* **2016,** *8* (12), 6820-6836.
23. Sarkar, K.; Madras, G.; Chatterjee, K., Dendron conjugation to graphene oxide using click chemistry for efficient gene delivery. *RSC Advances* **2015,** *5* (62), 50196-50211.
24. Sheng, Y.; Tang, X.; Peng, E.; Xue, J., Graphene oxide based fluorescent nanocomposites for cellular imaging. *Journal of Materials Chemistry B* **2013,** *1* (4), 512-521.
25. Choi, J.; Wang, M. C.; Cha, R. Y. S.; Park, W. I.; Nam, S., Graphene bioelectronics. *Biomedical Engineering Letters* **2013,** *3* (4), 201-208. DOI: 10.1007/s13534-013-0113-z.
26. Park, S.; An, J.; Jung, I.; Piner, R. D.; An, S. J.; Li, X.; Velamakanni, A.; Ruoff, R. S., Colloidal suspensions of highly reduced graphene oxide in a wide variety of organic solvents. *Nano letters* **2009,** *9* (4), 1593-1597.
27. Chen, Z.; Ren, W.; Gao, L.; Liu, B.; Pei, S.; Cheng, H.-M., Three-dimensional flexible and conductive interconnected graphene networks grown by chemical vapour deposition. *Nature materials* **2011,** *10* (6), 424-428.
28. Terasawa, T.-o.; Saiki, K., Synthesis of nitrogen-doped graphene by plasma-enhanced chemical vapor deposition. *Japanese Journal of Applied Physics* **2012,** *51* (5R), 055101.
29. Jayasena, B.; Subbiah, S., A novel mechanical cleavage method for synthesizing few-layer graphenes. *Nanoscale research letters* **2011,** *6* (1), 95.
30. Yang, W.; Chen, G.; Shi, Z.; Liu, C.-C.; Zhang, L.; Xie, G.; Cheng, M.; Wang, D.; Yang, R.; Shi, D., Epitaxial growth of single-domain graphene on hexagonal boron nitride. *Nature materials* **2013,** *12* (9), 792-797.
31. Veeramani, V.; Sivakumar, M.; Chen, S.-M.; Madhu, R.; Alamri, H. R.; Alothman, Z. A.; Hossain, M. S. A.; Chen, C.-K.; Yamauchi, Y.; Miyamoto, N.; Wu, K. C. W., Lignocellulosic biomass-derived, graphene sheet-like porous activated carbon for electrochemical supercapacitor and catechin sensing. *RSC Advances* **2017,** *7* (72), 45668-45675. DOI: 10.1039/C7RA07810B.
32. Purkait, T.; Singh, G.; Singh, M.; Kumar, D.; Dey, R. S., Large area few-layer graphene with scalable preparation from waste biomass for high-performance supercapacitor. *Scientific Reports* **2017,** *7* (1), 15239. DOI: 10.1038/s41598-017-15463-w.
33. Shams, S. S.; Zhang, L. S.; Hu, R.; Zhang, R.; Zhu, J., Synthesis of graphene from biomass: A green chemistry approach. *Materials Letters* **2015,** *161*, 476-479. DOI: https://doi.org/10.1016/j.matlet.2015.09.022.
34. Al-Hazmi, F.; Al-Harbi, G. H.; Beall, G. W.; Al-Ghamdi, A.; Obaid, A.; Mahmoud, W. E., One pot synthesis of graphene based on microwave assisted solvothermal technique. *Synthetic Metals* **2015,** *200*, 54-57.
35. Kumar, D.; Singh, K.; Verma, V.; Bhatti, H. S., Microwave assisted synthesis and characterization of graphene nanoplatelets. *Applied Nanoscience* **2016,** *6* (1), 97-103. DOI: 10.1007/s13204-015-0415-9.
36. Emtsev, K. V.; Bostwick, A.; Horn, K.; Jobst, J.; Kellogg, G. L.; Ley, L.; McChesney, J. L.; Ohta, T.; Reshanov, S. A.; Röhrl, J., Towards wafer-size graphene layers by atmospheric pressure graphitization of silicon carbide. *Nature materials* **2009,** *8* (3), 203-207.

37. Yu, Q.; Lian, J.; Siriponglert, S.; Li, H.; Chen, Y. P.; Pei, S.-S., Graphene segregated on Ni surfaces and transferred to insulators. *Applied Physics Letters* **2008,** *93* (11), 113103.
38. May, J. W., Platinum surface LEED rings. *Surface Science* **1969,** *17* (1), 267-270.
39. Angermann, H. H.; Hörz, G., Influence of sulfur on surface carbon monolayer formation and graphite growth on nickel. *Applied Surface Science* **1993,** *70-71*, 163-168. DOI: https://doi.org/10.1016/0169-4332(93)90419-C.
40. Land, T.; Michely, T.; Behm, R.; Hemminger, J.; Comsa, G., STM investigation of single layer graphite structures produced on Pt (111) by hydrocarbon decomposition. *Surface Science* **1992,** *264* (3), 261-270.
41. Reina, A.; Jia, X.; Ho, J.; Nezich, D.; Son, H.; Bulovic, V.; Dresselhaus, M. S.; Kong, J., Large area, few-layer graphene films on arbitrary substrates by chemical vapor deposition. *Nano letters* **2008,** *9* (1), 30-35.
42. Cai, W.; Piner, R. D.; Zhu, Y.; Li, X.; Tan, Z.; Floresca, H. C.; Yang, C.; Lu, L.; Kim, M.; Ruoff, R. S., Synthesis of isotopically-labeled graphite films by cold-wall chemical vapor deposition and electronic properties of graphene obtained from such films. *Nano Research* **2009,** *2* (11), 851-856.
43. Chen, S.; Cai, W.; Piner, R. D.; Suk, J. W.; Wu, Y.; Ren, Y.; Kang, J.; Ruoff, R. S., Synthesis and characterization of large-area graphene and graphite films on commercial Cu–Ni alloy foils. *Nano letters* **2011,** *11* (9), 3519-3525.
44. Marchini, S.; Günther, S.; Wintterlin, J., Scanning tunneling microscopy of graphene on Ru (0001). *Physical Review B* **2007,** *76* (7), 075429.
45. Coraux, J.; N 'Diaye, A. T.; Busse, C.; Michely, T., Structural coherency of graphene on Ir (111). *Nano letters* **2008,** *8* (2), 565-570.
46. Wu, Y.; Hao, Y.; Jeong, H. Y.; Lee, Z.; Chen, S.; Jiang, W.; Wu, Q.; Piner, R. D.; Kang, J.; Ruoff, R. S., Crystal Structure Evolution of Individual Graphene Islands During CVD Growth on Copper Foil. *Advanced Materials* **2013,** *25* (46), 6744-6751. DOI: 10.1002/adma.201302208.
47. Lin, Y.-M.; Dimitrakopoulos, C.; Jenkins, K. A.; Farmer, D. B.; Chiu, H.-Y.; Grill, A.; Avouris, P., 100-GHz transistors from wafer-scale epitaxial graphene. *Science* **2010,** *327* (5966), 662-662.
48. Tairov, Y. M.; Tsvetkov, V., Investigation of growth processes of ingots of silicon carbide single crystals. *Journal of crystal growth* **1978,** *43* (2), 209-212.
49. Van Bommel, A.; Crombeen, J.; Van Tooren, A., LEED and Auger electron observations of the SiC (0001) surface. *Surface Science* **1975,** *48* (2), 463-472.
50. Fan, Z.-J.; Kai, W.; Yan, J.; Wei, T.; Zhi, L.-J.; Feng, J.; Ren, Y.-m.; Song, L.-P.; Wei, F., Facile synthesis of graphene nanosheets via Fe reduction of exfoliated graphite oxide. *ACS nano* **2010,** *5* (1), 191-198.
51. Yang, X.; Dou, X.; Rouhanipour, A.; Zhi, L.; Räder, H. J.; Müllen, K., Two-dimensional graphene nanoribbons. *Journal of the American Chemical Society* **2008,** *130* (13), 4216-4217.
52. Duan, H.; Xie, E.; Han, L.; Xu, Z., Turning PMMA nanofibers into graphene nanoribbons by in situ electron beam irradiation. *Advanced Materials* **2008,** *20* (17), 3284-3288.
53. Vallés, C.; Drummond, C.; Saadaoui, H.; Furtado, C. A.; He, M.; Roubeau, O.; Ortolani, L.; Monthioux, M.; Pénicaud, A., Solutions of negatively charged graphene sheets and ribbons. *Journal of the American Chemical Society* **2008,** *130* (47), 15802-15804.
54. Choucair, M.; Thordarson, P.; Stride, J. A., Gram-scale production of graphene based on solvothermal synthesis and sonication. *Nature nanotechnology* **2009,** *4* (1), 30-33.
55. Li, D.; Müller, M. B.; Gilje, S.; Kaner, R. B.; Wallace, G. G., Processable aqueous dispersions of graphene nanosheets. *Nature nanotechnology* **2008,** *3* (2), 101.
56. Veeramani, V.; Sivakumar, M.; Chen, S.-M.; Madhu, R.; Alamri, H. R.; Alothman, Z. A.; Hossain, M. S. A.; Chen, C.-K.; Yamauchi, Y.; Miyamoto, N., Lignocellulosic biomass-derived, graphene sheet-like porous activated carbon for electrochemical supercapacitor and catechin sensing. *Rsc Advances* **2017,** *7* (72), 45668-45675.

57. Berger, C.; Song, Z.; Li, X.; Wu, X.; Brown, N.; Naud, C.; Mayou, D.; Li, T.; Hass, J.; Marchenkov, A. N., Electronic confinement and coherence in patterned epitaxial graphene. *Science* **2006,** *312* (5777), 1191-1196.
58. Eda, G.; Fanchini, G.; Chhowalla, M., Large-area ultrathin films of reduced graphene oxide as a transparent and flexible electronic material. *Nature nanotechnology* **2008,** *3* (5), 270-274.
59. Sutter, P. W.; Flege, J.-I.; Sutter, E. A., Epitaxial graphene on ruthenium. *Nature materials* **2008,** *7* (5), 406-411.
60. Subrahmanyam, K. S.; Vivekchand, S. R. C.; Govindaraj, A.; Rao, C. N. R., A study of graphenes prepared by different methods: characterization, properties and solubilization. *Journal of Materials Chemistry* **2008,** *18* (13), 1517-1523. DOI: 10.1039/B716536F.
61. Subrahmanyam, K.; Panchakarla, L.; Govindaraj, A.; Rao, C., Simple method of preparing graphene flakes by an arc-discharge method. *The Journal of Physical Chemistry C* **2009,** *113* (11), 4257-4259.
62. Kosynkin, D. V.; Higginbotham, A. L.; Sinitskii, A.; Lomeda, J. R.; Dimiev, A.; Price, B. K.; Tour, J. M., Longitudinal unzipping of carbon nanotubes to form graphene nanoribbons. *Nature* **2009,** *458* (7240), 872-876.
63. Wang, X.; Zhi, L.; Tsao, N.; Tomović, Ž.; Li, J.; Müllen, K., Transparent carbon films as electrodes in organic solar cells. *Angewandte Chemie International Edition* **2008,** *47* (16), 2990-2992.
64. Hernandez, Y.; Nicolosi, V.; Lotya, M.; Blighe, F. M.; Sun, Z.; De, S.; McGovern, I.; Holland, B.; Byrne, M.; Gun'Ko, Y. K., High-yield production of graphene by liquid-phase exfoliation of graphite. *Nature nanotechnology* **2008,** *3* (9), 563-568.
65. Levendorf, M. P.; Ruiz-Vargas, C. S.; Garg, S.; Park, J., Transfer-free batch fabrication of single layer graphene transistors. *Nano letters* **2009,** *9* (12), 4479-4483.
66. Zhan, N.; Olmedo, M.; Wang, G.; Liu, J., Layer-by-layer synthesis of large-area graphene films by thermal cracker enhanced gas source molecular beam epitaxy. *Carbon* **2011,** *49* (6), 2046-2052.
67. Brodie, B., Sur le poids atomique du graphite. *Ann. Chim. Phys* **1860,** *59* (466), e472.
68. Staudenmaier, L., Verfahren zur darstellung der graphitsäure. *European Journal of Inorganic Chemistry* **1899,** *32* (2), 1394-1399.
69. Hummers Jr, W. S.; Offeman, R. E., Preparation of graphitic oxide. *Journal of the American Chemical Society* **1958,** *80* (6), 1339-1339.
70. Gao, W., The chemistry of graphene oxide. In *Graphene oxide*, Springer: 2015; pp 61-95.
71. Koch, K. R., Oxidation by Mn207: An impressive demonstration of the powerful oxidizing property of dimanganeseheptoxide. *J. Chem. Educ* **1982,** *59* (11), 973.
72. Simon, A.; Dronskowski, R.; Krebs, B.; Hettich, B., The crystal structure of Mn2O7. *Angewandte Chemie International Edition* **1987,** *26* (2), 139-140.
73. Marcano, D. C.; Kosynkin, D. V.; Berlin, J. M.; Sinitskii, A.; Sun, Z.; Slesarev, A.; Alemany, L. B.; Lu, W.; Tour, J. M., Improved Synthesis of Graphene Oxide. *ACS Nano* **2010,** *4* (8), 4806-4814. DOI: 10.1021/nn1006368.
74. Segal, M., Selling graphene by the ton. *Nature nanotechnology* **2009,** *4* (10), 612-614.
75. Wang, X.; Tang, H.; Huang, S.; Zhu, L., Fast and facile microwave-assisted synthesis of graphene oxide nanosheets. *RSC Advances* **2014,** *4* (104), 60102-60105.
76. Patel, M.; Feng, W.; Savaram, K.; Khoshi, M. R.; Huang, R.; Sun, J.; Rabie, E.; Flach, C.; Mendelsohn, R.; Garfunkel, E., Microwave Enabled One-Pot, One-Step Fabrication and Nitrogen Doping of Holey Graphene Oxide for Catalytic Applications. *Small* **2015,** *11* (27), 3358-3368.
77. Kumar, P. V.; Bardhan, N. M.; Tongay, S.; Wu, J.; Belcher, A. M.; Grossman, J. C., Scalable enhancement of graphene oxide properties by thermally driven phase transformation. *Nature chemistry* **2014,** *6* (2), 151.
78. Hisato, Y.; Shuichi, O.; Daiki, W.; Hideaki, H.; Yongqian, G.; Goki, E.; Cecilia, M.; Takeshi, F.; Akitaka, Y.; Shinji, I.; Lyudmyla, A.; Takatoshi, Y.; M., D. A.; Gautam, G.; K., D. S.; A., V. K.; Yuden, T.; Mingwei, C.; Han, H.; Manish, C.; D., M. A.; Yuji, T., Valence-band electronic structure evolution of

graphene oxide upon thermal annealing for optoelectronics. *physica status solidi (a)* **2016,** *213* (9), 2380-2386. DOI: doi:10.1002/pssa.201532855.

79. Stankovich, S.; Dikin, D. A.; Piner, R. D.; Kohlhaas, K. A.; Kleinhammes, A.; Jia, Y.; Wu, Y.; Nguyen, S. T.; Ruoff, R. S., Synthesis of graphene-based nanosheets via chemical reduction of exfoliated graphite oxide. *carbon* **2007,** *45* (7), 1558-1565.

80. Li, D.; Müller, M. B.; Gilje, S.; Kaner, R. B.; Wallace, G. G., Processable aqueous dispersions of graphene nanosheets. *Nature nanotechnology* **2008,** *3* (2), 101-105.

81. Becerril, H. A.; Mao, J.; Liu, Z.; Stoltenberg, R. M.; Bao, Z.; Chen, Y., Evaluation of solution-processed reduced graphene oxide films as transparent conductors. *ACS nano* **2008,** *2* (3), 463-470.

82. Fernández-Merino, M. J.; Guardia, L.; Paredes, J.; Villar-Rodil, S.; Solís-Fernández, P.; Martínez-Alonso, A.; Tascon, J., Vitamin C is an ideal substitute for hydrazine in the reduction of graphene oxide suspensions. *The Journal of Physical Chemistry C* **2010,** *114* (14), 6426-6432.

83. Shin, H. J.; Kim, K. K.; Benayad, A.; Yoon, S. M.; Park, H. K.; Jung, I. S.; Jin, M. H.; Jeong, H. K.; Kim, J. M.; Choi, J. Y., Efficient reduction of graphite oxide by sodium borohydride and its effect on electrical conductance. *Advanced Functional Materials* **2009,** *19* (12), 1987-1992.

84. Pei, S.; Zhao, J.; Du, J.; Ren, W.; Cheng, H.-M., Direct reduction of graphene oxide films into highly conductive and flexible graphene films by hydrohalic acids. *Carbon* **2010,** *48* (15), 4466-4474.

85. Kumar, P. V.; Bardhan, N. M.; Chen, G.-Y.; Li, Z.; Belcher, A. M.; Grossman, J. C., New insights into the thermal reduction of graphene oxide: Impact of oxygen clustering. *Carbon* **2016,** *100*, 90-98. DOI: https://doi.org/10.1016/j.carbon.2015.12.087.

86. Shen, Y.; Boffa, V.; Corazzari, I.; Qiao, A.; Tao, H.; Yue, Y., Revealing hidden endotherm of Hummers' graphene oxide during low-temperature thermal reduction. *Carbon* **2018**. DOI: https://doi.org/10.1016/j.carbon.2018.05.018.

87. Niu, Y.; Zhang, Q.; Li, Y.; Fang, Q.; Zhang, X., Reduction, dispersity and electrical properties of graphene oxide sheets under low-temperature thermal treatments. *Journal of Materials Science: Materials in Electronics* **2017,** *28* (1), 729-733. DOI: 10.1007/s10854-016-5583-1.

88. Shen, J.; Zhu, Y.; Yang, X.; Li, C., Graphene quantum dots: emergent nanolights for bioimaging, sensors, catalysis and photovoltaic devices. *Chemical communications* **2012,** *48* (31), 3686-3699.

89. Bak, S.; Kim, D.; Lee, H., Graphene quantum dots and their possible energy applications: A review. *Current Applied Physics* **2016,** *16* (9), 1192-1201.

90. Pan, D.; Zhang, J.; Li, Z.; Wu, M., Hydrothermal route for cutting graphene sheets into blue-luminescent graphene quantum dots. *Advanced materials* **2010,** *22* (6), 734-738.

91. Shen, J.; Zhu, Y.; Yang, X.; Zong, J.; Zhang, J.; Li, C., One-pot hydrothermal synthesis of graphene quantum dots surface-passivated by polyethylene glycol and their photoelectric conversion under near-infrared light. *New Journal of Chemistry* **2012,** *36* (1), 97-101.

92. Zhu, S.; Zhang, J.; Qiao, C.; Tang, S.; Li, Y.; Yuan, W.; Li, B.; Tian, L.; Liu, F.; Hu, R., Strongly green-photoluminescent graphene quantum dots for bioimaging applications. *Chemical Communications* **2011,** *47* (24), 6858-6860.

93. Shen, J.; Zhu, Y.; Chen, C.; Yang, X.; Li, C., Facile preparation and upconversion luminescence of graphene quantum dots. *Chemical communications* **2011,** *47* (9), 2580-2582.

94. Eda, G.; Lin, Y. Y.; Mattevi, C.; Yamaguchi, H.; Chen, H. A.; Chen, I.; Chen, C. W.; Chhowalla, M., Blue photoluminescence from chemically derived graphene oxide. *Advanced materials* **2010,** *22* (4), 505-509.

95. Zhao, Q.-L.; Zhang, Z.-L.; Huang, B.-H.; Peng, J.; Zhang, M.; Pang, D.-W., Facile preparation of low cytotoxicity fluorescent carbon nanocrystals by electrooxidation of graphite. *Chemical Communications* **2008,** (41), 5116-5118.

96. Zheng, L.; Chi, Y.; Dong, Y.; Lin, J.; Wang, B., Electrochemiluminescence of water-soluble carbon nanocrystals released electrochemically from graphite. *Journal of the American Chemical Society* **2009,** *131* (13), 4564-4565.

97. Li, Y.; Hu, Y.; Zhao, Y.; Shi, G.; Deng, L.; Hou, Y.; Qu, L., An electrochemical avenue to green-luminescent graphene quantum dots as potential electron-acceptors for photovoltaics. *Advanced Materials* **2011,** *23* (6), 776-780.
98. Li, Y.; Zhao, Y.; Cheng, H.; Hu, Y.; Shi, G.; Dai, L.; Qu, L., Nitrogen-doped graphene quantum dots with oxygen-rich functional groups. *Journal of the American Chemical Society* **2011,** *134* (1), 15-18.
99. Chua, C. K.; Sofer, Z.; Simek, P.; Jankovsky, O.; Klimova, K.; Bakardjieva, S.; Hrdličková Kučková, S. t. p. n.; Pumera, M., Synthesis of strongly fluorescent graphene quantum dots by cage-opening buckminsterfullerene. *Acs Nano* **2015,** *9* (3), 2548-2555.
100. Lu, J.; Yeo, P. S. E.; Gan, C. K.; Wu, P.; Loh, K. P., Transforming C60 molecules into graphene quantum dots. *Nature nanotechnology* **2011,** *6* (4), 247-252.
101. Yan, X.; Cui, X.; Li, L.-s., Synthesis of large, stable colloidal graphene quantum dots with tunable size. *Journal of the American Chemical Society* **2010,** *132* (17), 5944-5945.
102. Liu, R.; Wu, D.; Feng, X.; Müllen, K., Bottom-up fabrication of photoluminescent graphene quantum dots with uniform morphology. *Journal of the American Chemical Society* **2011,** *133* (39), 15221-15223.
103. Wu, X.; Tian, F.; Wang, W.; Chen, J.; Wu, M.; Zhao, J. X., Fabrication of highly fluorescent graphene quantum dots using L-glutamic acid for in vitro/in vivo imaging and sensing. *Journal of Materials Chemistry C* **2013,** *1* (31), 4676-4684.
104. Zhang, C.; Cui, Y.; Song, L.; Liu, X.; Hu, Z., Microwave assisted one-pot synthesis of graphene quantum dots as highly sensitive fluorescent probes for detection of iron ions and pH value. *Talanta* **2016,** *150*, 54-60.
105. Li, L. L.; Ji, J.; Fei, R.; Wang, C. Z.; Lu, Q.; Zhang, J. R.; Jiang, L. P.; Zhu, J. J., A Facile Microwave Avenue to Electrochemiluminescent Two-Color Graphene Quantum Dots. *Advanced Functional Materials* **2012,** *22* (14), 2971-2979.
106. Yin, P. T.; Shah, S.; Chhowalla, M.; Lee, K.-B., Design, synthesis, and characterization of graphene–nanoparticle hybrid materials for bioapplications. *Chemical reviews* **2015,** *115* (7), 2483-2531.
107. Servant, A.; Bianco, A.; Prato, M.; Kostarelos, K., Graphene for multi-functional synthetic biology: The last 'zeitgeist' in nanomedicine. *Bioorganic & Medicinal Chemistry Letters* **2014,** *24* (7), 1638-1649. DOI: https://doi.org/10.1016/j.bmcl.2014.01.051.
108. Wang, K.; Ruan, J.; Song, H.; Zhang, J.; Wo, Y.; Guo, S.; Cui, D., Biocompatibility of Graphene Oxide. *Nanoscale Res Lett* **2010,** *6* (1), 8. DOI: 10.1007/s11671-010-9751-6.
109. Sasidharan, A.; Panchakarla, L.; Chandran, P.; Menon, D.; Nair, S.; Rao, C.; Koyakutty, M., Differential nano-bio interactions and toxicity effects of pristine versus functionalized graphene. *Nanoscale* **2011,** *3* (6), 2461-2464.
110. Sasidharan, A.; Panchakarla, L. S.; Sadanandan, A. R.; Ashokan, A.; Chandran, P.; Girish, C. M.; Menon, D.; Nair, S. V.; Rao, C.; Koyakutty, M., Hemocompatibility and macrophage response of pristine and functionalized graphene. *Small* **2012,** *8* (8), 1251-1263.
111. Liao, K.-H.; Lin, Y.-S.; Macosko, C. W.; Haynes, C. L., Cytotoxicity of graphene oxide and graphene in human erythrocytes and skin fibroblasts. *ACS applied materials & interfaces* **2011,** *3* (7), 2607-2615.
112. Gollavelli, G.; Ling, Y.-C., Multi-functional graphene as an in vitro and in vivo imaging probe. *Biomaterials* **2012,** *33* (8), 2532-2545.
113. Bianco, A., Graphene: Safe or Toxic? The Two Faces of the Medal. *Angewandte Chemie International Edition* **2013,** *52* (19), 4986-4997. DOI: 10.1002/anie.201209099.
114. Park, S. Y.; Park, J.; Sim, S. H.; Sung, M. G.; Kim, K. S.; Hong, B. H.; Hong, S., Enhanced differentiation of human neural stem cells into neurons on graphene. *Advanced Materials* **2011,** *23* (36).
115. Chen, G.-Y.; Pang, D.-P.; Hwang, S.-M.; Tuan, H.-Y.; Hu, Y.-C., A graphene-based platform for induced pluripotent stem cells culture and differentiation. *Biomaterials* **2012,** *33* (2), 418-427.

116. Bardhan, N. M.; Kumar, P. V.; Li, Z.; Ploegh, H. L.; Grossman, J. C.; Belcher, A. M.; Chen, G.-Y., Enhanced Cell Capture on Functionalized Graphene Oxide Nanosheets through Oxygen Clustering. *ACS Nano* **2017,** *11* (2), 1548-1558. DOI: 10.1021/acsnano.6b06979.
117. Yang, J.-W.; Hsieh, K. Y.; Kumar, P. V.; Cheng, S.-J.; Lin, Y.-R.; Shen, Y.-C.; Chen, G.-Y., Enhanced Osteogenic Differentiation of Stem Cells on Phase-Engineered Graphene Oxide. *ACS Applied Materials & Interfaces* **2018,** *10* (15), 12497-12503. DOI: 10.1021/acsami.8b02225.
118. Yue, H.; Wei, W.; Yue, Z.; Wang, B.; Luo, N.; Gao, Y.; Ma, D.; Ma, G.; Su, Z., The role of the lateral dimension of graphene oxide in the regulation of cellular responses. *Biomaterials* **2012,** *33* (16), 4013-4021.
119. Shang, W.; Zhang, X.; Zhang, M.; Fan, Z.; Sun, Y.; Han, M.; Fan, L., The uptake mechanism and biocompatibility of graphene quantum dots with human neural stem cells. *Nanoscale* **2014,** *6* (11), 5799-5806.
120. Girish, C. M.; Sasidharan, A.; Gowd, G. S.; Nair, S.; Koyakutty, M., Confocal Raman Imaging Study Showing Macrophage Mediated Biodegradation of Graphene In Vivo. *Advanced Healthcare Materials* **2013,** *2* (11), 1489-1500. DOI: 10.1002/adhm.201200489.
121. Liu, J.-H.; Yang, S.-T.; Wang, H.; Chang, Y.; Cao, A.; Liu, Y., Effect of size and dose on the biodistribution of graphene oxide in mice. *Nanomedicine* **2012,** *7* (12), 1801-1812. DOI: 10.2217/nnm.12.60.
122. Singh, S. K.; Singh, M. K.; Nayak, M. K.; Kumari, S.; Shrivastava, S.; Grácio, J. J.; Dash, D., Thrombus inducing property of atomically thin graphene oxide sheets. *Acs Nano* **2011,** *5* (6), 4987-4996.
123. Duch, M. C.; Budinger, G. R. S.; Liang, Y. T.; Soberanes, S.; Urich, D.; Chiarella, S. E.; Campochiaro, L. A.; Gonzalez, A.; Chandel, N. S.; Hersam, M. C.; Mutlu, G. M., Minimizing Oxidation and Stable Nanoscale Dispersion Improves the Biocompatibility of Graphene in the Lung. *Nano Letters* **2011,** *11* (12), 5201-5207. DOI: 10.1021/nl202515a.
124. Zhang, X.; Yin, J.; Peng, C.; Hu, W.; Zhu, Z.; Li, W.; Fan, C.; Huang, Q., Distribution and biocompatibility studies of graphene oxide in mice after intravenous administration. *carbon* **2011,** *49* (3), 986-995.
125. Sydlik, S. A.; Jhunjhunwala, S.; Webber, M. J.; Anderson, D. G.; Langer, R., In Vivo Compatibility of Graphene Oxide with Differing Oxidation States. *ACS nano* **2015,** *9* (4), 3866-3874. DOI: 10.1021/acsnano.5b01290.
126. Yang, K.; Wan, J.; Zhang, S.; Zhang, Y.; Lee, S.-T.; Liu, Z., In vivo pharmacokinetics, long-term biodistribution, and toxicology of PEGylated graphene in mice. *ACS nano* **2010,** *5* (1), 516-522.
127. Zhang, W.; Wang, C.; Li, Z.; Lu, Z.; Li, Y.; Yin, J. J.; Zhou, Y. T.; Gao, X.; Fang, Y.; Nie, G., Unraveling Stress-Induced Toxicity Properties of Graphene Oxide and the Underlying Mechanism. *Advanced Materials* **2012,** *24* (39), 5391-5397.
128. Pumera, M., Graphene in biosensing. *Materials today* **2011,** *14* (7), 308-315.
129. Pumera, M., Graphene-based nanomaterials and their electrochemistry. *Chemical Society Reviews* **2010,** *39* (11), 4146-4157.
130. Wilson, G. S.; Hu, Y., Enzyme-based biosensors for in vivo measurements. *Chemical Reviews* **2000,** *100* (7), 2693-2704.
131. Fu, C.; Yang, W.; Chen, X.; Evans, D. G., Direct electrochemistry of glucose oxidase on a graphite nanosheet–Nafion composite film modified electrode. *Electrochemistry Communications* **2009,** *11* (5), 997-1000.
132. Song, Y.; Qu, K.; Zhao, C.; Ren, J.; Qu, X., Graphene Oxide: Intrinsic Peroxidase Catalytic Activity and Its Application to Glucose Detection. *Advanced Materials* **2010,** *22* (19), 2206-2210. DOI: 10.1002/adma.200903783.
133. Shan, C.; Yang, H.; Song, J.; Han, D.; Ivaska, A.; Niu, L., Direct electrochemistry of glucose oxidase and biosensing for glucose based on graphene. *Analytical Chemistry* **2009,** *81* (6), 2378-2382.

134. Wang, K.; Liu, Q.; Guan, Q.-M.; Wu, J.; Li, H.-N.; Yan, J.-J., Enhanced direct electrochemistry of glucose oxidase and biosensing for glucose via synergy effect of graphene and CdS nanocrystals. *Biosensors and Bioelectronics* **2011,** *26* (5), 2252-2257. DOI: https://doi.org/10.1016/j.bios.2010.09.043.
135. Razmi, H.; Mohammad-Rezaei, R., Graphene quantum dots as a new substrate for immobilization and direct electrochemistry of glucose oxidase: application to sensitive glucose determination. *Biosensors and Bioelectronics* **2013,** *41*, 498-504.
136. Shan, C.; Yang, H.; Han, D.; Zhang, Q.; Ivaska, A.; Niu, L., Graphene/AuNPs/chitosan nanocomposites film for glucose biosensing. *Biosensors and bioelectronics* **2010,** *25* (5), 1070-1074.
137. Liu, H.; Gao, J.; Xue, M.; Zhu, N.; Zhang, M.; Cao, T., Processing of graphene for electrochemical application: noncovalently functionalize graphene sheets with water-soluble electroactive methylene green. *Langmuir* **2009,** *25* (20), 12006-12010.
138. Kuila, T.; Bose, S.; Khanra, P.; Mishra, A. K.; Kim, N. H.; Lee, J. H., Recent advances in graphene-based biosensors. *Biosensors and Bioelectronics* **2011,** *26* (12), 4637-4648.
139. Tang, L.; Wang, Y.; Li, Y.; Feng, H.; Lu, J.; Li, J., Preparation, structure, and electrochemical properties of reduced graphene sheet films. *Advanced Functional Materials* **2009,** *19* (17), 2782-2789.
140. Shan, C.; Yang, H.; Han, D.; Zhang, Q.; Ivaska, A.; Niu, L., Electrochemical determination of NADH and ethanol based on ionic liquid-functionalized graphene. *Biosensors and Bioelectronics* **2010,** *25* (6), 1504-1508.
141. Wei, F.; Lillehoj, P. B.; Ho, C.-M., DNA diagnostics: nanotechnology-enhanced electrochemical detection of nucleic acids. *Pediatric research* **2010,** *67* (5), 458-468.
142. Palek, E.; Fojta, M., Peer reviewed: detecting DNA hybridization and damage. ACS Publications: 2001.
143. Zhou, M.; Zhai, Y.; Dong, S., Electrochemical sensing and biosensing platform based on chemically reduced graphene oxide. *Analytical chemistry* **2009,** *81* (14), 5603-5613.
144. Lim, C. X.; Hoh, H. Y.; Ang, P. K.; Loh, K. P., Direct voltammetric detection of DNA and pH sensing on epitaxial graphene: an insight into the role of oxygenated defects. *Analytical chemistry* **2010,** *82* (17), 7387-7393.
145. Ambrosi, A.; Pumera, M., Stacked graphene nanofibers for electrochemical oxidation of DNA bases. *Physical Chemistry Chemical Physics* **2010,** *12* (31), 8943-8947.
146. Zhao, J.; Chen, G.; Zhu, L.; Li, G., Graphene quantum dots-based platform for the fabrication of electrochemical biosensors. *Electrochemistry Communications* **2011,** *13* (1), 31-33.
147. Xu, H.; Dai, H.; Chen, G., Direct electrochemistry and electrocatalysis of hemoglobin protein entrapped in graphene and chitosan composite film. *Talanta* **2010,** *81* (1), 334-338.
148. Wang, Z.; Li, F.; Xia, J.; Xia, L.; Zhang, F.; Bi, S.; Shi, G.; Xia, Y.; Liu, J.; Li, Y., An ionic liquid-modified graphene based molecular imprinting electrochemical sensor for sensitive detection of bovine hemoglobin. *Biosensors and Bioelectronics* **2014,** *61*, 391-396.
149. Luo, J.; Jiang, S.; Liu, X., Electrochemical sensor for bovine hemoglobin based on a novel graphene-molecular imprinted polymers composite as recognition element. *Sensors and Actuators B: Chemical* **2014,** *203*, 782-789.
150. Zhou, K.; Zhu, Y.; Yang, X.; Luo, J.; Li, C.; Luan, S., A novel hydrogen peroxide biosensor based on Au–graphene–HRP–chitosan biocomposites. *Electrochimica Acta* **2010,** *55* (9), 3055-3060.
151. Zeng, Q.; Cheng, J.; Tang, L.; Liu, X.; Liu, Y.; Li, J.; Jiang, J., Self-Assembled Graphene–Enzyme Hierarchical Nanostructures for Electrochemical Biosensing. *Advanced Functional Materials* **2010,** *20* (19), 3366-3372.
152. Muthurasu, A.; Ganesh, V., Horseradish peroxidase enzyme immobilized graphene quantum dots as electrochemical biosensors. *Applied biochemistry and biotechnology* **2014,** *174* (3), 945-959.
153. Dey, R. S.; Raj, C. R., Development of an amperometric cholesterol biosensor based on graphene− Pt nanoparticle hybrid material. *The Journal of Physical Chemistry C* **2010,** *114* (49), 21427-21433.

154. Ruecha, N.; Rangkupan, R.; Rodthongkum, N.; Chailapakul, O., Novel paper-based cholesterol biosensor using graphene/polyvinylpyrrolidone/polyaniline nanocomposite. *Biosensors and Bioelectronics* **2014,** *52*, 13-19.
155. Simoni, R.; Gomes, L. F.; Scalco, F.; Oliveira, C.; Neto, F. A.; de Oliveira, M. C., Uric acid changes in urine and plasma: an effective tool in screening for purine inborn errors of metabolism and other pathological conditions. *Journal of inherited metabolic disease* **2007,** *30* (3), 295-309.
156. Guo, X.; Guo, B.; Li, C.; Wang, Y., Amperometric Highly Sensitive Uric Acid sensor Based on Manganese (III) porphyrin-Graphene Modified Glassy Carbon Electrode. *Journal of Electroanalytical Chemistry* **2016,** *783*, 8-14.
157. Liang, Z.; Zhai, H.; Chen, Z.; Wang, H.; Wang, S.; Zhou, Q.; Huang, X., A simple, ultrasensitive sensor for gallic acid and uric acid based on gold microclusters/sulfonate functionalized graphene modified glassy carbon electrode. *Sensors and Actuators B: Chemical* **2016,** *224*, 915-925.
158. Feng, L.; Chen, Y.; Ren, J.; Qu, X., A graphene functionalized electrochemical aptasensor for selective label-free detection of cancer cells. *Biomaterials* **2011,** *32* (11), 2930-2937.
159. Feng, L.; Wu, L.; Wang, J.; Ren, J.; Miyoshi, D.; Sugimoto, N.; Qu, X., Detection of a Prognostic Indicator in Early-Stage Cancer Using Functionalized Graphene-Based Peptide Sensors. *Advanced Materials* **2012,** *24* (1), 125-131.
160. Castillo, J. J.; Svendsen, W. E.; Rozlosnik, N.; Escobar, P.; Martínez, F.; Castillo-León, J., Detection of cancer cells using a peptide nanotube–folic acid modified graphene electrode. *Analyst* **2013,** *138* (4), 1026-1031.
161. Du, D.; Zou, Z.; Shin, Y.; Wang, J.; Wu, H.; Engelhard, M. H.; Liu, J.; Aksay, I. A.; Lin, Y., Sensitive immunosensor for cancer biomarker based on dual signal amplification strategy of graphene sheets and multienzyme functionalized carbon nanospheres. *Analytical Chemistry* **2010,** *82* (7), 2989-2995.
162. Du, D.; Wang, L.; Shao, Y.; Wang, J.; Engelhard, M. H.; Lin, Y., Functionalized graphene oxide as a nanocarrier in a multienzyme labeling amplification strategy for ultrasensitive electrochemical immunoassay of phosphorylated p53 (S392). *Analytical chemistry* **2011,** *83* (3), 746-752.
163. Chang, H.; Tang, L.; Wang, Y.; Jiang, J.; Li, J., Graphene fluorescence resonance energy transfer aptasensor for the thrombin detection. *Analytical Chemistry* **2010,** *82* (6), 2341-2346.
164. Zhang, H. L.; Wei, X. L.; Zang, Y.; Cao, J. Y.; Liu, S.; He, X. P.; Chen, Q.; Long, Y. T.; Li, J.; Chen, G. R., Fluorogenic probing of specific recognitions between sugar ligands and glycoprotein receptors on cancer cells by an economic graphene nanocomposite. *Advanced Materials* **2013,** *25* (30), 4097-4101.
165. Kushwaha, H.; Sao, R.; Vaish, R., Label free selective detection of estriol using graphene oxide-based fluorescence sensor. *Journal of Applied Physics* **2014,** *116* (3), 034701.
166. He, S.; Song, B.; Li, D.; Zhu, C.; Qi, W.; Wen, Y.; Wang, L.; Song, S.; Fang, H.; Fan, C., A graphene nanoprobe for rapid, sensitive, and multicolor fluorescent DNA analysis. *Advanced Functional Materials* **2010,** *20* (3), 453-459.
167. Zhang, C.; Yuan, Y.; Zhang, S.; Wang, Y.; Liu, Z., Biosensing platform based on fluorescence resonance energy transfer from upconverting nanocrystals to graphene oxide. *Angewandte Chemie International Edition* **2011,** *50* (30), 6851-6854.
168. Chun-Hua, L.; Huang-Hao, Y.; Chun-Ling, Z.; Xi, C.; Guo-Nan, C., A Graphene Platform for Sensing Biomolecules. *Angewandte Chemie International Edition* **2009,** *48* (26), 4785-4787. DOI: doi:10.1002/anie.200901479.
169. Lu, C.-H.; Zhu, C.-L.; Li, J.; Liu, J.-J.; Chen, X.; Yang, H.-H., Using graphene to protect DNA from cleavage during cellular delivery. *Chemical Communications* **2010,** *46* (18), 3116-3118.
170. Zhang, H.; Wang, Y.; Zhao, D.; Zeng, D.; Xia, J.; Aldalbahi, A.; Wang, C.; San, L.; Fan, C.; Zuo, X.; Mi, X., Universal Fluorescence Biosensor Platform Based on Graphene Quantum Dots and Pyrene-Functionalized Molecular Beacons for Detection of MicroRNAs. *ACS Applied Materials & Interfaces* **2015,** *7* (30), 16152-16156. DOI: 10.1021/acsami.5b04773.

171. He, Y.; Lin, Y.; Tang, H.; Pang, D., A graphene oxide-based fluorescent aptasensor for the turn-on detection of epithelial tumor marker mucin 1. *Nanoscale* **2012,** *4* (6), 2054-2059.
172. Jung, J. H.; Cheon, D. S.; Liu, F.; Lee, K. B.; Seo, T. S., A graphene oxide based immuno-biosensor for pathogen detection. *Angewandte Chemie International Edition* **2010,** *49* (33), 5708-5711.
173. Ran, X.; Sun, H.; Pu, F.; Ren, J.; Qu, X., Ag nanoparticle-decorated graphene quantum dots for label-free, rapid and sensitive detection of Ag+ and biothiols. *Chemical Communications* **2013,** *49* (11), 1079-1081.
174. He, Y.; Wang, X.; Sun, J.; Jiao, S.; Chen, H.; Gao, F.; Wang, L., Fluorescent blood glucose monitor by hemin-functionalized graphene quantum dots based sensing system. *Analytica Chimica Acta* **2014,** *810*, 71-78. DOI: https://doi.org/10.1016/j.aca.2013.11.059.
175. Wang, Y.; Zhang, L.; Liang, R.-P.; Bai, J.-M.; Qiu, J.-D., Using Graphene Quantum Dots as Photoluminescent Probes for Protein Kinase Sensing. *Analytical Chemistry* **2013,** *85* (19), 9148-9155. DOI: 10.1021/ac401807b.
176. Zhang, L.; Zhang, Z.-Y.; Liang, R.-P.; Li, Y.-H.; Qiu, J.-D., Boron-Doped Graphene Quantum Dots for Selective Glucose Sensing Based on the "Abnormal" Aggregation-Induced Photoluminescence Enhancement. *Analytical Chemistry* **2014,** *86* (9), 4423-4430. DOI: 10.1021/ac500289c.
177. Zhao, H.; Chang, Y.; Liu, M.; Gao, S.; Yu, H.; Quan, X., A universal immunosensing strategy based on regulation of the interaction between graphene and graphene quantum dots. *Chemical Communications* **2013,** *49* (3), 234-236.
178. Qian, Z. S.; Shan, X. Y.; Chai, L. J.; Ma, J. J.; Chen, J. R.; Feng, H., DNA nanosensor based on biocompatible graphene quantum dots and carbon nanotubes. *Biosensors and Bioelectronics* **2014,** *60*, 64-70.
179. Ahn, J.-H.; Choi, S.-J.; Han, J.-W.; Park, T. J.; Lee, S. Y.; Choi, Y.-K., Double-gate nanowire field effect transistor for a biosensor. *Nano letters* **2010,** *10* (8), 2934-2938.
180. Wallace, P. R., The band theory of graphite. *Physical Review* **1947,** *71* (9), 622.
181. Mohanty, N.; Berry, V., Graphene-based single-bacterium resolution biodevice and DNA transistor: interfacing graphene derivatives with nanoscale and microscale biocomponents. *Nano letters* **2008,** *8* (12), 4469-4476.
182. Dong, X.; Shi, Y.; Huang, W.; Chen, P.; Li, L. J., Electrical detection of DNA hybridization with single-base specificity using transistors based on CVD-grown graphene sheets. *Advanced Materials* **2010,** *22* (14), 1649-1653.
183. Stine, R.; Robinson, J. T.; Sheehan, P. E.; Tamanaha, C. R., Real-Time DNA Detection Using Reduced Graphene Oxide Field Effect Transistors. *Advanced Materials* **2010,** *22* (46), 5297-5300.
184. Mao, S.; Lu, G.; Yu, K.; Bo, Z.; Chen, J., Specific protein detection using thermally reduced graphene oxide sheet decorated with gold nanoparticle-antibody conjugates. *Advanced Materials* **2010,** *22* (32), 3521-3526.
185. Ohno, Y.; Maehashi, K.; Matsumoto, K., Label-free biosensors based on aptamer-modified graphene field-effect transistors. *Journal of the American Chemical Society* **2010,** *132* (51), 18012-18013.
186. You, X.; Pak, J. J., Graphene-based field effect transistor enzymatic glucose biosensor using silk protein for enzyme immobilization and device substrate. *Sensors and Actuators B: Chemical* **2014,** *202*, 1357-1365.
187. Luo, Z.; Yuwen, L.; Han, Y.; Tian, J.; Zhu, X.; Weng, L.; Wang, L., Reduced graphene oxide/PAMAM–silver nanoparticles nanocomposite modified electrode for direct electrochemistry of glucose oxidase and glucose sensing. *Biosensors and Bioelectronics* **2012,** *36* (1), 179-185. DOI: https://doi.org/10.1016/j.bios.2012.04.009.
188. Chu, Z.; Liu, Y.; Xu, Y.; Shi, L.; Peng, J.; Jin, W., In-situ fabrication of well-distributed gold nanocubes on thiol graphene as a third-generation biosensor for ultrasensitive glucose detection. *Electrochimica Acta* **2015,** *176*, 162-171. DOI: https://doi.org/10.1016/j.electacta.2015.06.123.

189. Liu, M.; Liu, R.; Chen, W., Graphene wrapped Cu2O nanocubes: Non-enzymatic electrochemical sensors for the detection of glucose and hydrogen peroxide with enhanced stability. *Biosensors and Bioelectronics* **2013,** *45*, 206-212. DOI: https://doi.org/10.1016/j.bios.2013.02.010.
190. Dhara, K.; Stanley, J.; T, R.; Nair, B. G.; T.G, S. B., Pt-CuO nanoparticles decorated reduced graphene oxide for the fabrication of highly sensitive non-enzymatic disposable glucose sensor. *Sensors and Actuators B: Chemical* **2014,** *195*, 197-205. DOI: https://doi.org/10.1016/j.snb.2014.01.044.
191. Ping, J.; Wang, Y.; Fan, K.; Wu, J.; Ying, Y., Direct electrochemical reduction of graphene oxide on ionic liquid doped screen-printed electrode and its electrochemical biosensing application. *Biosensors and Bioelectronics* **2011,** *28* (1), 204-209. DOI: https://doi.org/10.1016/j.bios.2011.07.018.
192. Wu, P.; Shao, Q.; Hu, Y.; Jin, J.; Yin, Y.; Zhang, H.; Cai, C., Direct electrochemistry of glucose oxidase assembled on graphene and application to glucose detection. *Electrochimica Acta* **2010,** *55* (28), 8606-8614. DOI: https://doi.org/10.1016/j.electacta.2010.07.079.
193. Mani, V.; Devadas, B.; Chen, S.-M., Direct electrochemistry of glucose oxidase at electrochemically reduced graphene oxide-multiwalled carbon nanotubes hybrid material modified electrode for glucose biosensor. *Biosensors and Bioelectronics* **2013,** *41*, 309-315. DOI: https://doi.org/10.1016/j.bios.2012.08.045.
194. Yang, J.; Deng, S.; Lei, J.; Ju, H.; Gunasekaran, S., Electrochemical synthesis of reduced graphene sheet–AuPd alloy nanoparticle composites for enzymatic biosensing. *Biosensors and Bioelectronics* **2011,** *29* (1), 159-166. DOI: https://doi.org/10.1016/j.bios.2011.08.011.
195. Zhang, Q.; Wu, S.; Zhang, L.; Lu, J.; Verproot, F.; Liu, Y.; Xing, Z.; Li, J.; Song, X.-M., Fabrication of polymeric ionic liquid/graphene nanocomposite for glucose oxidase immobilization and direct electrochemistry. *Biosensors and Bioelectronics* **2011,** *26* (5), 2632-2637. DOI: https://doi.org/10.1016/j.bios.2010.11.024.
196. Gu, H.; Yu, Y.; Liu, X.; Ni, B.; Zhou, T.; Shi, G., Layer-by-layer self-assembly of functionalized graphene nanoplates for glucose sensing in vivo integrated with on-line microdialysis system. *Biosensors and Bioelectronics* **2012,** *32* (1), 118-126. DOI: https://doi.org/10.1016/j.bios.2011.11.044.
197. Zheng, D.; Vashist, S. K.; Al-Rubeaan, K.; Luong, J. H. T.; Sheu, F.-S., Mediatorless amperometric glucose biosensing using 3-aminopropyltriethoxysilane-functionalized graphene. *Talanta* **2012,** *99*, 22-28. DOI: https://doi.org/10.1016/j.talanta.2012.05.014.
198. Baby, T. T.; Aravind, S. S. J.; Arockiadoss, T.; Rakhi, R. B.; Ramaprabhu, S., Metal decorated graphene nanosheets as immobilization matrix for amperometric glucose biosensor. *Sensors and Actuators B: Chemical* **2010,** *145* (1), 71-77. DOI: https://doi.org/10.1016/j.snb.2009.11.022.
199. Qiu, J.-D.; Huang, J.; Liang, R.-P., Nanocomposite film based on graphene oxide for high performance flexible glucose biosensor. *Sensors and Actuators B: Chemical* **2011,** *160* (1), 287-294. DOI: https://doi.org/10.1016/j.snb.2011.07.049.
200. Liu, S.; Tian, J.; Wang, L.; Luo, Y.; Lu, W.; Sun, X., Self-assembled graphene platelet–glucose oxidase nanostructures for glucose biosensing. *Biosensors and Bioelectronics* **2011,** *26* (11), 4491-4496. DOI: https://doi.org/10.1016/j.bios.2011.05.008.
201. Lu, W.; Luo, Y.; Chang, G.; Sun, X., Synthesis of functional SiO2-coated graphene oxide nanosheets decorated with Ag nanoparticles for H2O2 and glucose detection. *Biosensors and Bioelectronics* **2011,** *26* (12), 4791-4797. DOI: https://doi.org/10.1016/j.bios.2011.06.008.
202. Luo, Z.; Ma, X.; Yang, D.; Yuwen, L.; Zhu, X.; Weng, L.; Wang, L., Synthesis of highly dispersed titanium dioxide nanoclusters on reduced graphene oxide for increased glucose sensing. *Carbon* **2013,** *57*, 470-476. DOI: https://doi.org/10.1016/j.carbon.2013.02.020.
203. Li, S.-J.; Xia, N.; Lv, X.-L.; Zhao, M.-M.; Yuan, B.-Q.; Pang, H., A facile one-step electrochemical synthesis of graphene/NiO nanocomposites as efficient electrocatalyst for glucose and methanol. *Sensors and Actuators B: Chemical* **2014,** *190*, 809-817.

204. Wang, B.; Li, S.; Liu, J.; Yu, M., Preparation of nickel nanoparticle/graphene composites for non-enzymatic electrochemical glucose biosensor applications. *Materials Research Bulletin* **2014,** *49*, 521-524.
205. Zhang, X.; Xu, F.; Zhao, B.; Ji, X.; Yao, Y.; Wu, D.; Gao, Z.; Jiang, K., Synthesis of CdS quantum dots decorated graphene nanosheets and non-enzymatic photoelectrochemical detection of glucose. *Electrochimica Acta* **2014,** *133*, 615-622. DOI: https://doi.org/10.1016/j.electacta.2014.04.089.
206. Hsu, Y.-W.; Hsu, T.-K.; Sun, C.-L.; Nien, Y.-T.; Pu, N.-W.; Ger, M.-D., Synthesis of CuO/graphene nanocomposites for nonenzymatic electrochemical glucose biosensor applications. *Electrochimica Acta* **2012,** *82*, 152-157. DOI: https://doi.org/10.1016/j.electacta.2012.03.094.
207. Luo, J.; Jiang, S.; Zhang, H.; Jiang, J.; Liu, X., A novel non-enzymatic glucose sensor based on Cu nanoparticle modified graphene sheets electrode. *Analytica Chimica Acta* **2012,** *709*, 47-53. DOI: https://doi.org/10.1016/j.aca.2011.10.025.
208. Alwarappan, S.; Liu, C.; Kumar, A.; Li, C.-Z., Enzyme-Doped Graphene Nanosheets for Enhanced Glucose Biosensing. *The Journal of Physical Chemistry C* **2010,** *114* (30), 12920-12924. DOI: 10.1021/jp103273z.
209. Amouzadeh Tabrizi, M.; Jalilzadeh Azar, S.; Nadali Varkani, J., Eco-synthesis of graphene and its use in dihydronicotinamide adenine dinucleotide sensing. *Analytical Biochemistry* **2014,** *460*, 29-35. DOI: https://doi.org/10.1016/j.ab.2014.05.002.
210. Li, L.; Lu, H.; Deng, L., A sensitive NADH and ethanol biosensor based on graphene–Au nanorods nanocomposites. *Talanta* **2013,** *113*, 1-6. DOI: https://doi.org/10.1016/j.talanta.2013.03.074.
211. Yang, F.; Xin, Y.; Chunpeng, Y.; Jinhang, L., Au-TiO2/Graphene Nanocomposite Film for Electrochemical Sensing of Hydrogen Peroxide and NADH. *Electroanalysis* **2012,** *24* (6), 1334-1339. DOI: doi:10.1002/elan.201200008.
212. Wang, K.; Wu, J.; Liu, Q.; Jin, Y.; Yan, J.; Cai, J., Ultrasensitive photoelectrochemical sensing of nicotinamide adenine dinucleotide based on graphene-TiO2 nanohybrids under visible irradiation. *Analytica Chimica Acta* **2012,** *745*, 131-136. DOI: https://doi.org/10.1016/j.aca.2012.07.042.
213. Govindhan, M.; Amiri, M.; Chen, A., Au nanoparticle/graphene nanocomposite as a platform for the sensitive detection of NADH in human urine. *Biosensors and Bioelectronics* **2015,** *66*, 474-480. DOI: https://doi.org/10.1016/j.bios.2014.12.012.
214. Istrate, O.-M.; Rotariu, L.; Marinescu, V. E.; Bala, C., NADH sensing platform based on electrochemically generated reduced graphene oxide–gold nanoparticles composite stabilized with poly(allylamine hydrochloride). *Sensors and Actuators B: Chemical* **2016,** *223*, 697-704. DOI: https://doi.org/10.1016/j.snb.2015.09.142.
215. Chiang Lin, K.; Yu Lai, S.; Ming Chen, S., A highly sensitive NADH sensor based on a mycelium-like nanocomposite using graphene oxide and multi-walled carbon nanotubes to co-immobilize poly(luminol) and poly(neutral red) hybrid films. *Analyst* **2014,** *139* (16), 3991-3998. DOI: 10.1039/C4AN00536H.
216. Keeley, G. P.; O'Neill, A.; Holzinger, M.; Cosnier, S.; Coleman, J. N.; Duesberg, G. S., DMF-exfoliated graphene for electrochemical NADH detection. *Physical Chemistry Chemical Physics* **2011,** *13* (17), 7747-7750. DOI: 10.1039/C1CP20060G.
217. Lin, L.; Liu, Y.; Tang, L.; Li, J., Electrochemical DNA sensor by the assembly of graphene and DNA-conjugated gold nanoparticles with silver enhancement strategy. *Analyst* **2011,** *136* (22), 4732-4737. DOI: 10.1039/C1AN15610A.
218. Xueliang, N.; Wen, Z.; Xiaoyan, L.; Wenshu, Z.; Zuorui, W.; Qiutong, L.; Hui, X.; Wei, S., Electrochemical DNA Sensor Based on Chitosan-Graphene and Electrodeposited Gold Nanoparticle Modified Electrode for the Detection of Staphylococcus aureus nuc Gene Sequence. *Current Analytical Chemistry* **2018,** *14* (2), 159-165. DOI: http://dx.doi.org/10.2174/1573411013666170607123122.

219. Zheng, Q.; Wu, H.; Shen, Z.; Gao, W.; Yu, Y.; Ma, Y.; Guang, W.; Guo, Q.; Yan, R.; Wang, J., An electrochemical DNA sensor based on polyaniline/graphene: high sensitivity to DNA sequences in a wide range. *Analyst* **2015,** *140* (19), 6660-6670.
220. Chen, M.; Hou, C.; Huo, D.; Fa, H.; Zhao, Y.; Shen, C., A sensitive electrochemical DNA biosensor based on three-dimensional nitrogen-doped graphene and Fe3O4 nanoparticles. *Sensors and Actuators B: Chemical* **2017,** *239*, 421-429. DOI: https://doi.org/10.1016/j.snb.2016.08.036.
221. Bo, Y.; Yang, H.; Hu, Y.; Yao, T.; Huang, S., A novel electrochemical DNA biosensor based on graphene and polyaniline nanowires. *Electrochimica Acta* **2011,** *56* (6), 2676-2681. DOI: https://doi.org/10.1016/j.electacta.2010.12.034.
222. Rasheed, P. A.; Sandhyarani, N., Graphene-DNA electrochemical sensor for the sensitive detection of BRCA1 gene. *Sensors and Actuators B: Chemical* **2014,** *204*, 777-782. DOI: https://doi.org/10.1016/j.snb.2014.08.043.
223. Wang, Z.; Li, F.; Xia, J.; Xia, L.; Zhang, F.; Bi, S.; Shi, G.; Xia, Y.; Liu, J.; Li, Y.; Xia, L., An ionic liquid-modified graphene based molecular imprinting electrochemical sensor for sensitive detection of bovine hemoglobin. *Biosensors and Bioelectronics* **2014,** *61*, 391-396. DOI: https://doi.org/10.1016/j.bios.2014.05.043.
224. Dinesh, B.; Mani, V.; Saraswathi, R.; Chen, S.-M., Direct electrochemistry of cytochrome c immobilized on a graphene oxide-carbon nanotube composite for picomolar detection of hydrogen peroxide. *RSC Advances* **2014,** *4* (54), 28229-28237. DOI: 10.1039/C4RA02789B.
225. Mani, V.; Dinesh, B.; Chen, S.-M.; Saraswathi, R., Direct electrochemistry of myoglobin at reduced graphene oxide-multiwalled carbon nanotubes-platinum nanoparticles nanocomposite and biosensing towards hydrogen peroxide and nitrite. *Biosensors and Bioelectronics* **2014,** *53*, 420-427. DOI: https://doi.org/10.1016/j.bios.2013.09.075.
226. Cheng, Y.; Feng, B.; Yang, X.; Yang, P.; Ding, Y.; Chen, Y.; Fei, J., Electrochemical biosensing platform based on carboxymethyl cellulose functionalized reduced graphene oxide and hemoglobin hybrid nanocomposite film. *Sensors and Actuators B: Chemical* **2013,** *182*, 288-293. DOI: https://doi.org/10.1016/j.snb.2013.03.007.
227. Zhang, L.; Han, G.; Liu, Y.; Tang, J.; Tang, W., Immobilizing haemoglobin on gold/graphene–chitosan nanocomposite as efficient hydrogen peroxide biosensor. *Sensors and Actuators B: Chemical* **2014,** *197*, 164-171. DOI: https://doi.org/10.1016/j.snb.2014.02.077.
228. Maji, S. K.; Sreejith, S.; Mandal, A. K.; Ma, X.; Zhao, Y., Immobilizing Gold Nanoparticles in Mesoporous Silica Covered Reduced Graphene Oxide: A Hybrid Material for Cancer Cell Detection through Hydrogen Peroxide Sensing. *ACS Applied Materials & Interfaces* **2014,** *6* (16), 13648-13656. DOI: 10.1021/am503110s.
229. Li, L.; Du, Z.; Liu, S.; Hao, Q.; Wang, Y.; Li, Q.; Wang, T., A novel nonenzymatic hydrogen peroxide sensor based on MnO2/graphene oxide nanocomposite. *Talanta* **2010,** *82* (5), 1637-1641. DOI: https://doi.org/10.1016/j.talanta.2010.07.020.
230. Nalini, S.; Nandini, S.; Shanmugam, S.; Neelagund, S. E.; Melo, J. S.; Suresh, G. S., Amperometric hydrogen peroxide and cholesterol biosensors designed by using hierarchical curtailed silver flowers functionalized graphene and enzymes deposits. *Journal of Solid State Electrochemistry* **2014,** *18* (3), 685-701.
231. Radhakrishnan, S.; Kim, S. J., An enzymatic biosensor for hydrogen peroxide based on one-pot preparation of CeO2-reduced graphene oxide nanocomposite. *RSC Advances* **2015,** *5* (17), 12937-12943. DOI: 10.1039/C4RA12841A.
232. Song, H.; Ni, Y.; Kokot, S., Investigations of an electrochemical platform based on the layered MoS2–graphene and horseradish peroxidase nanocomposite for direct electrochemistry and electrocatalysis. *Biosensors and Bioelectronics* **2014,** *56*, 137-143. DOI: https://doi.org/10.1016/j.bios.2014.01.014.
233. Yuan, B.; Xu, C.; Liu, L.; Shi, Y.; Li, S.; Zhang, R.; Zhang, D., Polyethylenimine-bridged graphene oxide–gold film on glassy carbon electrode and its electrocatalytic activity toward nitrite

and hydrogen peroxide. *Sensors and Actuators B: Chemical* **2014,** *198*, 55-61. DOI: https://doi.org/10.1016/j.snb.2014.03.014.

234. Ju, J.; Chen, W., In Situ Growth of Surfactant-Free Gold Nanoparticles on Nitrogen-Doped Graphene Quantum Dots for Electrochemical Detection of Hydrogen Peroxide in Biological Environments. *Analytical Chemistry* **2015,** *87* (3), 1903-1910. DOI: 10.1021/ac5041555.

235. Jiang, B.-B.; Wei, X.-W.; Wu, F.-H.; Wu, K.-L.; Chen, L.; Yuan, G.-Z.; Dong, C.; Ye, Y., A non-enzymatic hydrogen peroxide sensor based on a glassy carbon electrode modified with cuprous oxide and nitrogen-doped graphene in a nafion matrix. *Microchimica Acta* **2014,** *181* (11), 1463-1470. DOI: 10.1007/s00604-014-1232-7.

236. Cheng, C.; Zhang, C.; Gao, X.; Zhuang, Z.; Du, C.; Chen, W., 3D Network and 2D Paper of Reduced Graphene Oxide/Cu2O Composite for Electrochemical Sensing of Hydrogen Peroxide. *Analytical Chemistry* **2018,** *90* (3), 1983-1991. DOI: 10.1021/acs.analchem.7b04070.

237. Amala, G.; Saravanan, J.; Jin Yoo, D.; Kim, A. R.; Gnana kumar, G., An environmentally benign one pot green synthesis of reduced graphene oxide based composites for the enzyme free electrochemical detection of hydrogen peroxide. *New Journal of Chemistry* **2017,** *41* (10), 4022-4030. DOI: 10.1039/C6NJ04030F.

238. Sheng, Z.-H.; Zheng, X.-Q.; Xu, J.-Y.; Bao, W.-J.; Wang, F.-B.; Xia, X.-H., Electrochemical sensor based on nitrogen doped graphene: Simultaneous determination of ascorbic acid, dopamine and uric acid. *Biosensors and Bioelectronics* **2012,** *34* (1), 125-131. DOI: https://doi.org/10.1016/j.bios.2012.01.030.

239. Kaur, B.; Pandiyan, T.; Satpati, B.; Srivastava, R., Simultaneous and sensitive determination of ascorbic acid, dopamine, uric acid, and tryptophan with silver nanoparticles-decorated reduced graphene oxide modified electrode. *Colloids and Surfaces B: Biointerfaces* **2013,** *111*, 97-106. DOI: https://doi.org/10.1016/j.colsurfb.2013.05.023.

240. Raj, M. A.; John, S. A., Simultaneous determination of uric acid, xanthine, hypoxanthine and caffeine in human blood serum and urine samples using electrochemically reduced graphene oxide modified electrode. *Analytica Chimica Acta* **2013,** *771*, 14-20. DOI: https://doi.org/10.1016/j.aca.2013.02.017.

241. Du, J.; Yue, R.; Yao, Z.; Jiang, F.; Du, Y.; Yang, P.; Wang, C., Nonenzymatic uric acid electrochemical sensor based on graphene-modified carbon fiber electrode. *Colloids and Surfaces A: Physicochemical and Engineering Aspects* **2013,** *419*, 94-99. DOI: https://doi.org/10.1016/j.colsurfa.2012.11.060.

242. Zhang, H.; Wang, Y.; Zhao, D.; Zeng, D.; Xia, J.; Aldalbahi, A.; Wang, C.; San, L.; Fan, C.; Zuo, X., Universal fluorescence biosensor platform based on graphene quantum dots and pyrene-functionalized molecular beacons for detection of microRNAs. *ACS applied materials & interfaces* **2015,** *7* (30), 16152-16156.

243. Zhou, L.; Mao, H.; Wu, C.; Tang, L.; Wu, Z.; Sun, H.; Zhang, H.; Zhou, H.; Jia, C.; Jin, Q., Label-free graphene biosensor targeting cancer molecules based on non-covalent modification. *Biosensors and Bioelectronics* **2017,** *87*, 701-707.

244. Xu, S.; Zhan, J.; Man, B.; Jiang, S.; Yue, W.; Gao, S.; Guo, C.; Liu, H.; Li, Z.; Wang, J., Real-time reliable determination of binding kinetics of DNA hybridization using a multi-channel graphene biosensor. *Nature communications* **2017,** *8*, 14902.

245. Said, K.; Ayesh, A. I.; Qamhieh, N. N.; Awwad, F.; Mahmoud, S. T.; Hisaindee, S., Fabrication and characterization of graphite oxide–nanoparticle composite based field effect transistors for non-enzymatic glucose sensor applications. *Journal of Alloys and Compounds* **2017,** *694*, 1061-1066.

246. Piccinini, E.; Bliem, C.; Reiner-Rozman, C.; Battaglini, F.; Azzaroni, O.; Knoll, W., Enzyme-polyelectrolyte multilayer assemblies on reduced graphene oxide field-effect transistors for biosensing applications. *Biosensors and Bioelectronics* **2017,** *92*, 661-667.

247. Khademhosseini, A.; Vacanti, J. P.; Langer, R., Progress in tissue engineering. *Scientific American* **2009,** *300* (5), 64-71.

248. Freed, L. E.; Vunjak-Novakovic, G.; Biron, R. J.; Eagles, D. B.; Lesnoy, D. C.; Barlow, S. K.; Langer, R., Biodegradable polymer scaffolds for tissue engineering. *Nature Biotechnology* **1994,** *12* (7), 689-693.
249. Tamayol, A.; Akbari, M.; Annabi, N.; Paul, A.; Khademhosseini, A.; Juncker, D., Fiber-based tissue engineering: progress, challenges, and opportunities. *Biotechnology advances* **2013,** *31* (5), 669-687.
250. Hubbell, J. A., Biomaterials in tissue engineering. *Nature Biotechnology* **1995,** *13* (6), 565-576.
251. Lutolf, M.; Hubbell, J., Synthetic biomaterials as instructive extracellular microenvironments for morphogenesis in tissue engineering. *Nature biotechnology* **2005,** *23* (1), 47-55.
252. Shin, S. R.; Aghaei-Ghareh-Bolagh, B.; Dang, T. T.; Topkaya, S. N.; Gao, X.; Yang, S. Y.; Jung, S. M.; Oh, J. H.; Dokmeci, M. R.; Tang, X. S., Cell-laden Microengineered and Mechanically Tunable Hybrid Hydrogels of Gelatin and Graphene Oxide. *Advanced materials* **2013,** *25* (44), 6385-6391.
253. Rowe, W. J., Extraordinary unremitting endurance exercise and permanent injury to normal heart. *The Lancet* **1992,** *340* (8821), 712-714.
254. You, J.-O.; Rafat, M.; Ye, G. J.; Auguste, D. T., Nanoengineering the heart: conductive scaffolds enhance connexin 43 expression. *Nano letters* **2011,** *11* (9), 3643-3648.
255. Liau, B.; Zhang, D.; Bursac, N., Functional cardiac tissue engineering. *Regenerative medicine* **2012,** *7* (2), 187-206.
256. Shin, S. R.; Li, Y.-C.; Jang, H. L.; Khoshakhlagh, P.; Akbari, M.; Nasajpour, A.; Zhang, Y. S.; Tamayol, A.; Khademhosseini, A., Graphene-based materials for tissue engineering. *Advanced drug delivery reviews* **2016,** *105*, 255-274.
257. Park, J.; Park, S.; Ryu, S.; Bhang, S. H.; Kim, J.; Yoon, J. K.; Park, Y. H.; Cho, S. P.; Lee, S.; Hong, B. H., Graphene–Regulated Cardiomyogenic Differentiation Process of Mesenchymal Stem Cells by Enhancing the Expression of Extracellular Matrix Proteins and Cell Signaling Molecules. *Advanced healthcare materials* **2014,** *3* (2), 176-181.
258. Park, J.; Kim, B.; Han, J.; Oh, J.; Park, S.; Ryu, S.; Jung, S.; Shin, J.-Y.; Lee, B. S.; Hong, B. H., Graphene oxide flakes as a cellular adhesive: prevention of reactive oxygen species mediated death of implanted cells for cardiac repair. *ACS nano* **2015,** *9* (5), 4987-4999.
259. Park, J.; Kim, Y. S.; Ryu, S.; Kang, W. S.; Park, S.; Han, J.; Jeong, H. C.; Hong, B. H.; Ahn, Y.; Kim, B. S., Graphene potentiates the myocardial repair efficacy of mesenchymal stem cells by stimulating the expression of angiogenic growth factors and gap junction protein. *Advanced Functional Materials* **2015,** *25* (17), 2590-2600.
260. Shin, S. R.; Aghaei-Ghareh-Bolagh, B.; Gao, X.; Nikkhah, M.; Jung, S. M.; Dolatshahi-Pirouz, A.; Kim, S. B.; Kim, S. M.; Dokmeci, M. R.; Tang, X. S., Layer-by-Layer Assembly of 3D Tissue Constructs with Functionalized Graphene. *Advanced functional materials* **2014,** *24* (39), 6136-6144.
261. Annabi, N.; Shin, S. R.; Tamayol, A.; Miscuglio, M.; Bakooshli, M. A.; Assmann, A.; Mostafalu, P.; Sun, J.-Y.; Mithieux, S.; Cheung, L.; Tang, X.; Weiss, A. S.; Khademhosseini, A., Highly Elastic and Conductive Human-Based Protein Hybrid Hydrogels. *Advanced Materials* **2016,** *28* (1), 40-49. DOI: 10.1002/adma.201503255.
262. Shi, X.; Chang, H.; Chen, S.; Lai, C.; Khademhosseini, A.; Wu, H., Regulating Cellular Behavior on Few-Layer Reduced Graphene Oxide Films with Well-Controlled Reduction States. *Advanced Functional Materials* **2012,** *22* (4), 751-759.
263. Nayak, T. R.; Andersen, H.; Makam, V. S.; Khaw, C.; Bae, S.; Xu, X.; Ee, P.-L. R.; Ahn, J.-H.; Hong, B. H.; Pastorin, G., Graphene for controlled and accelerated osteogenic differentiation of human mesenchymal stem cells. *ACS nano* **2011,** *5* (6), 4670-4678.
264. Lee, W. C.; Lim, C. H. Y.; Shi, H.; Tang, L. A.; Wang, Y.; Lim, C. T.; Loh, K. P., Origin of enhanced stem cell growth and differentiation on graphene and graphene oxide. *ACS nano* **2011,** *5* (9), 7334-7341.
265. Kim, S.; Ku, S. H.; Lim, S. Y.; Kim, J. H.; Park, C. B., Graphene–biomineral hybrid materials. *Advanced Materials* **2011,** *23* (17), 2009-2014.

266. Lu, J.; He, Y. S.; Cheng, C.; Wang, Y.; Qiu, L.; Li, D.; Zou, D., Self-Supporting Graphene Hydrogel Film as an Experimental Platform to Evaluate the Potential of Graphene for Bone Regeneration. *Advanced Functional Materials* **2013,** *23* (28), 3494-3502.
267. Xie, H.; Cao, T.; Gomes, J. V.; Neto, A. H. C.; Rosa, V., Two and three-dimensional graphene substrates to magnify osteogenic differentiation of periodontal ligament stem cells. *Carbon* **2015,** *93*, 266-275.
268. Lee, J. H.; Shin, Y. C.; Lee, S.-M.; Jin, O. S.; Kang, S. H.; Hong, S. W.; Jeong, C.-M.; Huh, J. B.; Han, D.-W., Enhanced osteogenesis by reduced graphene oxide/hydroxyapatite nanocomposites. *Scientific reports* **2015,** *5*.
269. Liu, H.; Cheng, J.; Chen, F.; Hou, F.; Bai, D.; Xi, P.; Zeng, Z., Biomimetic and cell-mediated mineralization of hydroxyapatite by carrageenan functionalized graphene oxide. *ACS applied materials & interfaces* **2014,** *6* (5), 3132-3140.
270. Xie, X.; Hu, K.; Fang, D.; Shang, L.; Tran, S. D.; Cerruti, M., Graphene and hydroxyapatite self-assemble into homogeneous, free standing nanocomposite hydrogels for bone tissue engineering. *Nanoscale* **2015,** *7* (17), 7992-8002.
271. Lee, J. H.; Shin, Y. C.; Jin, O. S.; Kang, S. H.; Hwang, Y.-S.; Park, J.-C.; Hong, S. W.; Han, D.-W., Reduced graphene oxide-coated hydroxyapatite composites stimulate spontaneous osteogenic differentiation of human mesenchymal stem cells. *Nanoscale* **2015,** *7* (27), 11642-11651.
272. Kumar, S.; Chatterjee, K., Strontium eluting graphene hybrid nanoparticles augment osteogenesis in a 3D tissue scaffold. *Nanoscale* **2015,** *7* (5), 2023-2033.
273. Mehrali, M.; Moghaddam, E.; Shirazi, S. F. S.; Baradaran, S.; Mehrali, M.; Latibari, S. T.; Metselaar, H. S. C.; Kadri, N. A.; Zandi, K.; Osman, N. A. A., Synthesis, mechanical properties, and in vitro biocompatibility with osteoblasts of calcium silicate–reduced graphene oxide composites. *ACS applied materials & interfaces* **2014,** *6* (6), 3947-3962.
274. Gao, C.; Liu, T.; Shuai, C.; Peng, S., Enhancement mechanisms of graphene in nano-58S bioactive glass scaffold: mechanical and biological performance. *Scientific reports* **2014,** *4*.
275. Yang, X.; Qiu, L.; Cheng, C.; Wu, Y.; Ma, Z. F.; Li, D., Ordered gelation of chemically converted graphene for next-generation electroconductive hydrogel films. *Angewandte Chemie International Edition* **2011,** *50* (32), 7325-7328.
276. Kolanthai, E.; Sindu, P. A.; Khajuria, D. K.; Veerla, S. C.; Kuppuswamy, D.; Catalani, L. H.; Mahapatra, D. R., Graphene Oxide—A Tool for the Preparation of Chemically Crosslinking Free Alginate–Chitosan–Collagen Scaffolds for Bone Tissue Engineering. *ACS Applied Materials & Interfaces* **2018,** *10* (15), 12441-12452. DOI: 10.1021/acsami.8b00699.
277. Buckwalter, J. A.; Mankin, H. J.; Grodzinsky, A. J., Articular cartilage and osteoarthritis. *Instructional Course Lectures-American Academy of Orthopaedic Surgeons* **2005,** *54*, 465.
278. Liao, J.; Qu, Y.; Chu, B.; Zhang, X.; Qian, Z., Biodegradable CSMA/PECA/graphene porous hybrid scaffold for cartilage tissue engineering. *Scientific reports* **2015,** *5*.
279. Yoon, H. H.; Bhang, S. H.; Kim, T.; Yu, T.; Hyeon, T.; Kim, B. S., Dual Roles of Graphene Oxide in Chondrogenic Differentiation of Adult Stem Cells: Cell-Adhesion Substrate and Growth Factor-Delivery Carrier. *Advanced Functional Materials* **2014,** *24* (41), 6455-6464.
280. Lee, W. C.; Lim, C. H.; Su, C.; Loh, K. P.; Lim, C. T., Cell-assembled graphene biocomposite for enhanced chondrogenic differentiation. *Small* **2015,** *11* (8), 963-969.
281. Picciotto, M. R.; Higley, M. J.; Mineur, Y. S., Acetylcholine as a neuromodulator: cholinergic signaling shapes nervous system function and behavior. *Neuron* **2012,** *76* (1), 116-129.
282. Yang, D.; Li, T.; Xu, M.; Gao, F.; Yang, J.; Yang, Z.; Le, W., Graphene oxide promotes the differentiation of mouse embryonic stem cells to dopamine neurons. *Nanomedicine* **2014,** *9* (16), 2445-2455.
283. Tu, Q.; Pang, L.; Chen, Y.; Zhang, Y.; Zhang, R.; Lu, B.; Wang, J., Effects of surface charges of graphene oxide on neuronal outgrowth and branching. *Analyst* **2014,** *139* (1), 105-115.

284. Tu, Q.; Pang, L.; Wang, L.; Zhang, Y.; Zhang, R.; Wang, J., Biomimetic choline-like graphene oxide composites for neurite sprouting and outgrowth. *ACS applied materials & interfaces* **2013,** *5* (24), 13188-13197.
285. Weaver, C. L.; Cui, X. T., Directed neural stem cell differentiation with a functionalized graphene oxide nanocomposite. *Advanced healthcare materials* **2015,** *4* (9), 1408-1416.
286. Lorenzoni, M.; Brandi, F.; Dante, S.; Giugni, A.; Torre, B., Simple and effective graphene laser processing for neuron patterning application. *Scientific reports* **2013,** *3*.
287. Solanki, A.; Chueng, S. T. D.; Yin, P. T.; Kappera, R.; Chhowalla, M.; Lee, K. B., Axonal Alignment and Enhanced Neuronal Differentiation of Neural Stem Cells on Graphene-Nanoparticle Hybrid Structures. *Advanced Materials* **2013,** *25* (38), 5477-5482.
288. Kim, T.-H.; Shah, S.; Yang, L.; Yin, P. T.; Hossain, M. K.; Conley, B.; Choi, J.-W.; Lee, K.-B., Controlling differentiation of adipose-derived stem cells using combinatorial graphene hybrid-pattern arrays. *ACS nano* **2015,** *9* (4), 3780-3790.
289. Akhavan, O.; Ghaderi, E., Differentiation of human neural stem cells into neural networks on graphene nanogrids. *Journal of Materials Chemistry B* **2013,** *1* (45), 6291-6301.
290. Fattahi, P.; Yang, G.; Kim, G.; Abidian, M. R., A review of organic and inorganic biomaterials for neural interfaces. *Advanced materials* **2014,** *26* (12), 1846-1885.
291. Liu, T.-C.; Chuang, M.-C.; Chu, C.-Y.; Huang, W.-C.; Lai, H.-Y.; Wang, C.-T.; Chu, W.-L.; Chen, S.-Y.; Chen, Y.-Y., Implantable graphene-based neural electrode interfaces for electrophysiology and neurochemistry in in vivo hyperacute stroke model. *ACS applied materials & interfaces* **2015,** *8* (1), 187-196.
292. Li, N.; Zhang, Q.; Gao, S.; Song, Q.; Huang, R.; Wang, L.; Liu, L.; Dai, J.; Tang, M.; Cheng, G., Three-dimensional graphene foam as a biocompatible and conductive scaffold for neural stem cells. *Scientific reports* **2013,** *3*, 1604.
293. Zhi, F.; Dong, H.; Jia, X.; Guo, W.; Lu, H.; Yang, Y.; Ju, H.; Zhang, X.; Hu, Y., Functionalized graphene oxide mediated adriamycin delivery and miR-21 gene silencing to overcome tumor multidrug resistance in vitro. *PloS one* **2013,** *8* (3), e60034.
294. Ahadian, S.; Ramón-Azcón, J.; Chang, H.; Liang, X.; Kaji, H.; Shiku, H.; Nakajima, K.; Ramalingam, M.; Wu, H.; Matsue, T., Electrically regulated differentiation of skeletal muscle cells on ultrathin graphene-based films. *RSC Advances* **2014,** *4* (19), 9534-9541.
295. Bajaj, P.; Rivera, J. A.; Marchwiany, D.; Solovyeva, V.; Bashir, R., Graphene-based patterning and differentiation of C2C12 myoblasts. *Advanced healthcare materials* **2014,** *3* (7), 995-1000.
296. Lee, E. J.; Lee, J. H.; Shin, Y. C.; Hwang, D.-G.; Kim, J. S.; Jin, O. S.; Jin, L.; Hong, S. W.; Han, D.-W., Graphene oxide-decorated PLGA/collagen hybrid fiber sheets for application to tissue engineering scaffolds. *Biomater Res* **2014,** *18*, 18-24.
297. Smith, A. S.; Yoo, H.; Yi, H.; Ahn, E. H.; Lee, J. H.; Shao, G.; Nagornyak, E.; Laflamme, M. A.; Murry, C. E.; Kim, D.-H., Micro-and nano-patterned conductive graphene–PEG hybrid scaffolds for cardiac tissue engineering. *Chemical Communications* **2017,** *53* (53), 7412-7415.
298. Ameri, S. K.; Singh, P.; D'Angelo, R.; Stoppel, W.; Black, L.; Sonkusale, S. R. In *Three dimensional graphene scaffold for cardiac tissue engineering and in-situ electrical recording*, Engineering in Medicine and Biology Society (EMBC), 2016 IEEE 38th Annual International Conference of the, IEEE: 2016; pp 4201-4203.
299. Tang, M.; Song, Q.; Li, N.; Jiang, Z.; Huang, R.; Cheng, G., Enhancement of electrical signaling in neural networks on graphene films. *Biomaterials* **2013,** *34* (27), 6402-6411.
300. Hong, S. W.; Lee, J. H.; Kang, S. H.; Hwang, E. Y.; Hwang, Y.-S.; Lee, M. H.; Han, D.-W.; Park, J.-C., Enhanced neural cell adhesion and neurite outgrowth on graphene-based biomimetic substrates. *BioMed research international* **2014,** *2014*.
301. Kalbacova, M.; Broz, A.; Kong, J.; Kalbac, M., Graphene substrates promote adherence of human osteoblasts and mesenchymal stromal cells. *Carbon* **2010,** *48* (15), 4323-4329.

302. La, W. G.; Park, S.; Yoon, H. H.; Jeong, G. J.; Lee, T. J.; Bhang, S. H.; Han, J. Y.; Char, K.; Kim, B. S., Delivery of a therapeutic protein for bone regeneration from a substrate coated with graphene oxide. *Small* **2013,** *9* (23), 4051-4060.
303. Kim, J.; Choi, K. S.; Kim, Y.; Lim, K. T.; Seonwoo, H.; Park, Y.; Kim, D. H.; Choung, P. H.; Cho, C. S.; Kim, S. Y., Bioactive effects of graphene oxide cell culture substratum on structure and function of human adipose-derived stem cells. *Journal of Biomedical Materials Research Part A* **2013,** *101* (12), 3520-3530.
304. Akhavan, O.; Ghaderi, E.; Shahsavar, M., Graphene nanogrids for selective and fast osteogenic differentiation of human mesenchymal stem cells. *Carbon* **2013,** *59*, 200-211.
305. Saravanan, S.; Chawla, A.; Vairamani, M.; Sastry, T.; Subramanian, K.; Selvamurugan, N., Scaffolds containing chitosan, gelatin and graphene oxide for bone tissue regeneration in vitro and in vivo. *International journal of biological macromolecules* **2017,** *104*, 1975-1985.
306. Unnithan, A. R.; Sasikala, A. R. K.; Park, C. H.; Kim, C. S., A unique scaffold for bone tissue engineering: An osteogenic combination of graphene oxide–hyaluronic acid–chitosan with simvastatin. *Journal of Industrial and Engineering Chemistry* **2017,** *46*, 182-191.
307. Liao, J.; Qu, Y.; Chu, B.; Zhang, X.; Qian, Z., Biodegradable CSMA/PECA/graphene porous hybrid scaffold for cartilage tissue engineering. *Scientific reports* **2015,** *5*, 9879.
308. Li, Z.; Wang, H.; Yang, B.; Sun, Y.; Huo, R., Three-dimensional graphene foams loaded with bone marrow derived mesenchymal stem cells promote skin wound healing with reduced scarring. *Materials Science and Engineering: C* **2015,** *57*, 181-188.
309. Shah, S.; Solanki, A.; Sasmal, P. K.; Lee, K.-B., Single vehicular delivery of siRNA and small molecules to control stem cell differentiation. *Journal of the American Chemical Society* **2013,** *135* (42), 15682-15685.
310. Goenka, S.; Sant, V.; Sant, S., Graphene-based nanomaterials for drug delivery and tissue engineering. *Journal of Controlled Release* **2014,** *173*, 75-88.
311. Zhang, L.; Xia, J.; Zhao, Q.; Liu, L.; Zhang, Z., Functional graphene oxide as a nanocarrier for controlled loading and targeted delivery of mixed anticancer drugs. *Small* **2010,** *6* (4), 537-544.
312. Yang, X.; Zhang, X.; Ma, Y.; Huang, Y.; Wang, Y.; Chen, Y., Superparamagnetic graphene oxide–Fe 3 O 4 nanoparticles hybrid for controlled targeted drug carriers. *Journal of Materials Chemistry* **2009,** *19* (18), 2710-2714.
313. Liu, Z.; Robinson, J. T.; Sun, X.; Dai, H., PEGylated nanographene oxide for delivery of water-insoluble cancer drugs. *Journal of the American Chemical Society* **2008,** *130* (33), 10876-10877.
314. Depan, D.; Shah, J.; Misra, R., Controlled release of drug from folate-decorated and graphene mediated drug delivery system: synthesis, loading efficiency, and drug release response. *Materials Science and Engineering: C* **2011,** *31* (7), 1305-1312.
315. Pan, Y.; Bao, H.; Sahoo, N. G.; Wu, T.; Li, L., Water-soluble poly (N-isopropylacrylamide)–graphene sheets synthesized via click chemistry for drug delivery. *Advanced Functional Materials* **2011,** *21* (14), 2754-2763.
316. Wen, H.; Dong, C.; Dong, H.; Shen, A.; Xia, W.; Cai, X.; Song, Y.; Li, X.; Li, Y.; Shi, D., Engineered redox-responsive PEG detachment mechanism in PEGylated nano-graphene oxide for intracellular drug delivery. *Small* **2012,** *8* (5), 760-769.
317. Chen, M.-L.; Liu, J.-W.; Hu, B.; Chen, M.-L.; Wang, J.-H., Conjugation of quantum dots with graphene for fluorescence imaging of live cells. *Analyst* **2011,** *136* (20), 4277-4283.
318. Fan, X.; Jiao, G.; Gao, L.; Jin, P.; Li, X., The preparation and drug delivery of a graphene–carbon nanotube–Fe 3 O 4 nanoparticle hybrid. *Journal of Materials Chemistry B* **2013,** *1* (20), 2658-2664.
319. Chen, M.-L.; He, Y.-J.; Chen, X.-W.; Wang, J.-H., Quantum-dot-conjugated graphene as a probe for simultaneous cancer-targeted fluorescent imaging, tracking, and monitoring drug delivery. *Bioconjugate chemistry* **2013,** *24* (3), 387-397.

320. Högemann-Savellano, D.; Bos, E.; Blondet, C.; Sato, F.; Abe, T.; Josephson, L.; Weissleder, R.; Gaudet, J.; Sgroi, D.; Peters, P. J., The transferrin receptor: a potential molecular imaging marker for human cancer. *Neoplasia* **2003,** *5* (6), 495-506.
321. Shah, S.; Sasmal, P. K.; Lee, K.-B., Photo-triggerable hydrogel–nanoparticle hybrid scaffolds for remotely controlled drug delivery. *Journal of Materials Chemistry B* **2014,** *2* (44), 7685-7693.
322. He, D.; He, X.; Wang, K.; Zou, Z.; Yang, X.; Li, X., Remote-controlled drug release from graphene oxide-capped mesoporous silica to cancer cells by photoinduced pH-jump activation. *Langmuir* **2014,** *30* (24), 7182-7189.
323. Shirai, M.; Tsunooka, M., Photoacid and photobase generators: chemistry and applications to polymeric materials. *Progress in polymer science* **1996,** *21* (1), 1-45.
324. Kim, H.; Lee, D.; Kim, J.; Kim, T.-i.; Kim, W. J., Photothermally triggered cytosolic drug delivery via endosome disruption using a functionalized reduced graphene oxide. *ACS nano* **2013,** *7* (8), 6735-6746.
325. Wang, X.; Sun, X.; Lao, J.; He, H.; Cheng, T.; Wang, M.; Wang, S.; Huang, F., Multifunctional graphene quantum dots for simultaneous targeted cellular imaging and drug delivery. *Colloids and Surfaces B: Biointerfaces* **2014,** *122*, 638-644.
326. Iannazzo, D.; Pistone, A.; Salamò, M.; Galvagno, S.; Romeo, R.; Giofré, S. V.; Branca, C.; Visalli, G.; Di Pietro, A., Graphene quantum dots for cancer targeted drug delivery. *International journal of pharmaceutics* **2017,** *518* (1), 185-192.
327. Chen, H.; Wang, Z.; Zong, S.; Chen, P.; Zhu, D.; Wu, L.; Cui, Y., A graphene quantum dot-based FRET system for nuclear-targeted and real-time monitoring of drug delivery. *Nanoscale* **2015,** *7* (37), 15477-15486.
328. Zheng, F.-F.; Zhang, P.-H.; Xi, Y.; Chen, J.-J.; Li, L.-L.; Zhu, J.-J., Aptamer/graphene quantum dots nanocomposite capped fluorescent mesoporous silica nanoparticles for intracellular drug delivery and real-time monitoring of drug release. *Analytical chemistry* **2015,** *87* (23), 11739-11745.
329. Nigam, P.; Waghmode, S.; Louis, M.; Wangnoo, S.; Chavan, P.; Sarkar, D., Graphene quantum dots conjugated albumin nanoparticles for targeted drug delivery and imaging of pancreatic cancer. *Journal of Materials Chemistry B* **2014,** *2* (21), 3190-3195.
330. Wang, C.; Wu, C.; Zhou, X.; Han, T.; Xin, X.; Wu, J.; Zhang, J.; Guo, S., Enhancing cell nucleus accumulation and DNA cleavage activity of anti-cancer drug via graphene quantum dots. *Scientific reports* **2013,** *3*.
331. Edelstein, M., Vectors used in gene therapy clinical trials. *Gene Therapy Clinical Trials Worldwide* **2011**.
332. Vincent, M.; de Lázaro, I.; Kostarelos, K., Graphene materials as 2D non-viral gene transfer vector platforms. *Gene therapy* **2017,** *24* (3), 123.
333. Yin, H.; Kanasty, R. L.; Eltoukhy, A. A.; Vegas, A. J.; Dorkin, J. R.; Anderson, D. G., Non-viral vectors for gene-based therapy. *Nature Reviews Genetics* **2014,** *15* (8), 541-555.
334. Hunter, A. C., Molecular hurdles in polyfectin design and mechanistic background to polycation induced cytotoxicity. *Advanced drug delivery reviews* **2006,** *58* (14), 1523-1531.
335. Chua, C. K.; Pumera, M., Covalent chemistry on graphene. *Chemical Society Reviews* **2013,** *42* (8), 3222-3233.
336. Yan, L.; Zheng, Y. B.; Zhao, F.; Li, S.; Gao, X.; Xu, B.; Weiss, P. S.; Zhao, Y., Chemistry and physics of a single atomic layer: strategies and challenges for functionalization of graphene and graphene-based materials. *Chemical Society Reviews* **2012,** *41* (1), 97-114.
337. Dong, H.; Dai, W.; Ju, H.; Lu, H.; Wang, S.; Xu, L.; Zhou, S.-F.; Zhang, Y.; Zhang, X., Multifunctional Poly (l-lactide)–Polyethylene Glycol-Grafted Graphene Quantum Dots for Intracellular MicroRNA Imaging and Combined Specific-Gene-Targeting Agents Delivery for Improved Therapeutics. *ACS applied materials & interfaces* **2015,** *7* (20), 11015-11023.
338. Lungwitz, U.; Breunig, M.; Blunk, T.; Göpferich, A., Polyethylenimine-based non-viral gene delivery systems. *European Journal of Pharmaceutics and Biopharmaceutics* **2005,** *60* (2), 247-266.

339. Prencipe, G.; Tabakman, S. M.; Welsher, K.; Liu, Z.; Goodwin, A. P.; Zhang, L.; Henry, J.; Dai, H., PEG branched polymer for functionalization of nanomaterials with ultralong blood circulation. *Journal of the American Chemical Society* **2009,** *131* (13), 4783-4787.
340. Feng, L.; Yang, X.; Shi, X.; Tan, X.; Peng, R.; Wang, J.; Liu, Z., Polyethylene glycol and polyethylenimine dual-functionalized nano-graphene oxide for photothermally enhanced gene delivery. *Small* **2013,** *9* (11), 1989-1997.
341. Yin, D.; Li, Y.; Lin, H.; Guo, B.; Du, Y.; Li, X.; Jia, H.; Zhao, X.; Tang, J.; Zhang, L., Functional graphene oxide as a plasmid-based Stat3 siRNA carrier inhibits mouse malignant melanoma growth in vivo. *Nanotechnology* **2013,** *24* (10), 105102.
342. Zhang, L.; Wang, Z.; Lu, Z.; Shen, H.; Huang, J.; Zhao, Q.; Liu, M.; He, N.; Zhang, Z., PEGylated reduced graphene oxide as a superior ssRNA delivery system. *Journal of Materials Chemistry B* **2013,** *1* (6), 749-755.
343. Bao, H.; Pan, Y.; Ping, Y.; Sahoo, N. G.; Wu, T.; Li, L.; Li, J.; Gan, L. H., Chitosan-functionalized graphene oxide as a nanocarrier for drug and gene delivery. *Small* **2011,** *7* (11), 1569-1578.
344. Kean, T.; Roth, S.; Thanou, M., Trimethylated chitosans as non-viral gene delivery vectors: cytotoxicity and transfection efficiency. *Journal of Controlled Release* **2005,** *103* (3), 643-653.
345. Sarkar, K.; Kundu, P., PAMAM conjugated chitosan through naphthalimide moiety for enhanced gene transfection efficiency. *Carbohydrate polymers* **2013,** *98* (1), 495-504.
346. Xu, C.; Yang, D.; Mei, L.; Lu, B.; Chen, L.; Li, Q.; Zhu, H.; Wang, T., Encapsulating gold nanoparticles or nanorods in graphene oxide shells as a novel gene vector. *ACS applied materials & interfaces* **2013,** *5* (7), 2715-2724.
347. Imani, R.; Emami, S. H.; Faghihi, S., Synthesis and characterization of an octaarginine functionalized graphene oxide nano-carrier for gene delivery applications. *Physical Chemistry Chemical Physics* **2015,** *17* (9), 6328-6339.
348. Yang, X.; Zhao, N.; Xu, F.-J., Biocleavable graphene oxide based-nanohybrids synthesized via ATRP for gene/drug delivery. *Nanoscale* **2014,** *6* (11), 6141-6150.
349. Li, K.; Feng, L.; Shen, J.; Zhang, Q.; Liu, Z.; Lee, S.-T.; Liu, J., Patterned substrates of nano-graphene oxide mediating highly localized and efficient gene delivery. *ACS applied materials & interfaces* **2014,** *6* (8), 5900-5907.
350. Tripathi, S. K.; Goyal, R.; Gupta, K. C.; Kumar, P., Functionalized graphene oxide mediated nucleic acid delivery. *Carbon* **2013,** *51*, 224-235.
351. Kim, H.; Kim, W. J., Photothermally controlled gene delivery by reduced graphene oxide–polyethylenimine nanocomposite. *Small* **2014,** *10* (1), 117-126.
352. Zhang, L.; Lu, Z.; Zhao, Q.; Huang, J.; Shen, H.; Zhang, Z., Enhanced chemotherapy efficacy by sequential delivery of siRNA and anticancer drugs using PEI-grafted graphene oxide. *Small* **2011,** *7* (4), 460-464.
353. Paul, A.; Hasan, A.; Kindi, H. A.; Gaharwar, A. K.; Rao, V. T.; Nikkhah, M.; Shin, S. R.; Krafft, D.; Dokmeci, M. R.; Shum-Tim, D., Injectable graphene oxide/hydrogel-based angiogenic gene delivery system for vasculogenesis and cardiac repair. *ACS nano* **2014,** *8* (8), 8050-8062.
354. Liu, X.; Ma, D.; Tang, H.; Tan, L.; Xie, Q.; Zhang, Y.; Ma, M.; Yao, S., Polyamidoamine dendrimer and oleic acid-functionalized graphene as biocompatible and efficient gene delivery vectors. *ACS applied materials & interfaces* **2014,** *6* (11), 8173-8183.
355. Wang, Y.; Li, Z.; Hu, D.; Lin, C.-T.; Li, J.; Lin, Y., Aptamer/graphene oxide nanocomplex for in situ molecular probing in living cells. *Journal of the American Chemical Society* **2010,** *132* (27), 9274-9276.
356. Chen, B.; Liu, M.; Zhang, L.; Huang, J.; Yao, J.; Zhang, Z., Polyethylenimine-functionalized graphene oxide as an efficient gene delivery vector. *Journal of Materials Chemistry* **2011,** *21* (21), 7736-7741.
357. Feng, L.; Zhang, S.; Liu, Z., Graphene based gene transfection. *Nanoscale* **2011,** *3* (3), 1252-1257.

358. Huang, Y.-P.; Hung, C.-M.; Hsu, Y.-C.; Zhong, C.-Y.; Wang, W.-R.; Chang, C.-C.; Lee, M.-J., Suppression of breast cancer cell migration by small interfering RNA delivered by polyethylenimine-functionalized graphene oxide. *Nanoscale research letters* **2016,** *11* (1), 247.
359. Imani, R.; Shao, W.; Taherkhani, S.; Emami, S. H.; Prakash, S.; Faghihi, S., Dual-functionalized graphene oxide for enhanced siRNA delivery to breast cancer cells. *Colloids and Surfaces B: Biointerfaces* **2016,** *147*, 315-325.
360. Cheng, F.-F.; Chen, W.; Hu, L.-H.; Chen, G.; Miao, H.-T.; Li, C.; Zhu, J.-J., Highly dispersible PEGylated graphene/Au composites as gene delivery vector and potential cancer therapeutic agent. *Journal of Materials Chemistry B* **2013,** *1* (38), 4956-4962.
361. Yang, H.-W.; Huang, C.-Y.; Lin, C.-W.; Liu, H.-L.; Huang, C.-W.; Liao, S.-S.; Chen, P.-Y.; Lu, Y.-J.; Wei, K.-C.; Ma, C.-C. M., Gadolinium-functionalized nanographene oxide for combined drug and microRNA delivery and magnetic resonance imaging. *Biomaterials* **2014,** *35* (24), 6534-6542.
362. Wang, C.; Ravi, S.; Garapati, U. S.; Das, M.; Howell, M.; Mallela, J.; Alwarappan, S.; Mohapatra, S. S.; Mohapatra, S., Multifunctional chitosan magnetic-graphene (CMG) nanoparticles: a theranostic platform for tumor-targeted co-delivery of drugs, genes and MRI contrast agents. *Journal of Materials Chemistry B* **2013,** *1* (35), 4396-4405.
363. Wang, Z.; Shen, H.; Song, S.; Zhang, L.; Chen, W.; Dai, J.; Zhang, Z., Graphene Oxide Incorporated PLGA Nanofibrous Scaffold for Solid Phase Gene Delivery into Mesenchymal Stem Cells. *Journal of Nanoscience and Nanotechnology* **2018,** *18* (4), 2286-2293.
364. Baek, A.; Baek, Y. M.; Kim, H.-M.; Jun, B.-H.; Kim, D.-E., Polyethylene Glycol-Engrafted Graphene Oxide as Biocompatible Materials for Peptide Nucleic Acid Delivery into Cells. *Bioconjugate chemistry* **2018,** *29* (2), 528-537.
365. Zhang, Y.; Hong, H.; Cai, W., Imaging with Raman spectroscopy. *Current pharmaceutical biotechnology* **2010,** *11* (6), 654-661.
366. Huang, J.; Zhang, L.; Chen, B.; Ji, N.; Chen, F.; Zhang, Y.; Zhang, Z., Nanocomposites of size-controlled gold nanoparticles and graphene oxide: formation and applications in SERS and catalysis. *Nanoscale* **2010,** *2* (12), 2733-2738.
367. Liu, Q.; Wei, L.; Wang, J.; Peng, F.; Luo, D.; Cui, R.; Niu, Y.; Qin, X.; Liu, Y.; Sun, H., Cell imaging by graphene oxide based on surface enhanced Raman scattering. *Nanoscale* **2012,** *4* (22), 7084-7089.
368. Liu, Z.; Guo, Z.; Zhong, H.; Qin, X.; Wan, M.; Yang, B., Graphene oxide based surface-enhanced Raman scattering probes for cancer cell imaging. *Physical Chemistry Chemical Physics* **2013,** *15* (8), 2961-2966. DOI: 10.1039/C2CP43715E.
369. Zhang, Z.; Liu, Q.; Gao, D.; Luo, D.; Niu, Y.; Yang, J.; Li, Y., Graphene oxide as a multifunctional platform for Raman and Fluorescence imaging of cells. *Small* **2015,** *11* (25), 3000-3005.
370. Ntziachristos, V., Fluorescence molecular imaging. *Annu. Rev. Biomed. Eng.* **2006,** *8*, 1-33.
371. Sun, X.; Liu, Z.; Welsher, K.; Robinson, J. T.; Goodwin, A.; Zaric, S.; Dai, H., Nano-graphene oxide for cellular imaging and drug delivery. *Nano research* **2008,** *1* (3), 203-212.
372. Yang, K.; Zhang, S.; Zhang, G.; Sun, X.; Lee, S.-T.; Liu, Z., Graphene in mice: ultrahigh in vivo tumor uptake and efficient photothermal therapy. *Nano letters* **2010,** *10* (9), 3318-3323.
373. Ji, D.-K.; Zhang, Y.; Zang, Y.; Liu, W.; Zhang, X.; Li, J.; Chen, G.-R.; James, T. D.; He, X.-P., Receptor-targeting fluorescence imaging and theranostics using a graphene oxide based supramolecular glycocomposite. *Journal of Materials Chemistry B* **2015,** *3* (47), 9182-9185.
374. Zhang, M.; Bai, L.; Shang, W.; Xie, W.; Ma, H.; Fu, Y.; Fang, D.; Sun, H.; Fan, L.; Han, M., Facile synthesis of water-soluble, highly fluorescent graphene quantum dots as a robust biological label for stem cells. *Journal of Materials Chemistry* **2012,** *22* (15), 7461-7467.
375. Pan, D.; Guo, L.; Zhang, J.; Xi, C.; Xue, Q.; Huang, H.; Li, J.; Zhang, Z.; Yu, W.; Chen, Z., Cutting sp 2 clusters in graphene sheets into colloidal graphene quantum dots with strong green fluorescence. *Journal of Materials Chemistry* **2012,** *22* (8), 3314-3318.

376. Nahain, A.-A.; Lee, J.-E.; Jeong, J. H.; Park, S. Y., Photoresponsive fluorescent reduced graphene oxide by spiropyran conjugated hyaluronic acid for in vivo imaging and target delivery. *Biomacromolecules* **2013,** *14* (11), 4082-4090.
377. Patel, M. A.; Yang, H.; Chiu, P. L.; Mastrogiovanni, D. D.; Flach, C. R.; Savaram, K.; Gomez, L.; Hemnarine, A.; Mendelsohn, R.; Garfunkel, E., Direct production of graphene nanosheets for near infrared photoacoustic imaging. *ACS nano* **2013,** *7* (9), 8147-8157.
378. Yang, K.; Hu, L.; Ma, X.; Ye, S.; Cheng, L.; Shi, X.; Li, C.; Li, Y.; Liu, Z., Multimodal imaging guided photothermal therapy using functionalized graphene nanosheets anchored with magnetic nanoparticles. *Advanced materials* **2012,** *24* (14), 1868-1872.
379. Lalwani, G.; Cai, X.; Nie, L.; Wang, L. V.; Sitharaman, B., Graphene-based contrast agents for photoacoustic and thermoacoustic tomography. *Photoacoustics* **2013,** *1* (3), 62-67.
380. Moon, H.; Kumar, D.; Kim, H.; Sim, C.; Chang, J.-H.; Kim, J.-M.; Kim, H.; Lim, D.-K., Amplified photoacoustic performance and enhanced photothermal stability of reduced graphene oxide coated gold nanorods for sensitive photoacoustic imaging. *ACS nano* **2015,** *9* (3), 2711-2719.
381. Sheng, Z.; Song, L.; Zheng, J.; Hu, D.; He, M.; Zheng, M.; Gao, G.; Gong, P.; Zhang, P.; Ma, Y., Protein-assisted fabrication of nano-reduced graphene oxide for combined in vivo photoacoustic imaging and photothermal therapy. *Biomaterials* **2013,** *34* (21), 5236-5243.
382. Toumia, Y.; Domenici, F.; Orlanducci, S.; Mura, F.; Grishenkov, D.; Trochet, P.; Lacerenza, S.; Bordi, F.; Paradossi, G., Graphene Meets Microbubbles: A Superior Contrast Agent for Photoacoustic Imaging. *ACS applied materials & interfaces* **2016,** *8* (25), 16465-16475.
383. Kuo, W.-S.; Shao, Y.-T.; Huang, K.-S.; Chou, T.-M.; Yang, C.-H., Antimicrobial Amino-Functionalized Nitrogen-Doped Graphene Quantum Dots for Eliminating Multidrug-Resistant Species in Dual-Modality Photodynamic Therapy and Bioimaging under Two-Photon Excitation. *ACS applied materials & interfaces* **2018,** *10* (17), 14438-14446.
384. Zhou, F.; Xing, D.; Ou, Z.; Wu, B.; Resasco, D. E.; Chen, W. R., Cancer photothermal therapy in the near-infrared region by using single-walled carbon nanotubes. *Journal of biomedical optics* **2009,** *14* (2), 021009-021009-7.
385. Jaque, D.; Maestro, L. M.; Del Rosal, B.; Haro-Gonzalez, P.; Benayas, A.; Plaza, J.; Rodriguez, E. M.; Sole, J. G., Nanoparticles for photothermal therapies. *Nanoscale* **2014,** *6* (16), 9494-9530.
386. Tian, B.; Wang, C.; Zhang, S.; Feng, L.; Liu, Z., Photothermally enhanced photodynamic therapy delivered by nano-graphene oxide. *ACS nano* **2011,** *5* (9), 7000-7009.
387. Robinson, J. T.; Tabakman, S. M.; Liang, Y.; Wang, H.; Sanchez Casalongue, H.; Vinh, D.; Dai, H., Ultrasmall reduced graphene oxide with high near-infrared absorbance for photothermal therapy. *Journal of the American Chemical Society* **2011,** *133* (17), 6825-6831.
388. Akhavan, O.; Ghaderi, E., Graphene nanomesh promises extremely efficient in vivo photothermal therapy. *Small* **2013,** *9* (21), 3593-3601.
389. Wang, Y.; Wang, K.; Zhao, J.; Liu, X.; Bu, J.; Yan, X.; Huang, R., Multifunctional mesoporous silica-coated graphene nanosheet used for chemo-photothermal synergistic targeted therapy of glioma. *Journal of the American Chemical Society* **2013,** *135* (12), 4799-4804.
390. Li, M.; Yang, X.; Ren, J.; Qu, K.; Qu, X., Using Graphene Oxide High Near-Infrared Absorbance for Photothermal Treatment of Alzheimer's Disease. *Advanced materials* **2012,** *24* (13), 1722-1728.
391. Sahu, A.; Choi, W. I.; Lee, J. H.; Tae, G., Graphene oxide mediated delivery of methylene blue for combined photodynamic and photothermal therapy. *Biomaterials* **2013,** *34* (26), 6239-6248.
392. Ge, J.; Lan, M.; Zhou, B.; Liu, W.; Guo, L.; Wang, H.; Jia, Q.; Niu, G.; Huang, X.; Zhou, H., A graphene quantum dot photodynamic therapy agent with high singlet oxygen generation. *Nature communications* **2014,** *5*.
393. Thakur, M.; Kumawat, M. K.; Srivastava, R., Multifunctional graphene quantum dots for combined photothermal and photodynamic therapy coupled with cancer cell tracking applications. *RSC Advances* **2017,** *7* (9), 5251-5261.
394. Guo, M.; Xiang, H.-J.; Wang, Y.; Zhang, Q.-L.; An, L.; Yang, S.-P.; Ma, Y.; Wang, Y.; Liu, J.-G., Ruthenium nitrosyl functionalized graphene quantum dots as an efficient nanoplatform for NIR-light-

controlled and mitochondria-targeted delivery of nitric oxide combined with photothermal therapy. *Chemical Communications* **2017,** *53* (22), 3253-3256.

395. Shi, X.; Gong, H.; Li, Y.; Wang, C.; Cheng, L.; Liu, Z., Graphene-based magnetic plasmonic nanocomposite for dual bioimaging and photothermal therapy. *Biomaterials* **2013,** *34* (20), 4786-4793.

396. Taratula, O.; Patel, M.; Schumann, C.; Naleway, M. A.; Pang, A. J.; He, H.; Taratula, O., Phthalocyanine-loaded graphene nanoplatform for imaging-guided combinatorial phototherapy. *International journal of nanomedicine* **2015,** *10*, 2347.

397. Zhang, D.-Y.; Zheng, Y.; Tan, C.-P.; Sun, J.-H.; Zhang, W.; Ji, L.-N.; Mao, Z.-W., Graphene Oxide Decorated with Ru (II)–Polyethylene Glycol Complex for Lysosome-Targeted Imaging and Photodynamic/Photothermal Therapy. *ACS Applied Materials & Interfaces* **2017,** *9* (8), 6761-6771.

398. Reina, G.; González-Domínguez, J. M.; Criado, A.; Vázquez, E.; Bianco, A.; Prato, M., Promises, facts and challenges for graphene in biomedical applications. *Chemical Society Reviews* **2017,** *46* (15), 4400-4416.

399. Björnmalm, M.; Faria, M.; Caruso, F., Increasing the impact of materials in and beyond bio-nano science. *J. Am. Chem. Soc* **2016,** *138* (41), 13449-13456.

400. Mills, K. C.; Murry, D.; Guzan, K. A.; Ostraat, M. L., Nanomaterial registry: database that captures the minimal information about nanomaterial physico-chemical characteristics. *Journal of nanoparticle research* **2014,** *16* (2), 2219.

401. Wick, P.; Louw-Gaume, A. E.; Kucki, M.; Krug, H. F.; Kostarelos, K.; Fadeel, B.; Dawson, K. A.; Salvati, A.; Vázquez, E.; Ballerini, L., Classification framework for graphene-based materials. *Angewandte Chemie International Edition* **2014,** *53* (30), 7714-7718.

402. Leon, V.; Gonzalez-Dominguez, J.; Fierro, J. L.; Prato, M.; Vazquez, E., Production and stability of mechanochemically exfoliated graphene in water and culture media. *Nanoscale* **2016,** *8* (30), 14548-14555.

For Table of Contents use only

Biomedical Applications of Graphene Nanomaterials and Beyond

Krishanu Ghosal and Kishor Sarkar*

Gene Therapy and Tissue Engineering Lab

Department of Polymer Science & Technology, University of Calcutta, 92, A.P.C. Road, Kolkata-7 00 009

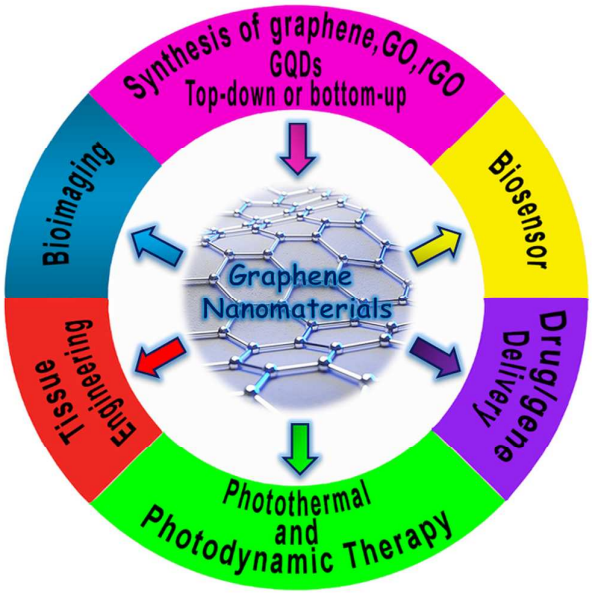

Table of Content